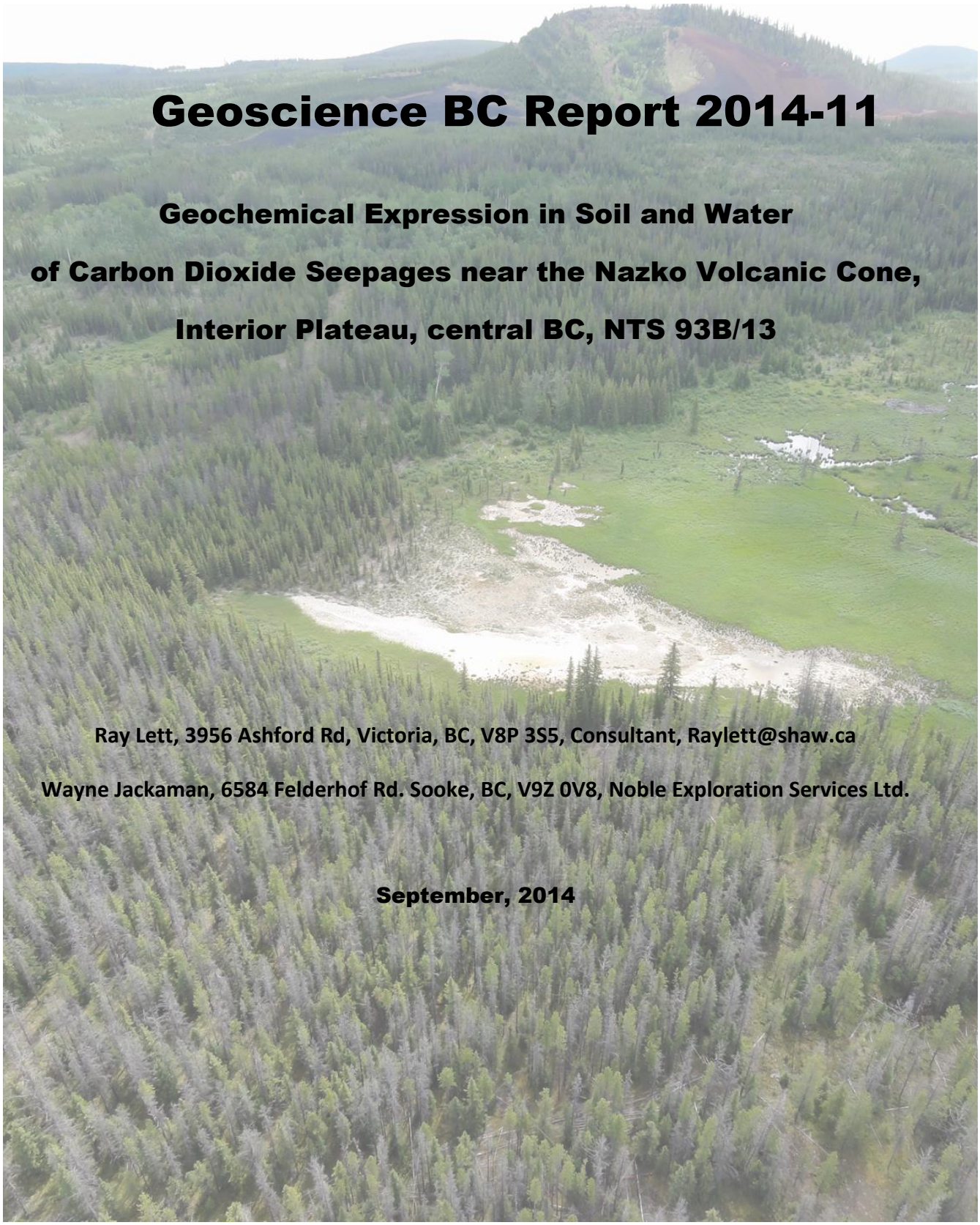

Geoscience BC Report 2014-11

Geochemical Expression in Soil and Water of Carbon Dioxide Seepages near the Nazko Volcanic Cone, Interior Plateau, central BC, NTS 93B/13

Ray Lett, 3956 Ashford Rd, Victoria, BC, V8P 3S5, Consultant, Raylett@shaw.ca

Wayne Jackaman, 6584 Felderhof Rd. Sooke, BC, V9Z 0V8, Noble Exploration Services Ltd.

September, 2014

Table of Contents

Figures 3
Introduction 7
Geology and Surface Environment 8
Field Work 12
Sample Preparation and Analysis 14
Water Sample Quality Control Data Analysis 15
Soil Sample Quality Control Data Analysis 18
Ground and Surface Water geochemistry 25
Soil Geochemistry 56
Rock Geochemistry 77
Discussion of the Results 81
Conclusions 85
Further studies 866
Acknowledgments 877
References 877
Appendix A - Water chemistry digital data
Appendix B - Soil chemistry digital data

Figures

Figure 1 Location of study area. 8
Figure 2 Fresh carbonate precipitate on the surface of the South Bog 9
Figure 3 Panorama of the North and South Bogs and Fishpot Lake to the west. 10
Figure 4 Drainages the Nazko Cone area through North and South Bogs to Fishpot Lake. 10
Figure 5 North and South Bog surface features and distribution of water samples. 11
Figure 6 Travertine mound with carbon dioxide vent in the North bog. 12
Figure 7 Ground water sampling with bailer and PVC pipe 13
Figure 8 Soil sampling using a Hiller auger. 14
Figure 9 Statistics (Median, 3rd quartile, Range) for elements and parameters in bog water 26
Figure 10 Statisitcs (Median, third quartile) for tace elements in bog water 27
Figure 11 TREK Geothermal Project stream and lake water sample locations. 29
Figure 12 TREK Geothermal project stream water pH. 30
Figure 13 TREK Geothermal project stream water temperature. 31
Figure 14 TREK Geothermal project stream water calcium.. 32
Figure 15 TREK Geothermal project and regional lake sediment stream sediment calcium. 33
Figure 16 TREK Geothermal project stream water lithium. 34
Figure 17 TREK Geothermal project stream water boron 35
Figure 18 TREK Geothermal project stream water silica 36
Figure 19 TREK Geothermal project stream water barium 37
Figure 20 TREK Geothermal project stream water strontium 38
Figure 21 TREK Geothermal project stream sediment and and lake sediment strontium 39
Figure 22 TREK Geothermal project stream sediment and lake sediment rhenium 40
Figure 23 TREK Geothermal project stream sediment and lake sediment molybdenum. 41
Figure 24 TREK Geothermal project stream sediment and lake sediment selenium. 42
Figure 25 TREK Geothermal project stream sediment and lake sediment merecury. 43
Figure 26 TREK Geothermal project stream sediment and lake sediment palladium 44
Figure 27 TREK Geothermal project stream and lake sediment nickel 45

Figure 28 TREK Geothermal Project North Bog water sample locations. 46
Figure 29 TREK Geothermal Project North Bog surface and ground water temperature..... 47
Figure 30 TREK Geothermal Project North Bog surface and ground water pH..... 47
Figure 31 TREK Geothermal project North Bog water dissolved carbon dioxide..... 48
Figure 32 TREK Geothermal project North Bog surface and ground water boron 48
Figure 33 TREK Geothermal North Bog stream, surface and ground water lithium..... 49
Figure 34 TREK Geothermal project North Bog surface and ground water calcium..... 49
Figure 35 TREK Geothermal project North Bog surface, and ground water magnesium. 50
Figure 36 TREK Geothermal project North Bog surface and ground water arsenic..... 50
Figure 37 TREK Geothermal project North Bog stream, surface, and ground water nickel..... 51
Figure 38 TREK Geothermal Project South Bog water samples locations..... 52
Figure 39 TREK Geothermal project South Bog travertine water and carbon dioxide seepage. . 52
Figure 40 TREK Geothermal project South Bog surface and ground water temperature..... 53
Figure 41 TREK Geothermal project South Bog surface and ground water pH..... 53
Figure 42 TREK Geothermal project South Bog water dissolved carbon dioxide..... 54
Figure 43 TREK Geothermal project South Bog surface and ground water calcium..... 54
Figure 44 TREK Geothermal project South Bog surface and ground water lithium..... 55
Figure 45 TREK Geothermal project South Bog surface and ground water boron. 55
Figure 46 TREK Geothermal project soil trace element statistics. 57
Figure 47 TREK Geothermal project trace and minor element statistics 58
Figure 48 TREK Geothermal project major oxide statistics. 59
Figure 49 TREK Geothermal project North Bog soil and rock sample locations..... 60
Figure 50 TREK Geothermal project calcium oxide in North Bog C horizon soil samples 60
Figure 51 TREK Geothermal project Silica in North Bog C soil samples 62
Figure 52 TREK Geothermal project magnesium oxide North Bog C soil samples 62
Figure 53 TREK Geothermal project carbon in North Bog C soil samples. 63
Figure 54 TREK Geothermal project sulphur in North Bog C soil samples. 63
Figure 55 TREK Geothermal project iron in North Bog C soil samples 64

Figure 56 .TREK Geothermal project boron in North Bog C soil horizon samples 64
Figure 57 TREK Geothermal project lithium in North Bog C soil horizon samples..... 65
Figure 58 TREK Geothermal project mercury in North Bog C soil horizon samples 65
Figure 59 TREK Geethermal project mercury profiles in the North Bog soil. 66
Figure 60 TREK Geothermal project arsenic profiles in North Bog soil. 67
Figure 61 TREK Geothermal project nickel profiles in North Bog soil. 67
Figure 62 TREK Geothermal project copper profile in North Bog soil. 68
Figure 63 TREK Geothermal project silver profiles in North Bog soil. 68
Figure 64 TREK Geothermal project molybdenum profiles in North Bog soil. 69
Figure 65 TREK Geothermal project rhenium profiles in North Bog soil. 69
Figure 66 TREK Geothermal project North Bog soil pH profiles. 70
Figure 67 TREK Geothermal project boron profiles in North Bog soil. 70
Figure 68 TREK Geothermal project lithium profiles in North Bog soil. 71
Figure 69 TREK Geothermal project calcium profiles in North Bog soil. 71
Figure 70 TREK Geothermal project silica profiles in North Bog soil. 72
Figure 71 TREK Geothermal project South Bog soil profile locations..... 73
Figure 72 TREK Geothermal project calcium profiles in South Bog soil 73
Figure 73 TREK Geothermal project silica profiles in South Bog soil. 74
Figure 74 TREK Geothermal boron profiles in South Bog soil. 74
Figure 75 TREK Geothermal project nickel in South Bog soil. 75
Figure 76 TREK Geothermal project North Bog C horizon and TREK regional till mercury 76
Figure 77 TREK Geothermal project North Bog C horizon and TREK regional till nickel 76
Figure 78 Rock sample locations in the Nazko TREK geothermal project area. 77
Figure 79 TREK Geothermal project,regional till survey mercury cinnabar grains in till..... 84
Figure 80 Processes responsible for soil mercury concentration and bog travertine..... 85

Introduction

Travertine deposits, soil gas seepages, organic soil mixed with calcium carbonate ($CaCO_3$)-mud and pools of stagnant or slow flowing water are among surface features observed in two wetlands informally named the North and South Bogs near the Nazko volcanic cone, BC (Figure 1). During preliminary geothermal exploration conducted at these wetlands in 2012, Alterra Power Corp. detected carbon dioxide with traces of methane and helium in the seepage gas (Hickson, pers comm, 2013; Vigouroux, pers comm, 2013). The isotopic composition ($\delta^{13}C$ between – 6.2 to – 6.9 per mil PDB) of the gases suggests that they are magmatic in origin (Williams-Jones, pers comm, 2013).

Analysis of the carbonate mud in the bogs by Vigouroux (pers comm, 2013), reveals a dominance of aragonite (66%), with equal parts remaining of calcite and dolomite, precipitated from the carbon-enriched surface water. Although the surface water temperature is typically below 12°C, the carbon dioxide seepages, travertine deposits and the nearby Nazko volcanic cone together suggest a magmatic, possibly geothermal source for the gas, similar to the setting described by Fouke et al. (2000) at Mammoth hot springs, Wyoming (Yellowstone) and at the Mt. Etna volcano (D'Alessandro et al. 2007). Magmatic carbon dioxide discharging into the near-surface environment forms "thermogenic" travertine that is predominantly calcite and aragonite enriched in ^{13}C and ^{18}O (Ford and Pedley, 1996; Pentecost, 1995).

While the cool surface waters do not suggest an active geothermal source beneath the Nazko wetlands, spring water temperatures in other areas of Canada where there are travertine deposits can be as low as 20°C, such as at the Rabbit Kettle springs, NWT (Fouke et al. 2000). The spring water chemistry in these areas typically shows elevated calcium, dissolved carbon dioxide, lithium and boron. At the Starlite mineral occurrence near the village of Hills, BC, travertine deposits on Arthur Creek are associated with warm springs (MINFILE 082KSW 074; BC Geological Survey, 2013).

Trace and minor element analyses of ground water, surface water, travertine and soil samples collected from the Nazko bogs and in the surrounding area to study the geochemical signature associated with the carbon dioxide gas seepages are documented in this final project report. This study is being supported by Geoscience BC as part of the 2013 TREK Project and was designed to complement earlier investigations on the potential for geothermal occurrences in the region (Williams-Jones, pers comm., 2013) and support local community interest in geothermal resources.

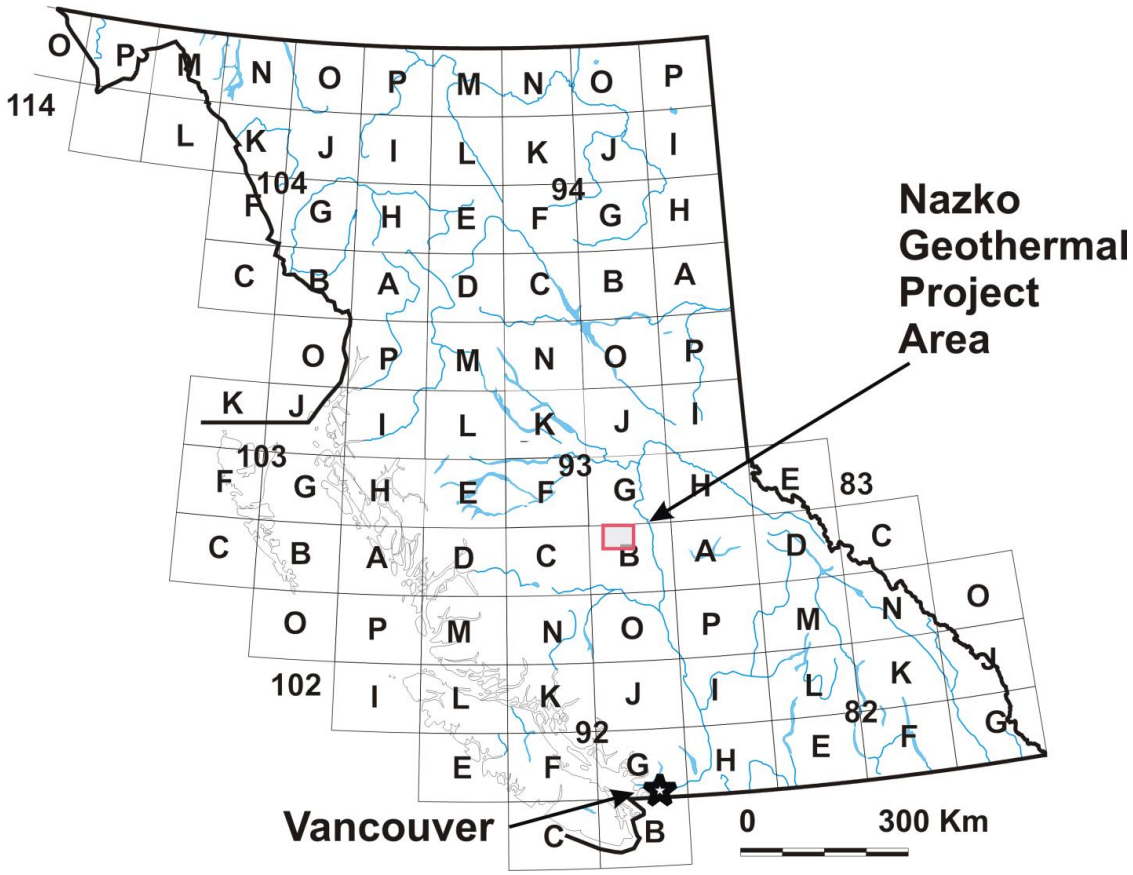

Figure 1 Location of study area.

Geology and Surface Environment

The North and South Bogs and surrounding area lie within the Anahim volcanic belt, an east-west trending belt of Pleistocene-Holocene age volcanoes that include the Nazko cone. (Riddell, 2011). Eocene Ootsa Lake, Miocene Endako and Pleistocene-Holocene volcanic rocks underlie the area. Souther at al. (1987) tentatively estimated that the Nazko volcanism began during the Fraser Glaciation, forming a hyaloclastite mound beneath the Cordilleran ice sheet. A subaerial, flow-layered, non-vesicular basalt buried by more recent tephra and till is the earliest eruptive rock. This unit is partially covered by a later blocky, highly vesicular basalt and tuff breccia forming the western part of the cone. Post glacial deposition of red pyroclastic ash, lapilli and volcanic bombs ejected from vents in the cone created the present-day edifice. During this eruption event, two olivine basalt lavas flowed for several hundred metres from the volcano to the south and west.

Glacial deposits in the area include tills and glacio-fluvial sediments (as eskers) that extend from the base of the cone into the wetlands. Souther et al. (1987) describe sampling a 6 metre vertical profile in the “Volcano Bog” 1.8 km north from the North Bog. Sediments sampled by

Souther et al.(1987) in the Volcano Bog were a mix of gravel and mud overlain by gyttja and more than 5 metres of peat interbedded with a tephra layer. This ash layer was interpreted by Souther et al. (1987) to have been deposited by an eruption from the cone between 7100 and 7200 years BP.

Parts of the North and South Bogs are covered by sedge and scattered wetland shrubs, calcium carbonate-rich mud, stagnant pools or slow moving streams, small, isolated outcrops of travertine, forest dominated bog and meandering streams flowing through the wetlands. In the carbonate-mud-dominated parts of the bog, carbon dioxide can be observed as bubbles seeping through the bottom sediment of stagnant ponds and a calcium carbonate (possibly aragonite) precipitate often occurs on the water surface (Figure 2). Two streams draining uplands to the east and south flow west though the bogs into Fishpot Lake (Figures 3 and 4). Luvisolic and brunisolic soils exist on the better drained hill slopes above the wetlands whereas gleyoslic soils have formed along the bog margin where the water table is close to the land surface. Peat mixed with calcium carbonate mud is the most common organic bog soil.

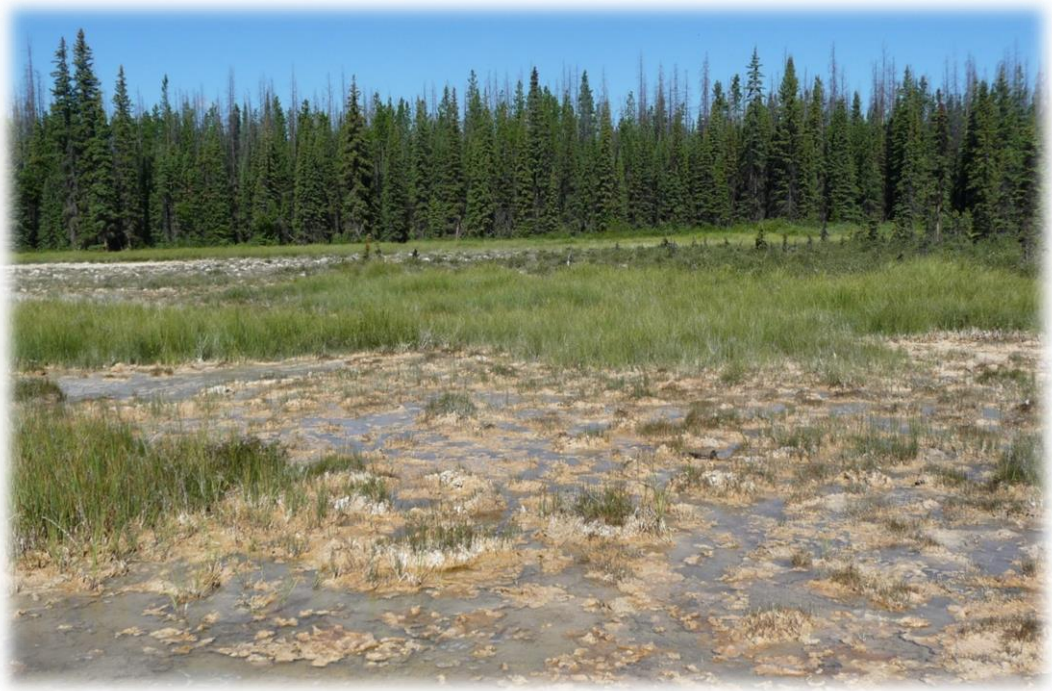

Figure 2 Fresh carbonate precipitate on the surface of the South Bog

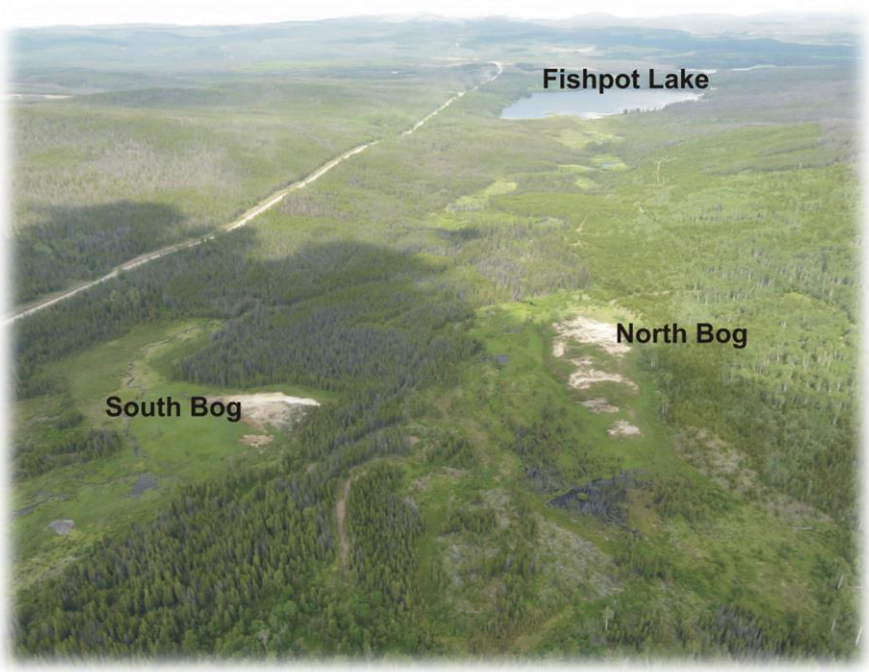

Figure 3 Panorama of the North and South Bogs and Fishpot Lake to the west.

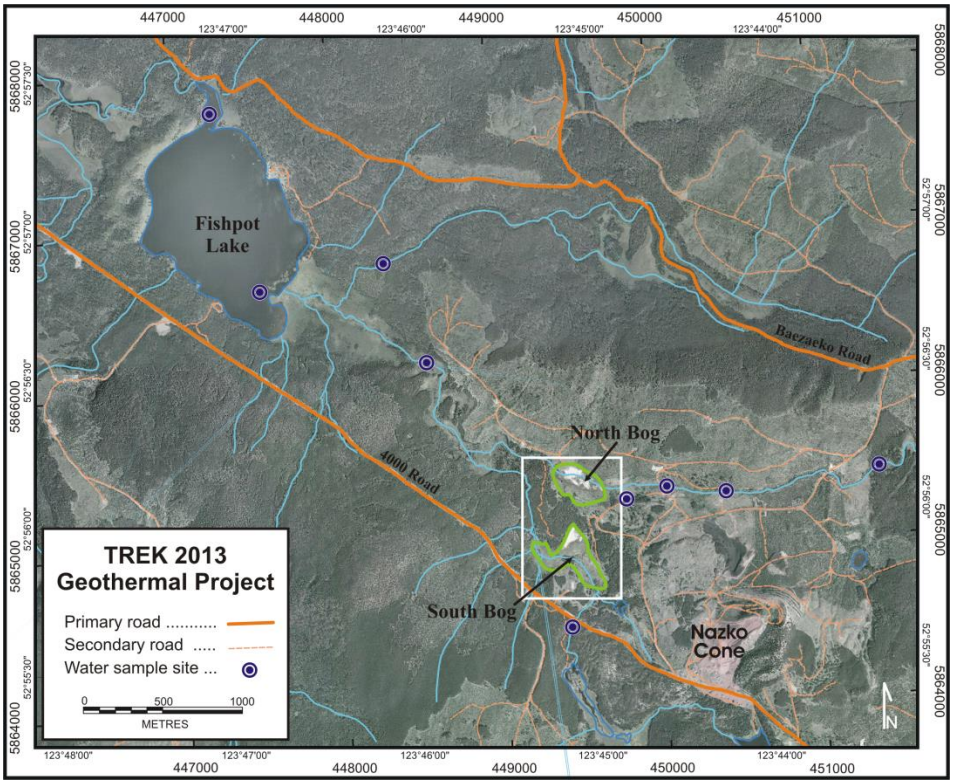

Figure 4 Drainages through North and South Bogs to Fishpot Lake.

Travertine is typically a rusty to white coloured rubble forming small, isolated and elevated areas in the bogs. Near the northern edge of the North Bog, there is a small, 35 centimetre-high inverted cone-shaped travertine deposit concealed by undergrowth. This cone encloses a partially submerged vent from which there is a steady flow of carbon dioxide. There is a less active carbon dioxide seep from another vent on a rusty travertine mound close to the edge of the southern bog. Figure 5 shows the wetland surface features including location of the two carbon dioxide discharging vents and Figure 6 shows the travertine mound vent feature.

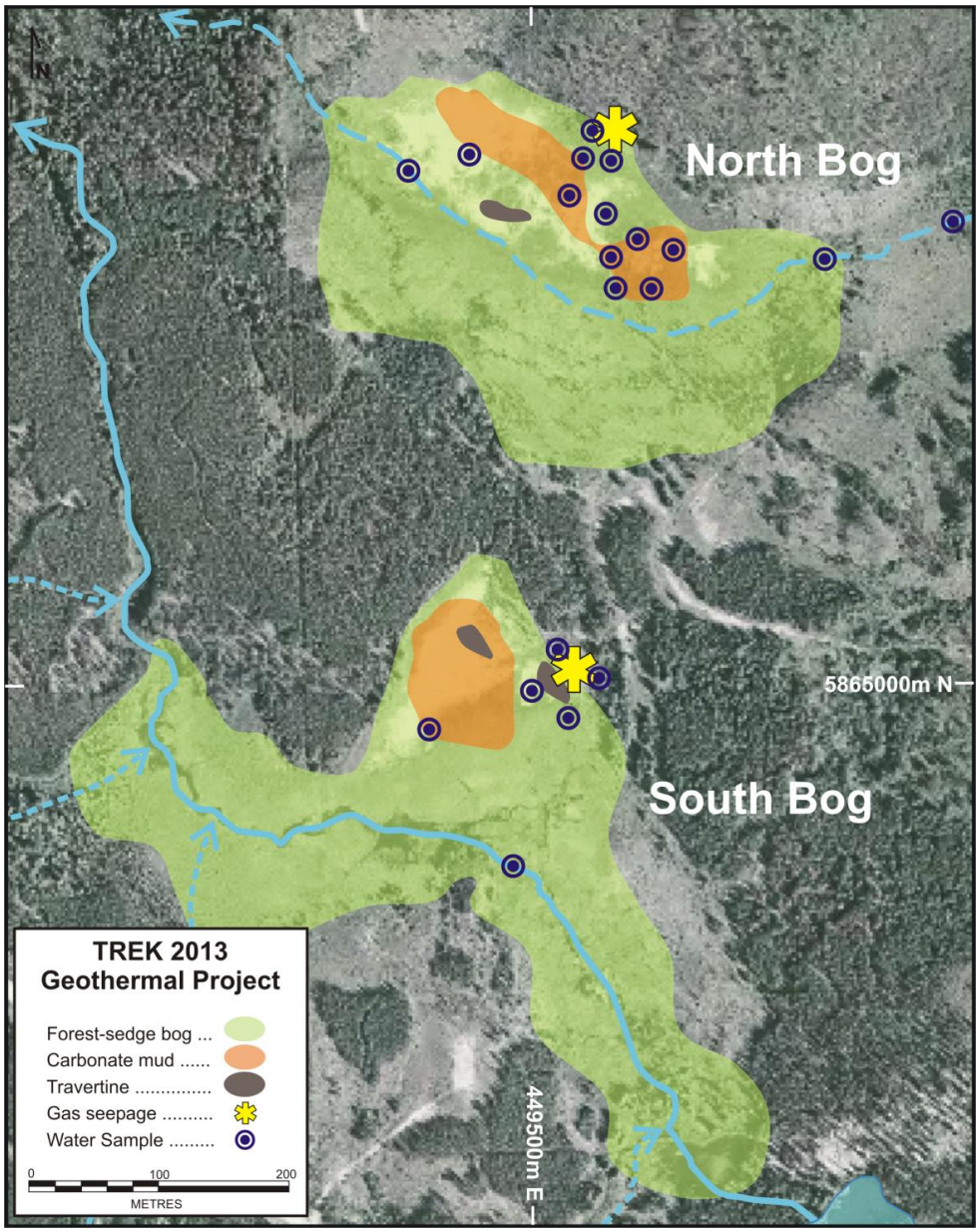

Figure 5 North and South bog surface features and distribution of water samples.

Figure 6 Travertine mound with bubbling carbon dioxide in the North Bog.

Field Work

Field work was carried out over two different periods in 2013. On June 24, 2013 the North and South Bogs were briefly visited, surface water pH, temperature and conductivity were measured and several water samples collected for analysis. Sampling was limited in late June because of high water levels in the wetland. Between July 28th and August 7th a more extensive sampling program was carried out in the two bogs and surrounding area. Field work in the North and South Bogs and surrounding area during July and August completed the following:

- Mapping bog surface features such as gas discharge vents and travertine deposits. Feature location coordinates were captured with a hand held Garmin 60 CX GPS and the area around each feature recorded with a Panasonic DCM-TZ4 camera.
- Sampling ground water from shallow dug pits, springs and gas vents. Samples were either collected with a bailer (Figure 6) from pits after the water had been allowed to settle or with a 30 mL PVC syringe. A sample of gas flowing from the travertine vent was also collected in a 30 mL PVC syringe, the syringe sealed and later discharged into distilled water. Sixty parts per million dissolved carbon dioxide were detected in the water using a Hatch test kit. Water pH, temperature, salinity and conductivity were measured on-site with an Oakton PCSTestr 35 multi meter. Details of the site such as

surface water flow rates, water table depth and presence of discharging carbon dioxide were recorded and are listed in Appendix A.

- Sampling surface water in bog pools, streams flowing into and out of the wetland and from Fishpot Lake using a bottle holder attached to a PVC pole. The sampler avoids disturbing surface carbonate precipitates that commonly formed on bog pool surfaces. Water pH, temperature, salinity and conductivity were measured and site details such as water flow rates, channel width and depth were recorded. Sample site details are recorded in Appendix A. Channel sediment was also collected at several stream sites. A total of 34 water and 6 sediment samples were collected
- Sampling bog and well-drained soil, travertine deposits and bedrock. In the bogs the soil was collected from dug pits or with a Hiller peat auger kindly loaned by Simon Fraser University (Figure 7, 8). A total of 54 soil samples were collected

Figure 7 Ground water sampling with bailer and PVC pipe

Figure 8 Soil sampling using a Hiller auger.

Sample Preparation and Analysis

Three water samples were collected in high-density polyethylene (HDPE) bottles at each site. The samples underwent the following analyses:

- Within 12 hours of collection, one sample was analysed for sodium with a HANNA model pHep pocket meter and total alkalinity and dissolved carbon dioxide were measured with Hach field test kits.
- A second sample was filtered through a Phenex™ polyethersulfone (*PES*) 0.45 micron membrane, and stored at 4°C for later analysis by ALS Global for hardness, total alkalinity, bicarbonate alkalinity and hydroxyl alkalinity by titration and for fluoride, chloride, bromide, nitrate, nitrite and sulphate by ion chromatography.
- A third sample was filtered through a Phenex™ polyethersulfone (*PES*) 0.45 micron membrane, filter, acidified with ultrapure nitric acid to pH 1 and later analysed by ALS Global for aluminium, arsenic, antimony, barium, beryllium, bismuth, boron, cadmium, calcium, cesium, chromium, cobalt, copper, gallium, iron, lead, lithium, manganese, molybdenum, nickel, phosphorus, potassium, rhenium, rubidium selenium, silica, silver,

sodium, strontium, tellurium, thallium, thorium, tin, titanium, uranium, vanadium, yttrium, zinc and zirconium by high resolution mass spectrometry. Four distilled-deionised water sample blanks and three samples of the National Research Council Canada (NRCC) river water standard, SLRS 3, were analysed with the field samples to monitor data accuracy and precision. Water chemistry data is listed in Appendix A.

Sediment and soil samples were dried at below 60°C, sieved to minus 80 mesh (< 0.177 mm). Rock samples were milled to minus 150 mesh. The prepared soil, sediment and rock samples were analysed at Acme Laboratories Ltd. for aluminium, arsenic, antimony, barium, beryllium, bismuth, boron, cadmium, calcium, cesium, chromium, cobalt, copper, gallium, iron, lead, lithium, manganese, mercury, molybdenum, nickel, phosphorus, potassium, rhenium, rubidium selenium, silica, silver, sodium, strontium, tellurium, thallium, thorium, tin, titanium, uranium, vanadium, yttrium, zinc, zirconium by aqua regia digestion and inductively coupled mass spectrometry (ICPMS). The samples were also analysed for major oxides (Al2O3, SiO2, Fe2O3, CaO, MgO, MnO, P2O5), minor elements (Cu, Ba, Zn, Ni, Co, Sr, Zr, Ce, Y, Nb, Sc), by lithium borate – ICPMS; for loss on ignition at 1100°C; carbon and sulphur by Leco combustion and boron by sodium peroxide sinter-ICPMS. Results are listed in Appendix B.

Water Sample Quality Control Data Analysis

Results of analysing four samples of ultrapure water samples and three samples of the National Research Council Canada (NRCC) water standard SLRS 3 analyses provide an estimate of the trace element data reliability (accuracy, precision). These data also indicate any contamination during sample collection in the field. Ultrapure water, supplied by ALS Chemex, was filtered and then acidified with nitric acid within 24 hours after collection to provide blanks. The SLRS 3 standard was kindly provided by the BC Geological Survey. Blanks and the standard were inserted randomly into samples collected in the field. Non-acidified ultrapure water and samples of the water standard SLRS 3 were also analysed for anions to monitor anion data reliability. Water from the bottom of the travertine cone- carbon dioxide vent in the North Bog was first sampled on June 30th, 2013 and then again on July 6th, 2013 to monitor both sampling variability and possible changes in the water chemistry over a time interval. The samples collected in July and August were not analysed for mercury because no mercury was detected the blank water sample, the SLRS 3 standard and the routine water samples collected on June 24th. Also no specific preservation method was used to limit possible mercury loss from the water over the interval between collection and analysis.

Analyte	Detect Limit	Mean Blank	Max Blank	Mean SLRS 3	RSD SLRS 3	SLRS 3*
Hardness	0.5	-0.5	-0.50	20.25	5.24	
Alk - CO_3^{2-}	1	-0.25	2.00	1.000	0.00	
Alk - HCO_3-	1	1.35	3.20	1.000	0.00	
Alk OH^-	1	-1	-1.00	1.000	0.00	
Alk-total	1	2.1	3.20	1.000	0.00	
Ag_ppb	0.005	-0.005	-0.01	0.005	0.00	
Al-ppb	1.000	-1	-1.00	32.80	0.92	31
As_ppb	0.050	-0.05	-0.05	0.829	2.42	0.72
B_ppb	5.000	-5	-5.00	9.467	8.54	
Ba_ppb	0.100	-0.1	-0.10	14.170	1.78	13.4
Be_ppb	0.005	-0.005	-0.01	0.011	21.65	0.005
Bi_ppb	0.050	-0.05	-0.05	0.050	0.00	
Br_ppm	0.050	-0.05	-0.05	2.500	0.00	
Ca_ppm	0.050	0.009	0.08	5.660	5.48	6
Cd_ppb	0.005	-0.005	-0.01	0.016	12.54	0.013
Cl_ppm	0.500	-0.5	-0.50	25.000	0.00	
Co_ppm	0.050	-0.05	-0.05	0.050	0.00	0.027
Cr_ppb	0.500	-0.5	-0.50	0.500	0.00	0.3
Cs_ppb	0.005	-0.005	-0.01	0.007	20.66	
Cu_ppb	0.500	-0.275	-0.20	1.510	1.75	1.35
F_ppm	0.020	-0.02	-0.02	1.000	0.00	
Fe_ppb	30.000	-30	-30	100	5.00	100
Ga_ppb	0.050	-0.05	-0.05	0.050	0.00	
Hg_ppb	0.050	-0.05	-0.05	0.050		
K_ppm	2.000	-2	-2	2.0	0.00	0.7
Li_ppb	0.200	-0.08	0.29	0.620	28.89	
Mg_ppm	0.100	-0.1	-0.10	1.620	6.64	1.6
Mn_ppb	0.200	-0.2	-0.20	4.070	3.40	3.9
Mo_ppb	0.050	-0.05	-0.05	0.230	1.68	0.19
Na_ppm	2.000	-2	-2	2.7	11.46	2.3
Ni_ppb	0.200	-0.2	-0.20	0.860	4.19	0.83
NO_2 ppm	0.001	-0.001	0.00	0.050	0.00	
NO_3 ppm	0.005	-0.005	-0.01	392	0.36	
P_ppm	0.300	-0.3	-0.30	0.300	0.00	
Pb_ppb	0.050	-0.05	-0.05	0.074	6.64	0.068
Rb_ppb	0.020	-0.02	-0.02	1.720	2.10	
Re_ppb	0.005	-0.005	-0.01	0.005	0.00	
Sb_ppb	0.010	-0.01	-0.01	0.169	0.91	0.12
Se_ppb	0.200	-0.2	-0.20	0.200	0.00	
Si_ppm	0.050	-0.05	-0.05	1.690	4.14	
Sn_ppb	0.200	-0.2	-0.20	0.200	0.00	
SO_4 ppm	0.500	-0.5	-0.50	25.000	0.00	
Sr_ppm	0.220	0.06	0.22	0.033	4.30	0.028
Te_ppb	0.010	-0.01	-0.01	0.010	0.00	
Th_ppb	0.005	-0.005	-0.01	0.014	4.03	
Ti_ppb	0.200	-0.2	-0.20	0.700	5.71	
Tl_ppb	0.002	-0.002	0.00	0.008	27.71	
U_ppb	0.002	-0.002	0.00	0.043	7.07	0.045
V_ppb	0.050	-0.05	-0.05	0.325	1.92	0.3
W_ppb	0.010	-0.01	-0.01	0.010	0.00	
Y_ppb	0.005	-0.005	-0.01	0.129	2.50	
Zn_ppb	1.000	-1	-1	1.53	7.53	1.04
Zr_ppb	0.050	-0.05	-0.05	0.081	6.24	

Table 1. Analytical detection limits, quadruple blank and results of National Research Council Canada river water standard SLRS 3 triplicate analysis. SLRS 3* - NRC recommended values. Alkalinity is in mg $CaCO_3$ L^{-1}

Analyte	201393B1013	201393B1038	Mean	RSD %
pH_field	6.48	6.37	6.4	1.2
Temp_field	5.6	5.9	5.8	3.7
Cond_us_field	3420	3580	3500	3.2
Na_ppm_field	190	160	175	12.1
Salinity_ppm_field	2460	1740	2100	24.2
TDS_ppm_field	1690	2520	2105	27.9
Alkalinity_total_field	2400	2200	2300	6.1
CO_2 _ppm_field	400	600	500	28.3
Hardness_ppm_lab	1490	1570	1530	3.7
Alk - HCO_3^-–Lab	2360	2410	2385	1.5
Alkalinity_total_Lab	2360	2410	2385	1.5
F_ppm	0.48	0.45	0.47	4.6
SO_4 ppm	18	18	18.0	0.0
Sb_ppb	0.055	0.039	0.047	24.1
As_ppb	2.02	2.5600	2.29	16.7
Ba_ppb	174	187	180.5	5.1
Be_ppb	0.04	0.044	0.042	6.7
B_ppb	380	343	362	7.2
Cd_ppb	0.0916	0.0376	0.0646	59.1
Ca_ppm	231	235	233	1.2
Cs_ppb	1.77	1.73	1.75	1.6
Co_ppm	2.230	2.240	2.235	0.3
Fe_ppb	446	3920	2183	112.5
Li_ppb	342	323	333	4.0
Mg_ppm	221	239	230	5.5
Mn_ppb	197	193	195	1.5
Mo_ppb	0.574	0.459	0.517	15.7
Ni_ppb	43.8	44	43.9	0.3
K_ppm	31.1	31.5	31.3	0.9
Re_ppb	0.0069	0.0064	0.0067	5.3
Rb_ppb	39.6	39.3	39.5	0.5
Si_ppm	9.75	9.63	9.69	0.9
Na_ppm	298	307	303	2.1
Sr_ppm	7.53	7.68	7.61	1.4
Tl_ppb	0.335	0.323	0.329	2.6
Ti_ppb	0.35	0.23	0.29	29.3
U_ppb	0.113	0.12	0.117	4.2
V_ppb	1.23	1.08	1.16	9.2
Y_ppb	0.27	0.358	0.314	19.8
Zn_ppb	11.2	10.5	10.9	4.6
Zr_ppb	2.43	1.73	2.08	23.8

Table 2. Analyses of water sample 201393B 1013 and 1038 from the travertine cone-CO_2 vent site . SLRS 3* - NRC recommended values. Alkalinity CO_3^{2-} , alkalinity OH^-, Ag, Al, Br, Cl, NO3, NO2, Bi, Cr, Cu, P, Pb, Te, Th, Sn and W are not reported because all values are below detection limit. Alkalinity in mg $CaCO_3$ L^{-1}

Table 1 lists element detection limits, the mean of the four blank water sample analyses and the maximum concentration detected in the blank. Also listed is the mean measured value for water standard SLRS 3, the percent relative standard deviation (%RSD) calculated from two SLRS 3 analyses and an element value for the SLRS 3 standard if reported by NRCC. Analyses of the filtered water blanks reveal that while lithium, strontium and calcium are detectable in the blanks their concentrations are less than twice the detection limit. Only %RSD values for beryllium, cadmium, cesium, lithium, sodium and thallium in the water standard SLRS 3 are more that 10 percent. The higher variability for these elements largely reflects their concentration close to detection limit in the standard. Where there is an NRCC recommended value for an element in the standard SLRS 3, it is within 10 percent of the recommended value.

A comparison of the chemistry of the water sampled from the bottom of the travertine-carbon dioxide vent in Table 2 reveals that most elements differ very little in their concentrations measured on June 30th and July 6th. Antimony, arsenic, cadmium, iron, molybdenum, titanium, yttrium and zirconium do have relative standard deviations (RSD) that are more than 10 percent, but except for iron (RSD 112%) and cadmium (RSD 59%) values for the other elements are less than 30 percent. Good precision (< 5% RSD) for the travertine-carbon dioxide vent water pH, temperature, and conductivity suggest that field measurements are very reliable and there no variation in the water chemistry over a one week interval.

Soil Sample Quality Control Data Analysis

Trace, minor and major element analysis of a quartz blank, standards and duplicate samples inserted randomly with the soil samples generated quality control data. These data monitored accuracy and precision of results reported by the laboratory and any contamination of the soil during preparation. The blank sample was created from high purity silica and the standards were an internal TREK project till analysed in duplicate and CANMET Till 1 analysed once. Table 3 shows that barium, cerium, copper, manganese, lead, nickel, strontium, yttrium, zinc and zirconium by aqua regia digestion-ICPMS are above detection limit in the silica blank and of these elements only copper and lead are significantly higher than a 0.01 ppm, but still below 1 ppm. Table 3 also reveals that the percent relative standard deviation (% RSD) calculated from first and second TREK till duplicate determination is less than 12 percent for most elements by aqua regia-ICPMS and only exceeds 10 percent for beryllium, tellurium and uranium. Element means calculated from duplicate TREK standard analyses are close to a recommended value. The CANMET TILL 1 standard was only analysed once, but the results are within 10 percent of recommended values for elements determined by CANMET in a digestion similar an aqua regia.

Analyte	IDL	Qtz. Blank	Mean TREK Std.	% RSD	TREK Std. Rec.	CANMET TILL	CANMET TILL 1 Rec.
Ag_ppb	2	-2	79.50	9.78	95.00	250	200
Al_pct	0.01	-0.01	1.93	1.10	1.99	1.72	
As_ppm	0.1	-0.1	7.40	1.91	7.30	17.9	13
Au_ppb	0.2	-0.2	7.20	1.96	11.03	14	13
B_ppm	20	-20	20.00	0.00	-20.00	-20	
Ba_ppm	0.5	2.5	51.60	1.37	50.90	85.5	
Be_ppm	0.1	-0.1	0.45	15.71	0.43	0.3	
Bi_ppm	0.02	-0.02	0.18	7.86	0.20	1.98	-3
Ca_pct	0.01	0.02	0.22	3.29	0.22	0.29	
Cd_ppm	0.01	-0.01	0.09	8.32	0.10	0.18	-0.2
Ce_ppm	0.1	0.9	45.55	2.02	49.81	47.2	
Co_ppm	0.1	0.1	14.35	0.49	14.99	13.5	12
Cr_ppm	0.5	-0.5	46.65	1.67	47.00	28.6	30
Cs_ppm	0.02	-0.02	1.06	3.35	0.98	0.61	
Cu_ppm	0.01	0.36	68.82	4.98	71.50	49.29	48
Fe_%	0.01	0.02	3.59	0.39	3.69	3.18	3.1
Ga_ppm	0.1	-0.1	5.05	4.20	5.21	6.4	
Ge_ppm	0.1	-0.1	0.10	0.00	-0.03	-0.1	
Hf_ppm	0.02	-0.02	0.02	0.00	-0.01	-0.02	
Hg_ppb	5	-5	59.00	2.40	60.00	102	92
In_ppm	0.02	-0.02	0.02	0.00	0.00	0.05	
K_pct	0.01	-0.01	0.10	7.44	0.10	0.05	
La_ppm	0.5	-0.5	18.10	1.56	20.11	16.5	
Li_ppm	0.1	0.1	27.90	7.60	30.49	10	
Mg_pct	0.01	-0.01	0.84	0.85	0.85	0.56	
Mn_ppm	1	2	305.00	6.03	335.71	1147	950
Mo_ppm	0.01	0.05	0.725	4.88	0.79	0.7	-2
Na_pct	0.001	0.003	0.01	8.32	0.00	0.03	
Nb_ppm	0.02	0.02	0.16	8.84	0.25	0.73	
Ni_ppm	0.1	0.5	36.85	5.95	38.76	18.4	18
P_pct	0.001	0.001	0.07	7.56	0.07	0.082	
Pb_ppm	0.01	0.57	9.53	1.86	9.80	13.83	12
Pd_ppb	10	-10	10.00	0.00	-10.00	-10	
Pt_ppb	2	-2	2.00	0.00	0.14	-2	
Rb_ppm	0.1	0.1	10.90	5.19	11.30	6	
Re_ppm	1	-1	1.00	0.00	-1.00	-1	
S_pct	0.02	-0.02	0.02	0.00	-0.02	0.02	
Sb_ppm	0.02	-0.02	0.32	6.73	0.25	5.62	
Sc_ppm	0.1	-0.1	4.30	3.29	4.27	4.6	
Se_ppm	0.1	-0.1	0.30	0.00	0.24	0.3	
Sn_ppm	0.1	-0.1	0.20	0.00	0.21	1	
Sr_ppm	0.5	2.2	21.90	0.65	21.87	10.9	
Ta_ppm	0.05	-0.05	0.05	0.00	-0.05	-0.05	
Te_ppm	0.02	-0.02	0.07	10.88	0.06	-0.02	
Th_ppm	0.1	0.1	6.10	2.32	6.51	2.6	5.6
Ti_pct	0.001	-0.001	0.05	1.37	0.06	0.069	
Tl_ppm	0.02	-0.02	0.09	0.00	0.09	0.1	
U_ppm	0.1	-0.1	0.55	12.86	0.59	0.7	2.2
V_ppm	2	-2	51.50	1.37	50.43	57	48
W_ppm	0.1	-0.1	0.10	0.00	0.09	0.1	
Y_ppm	0.01	0.71	4.96	5.85	5.12	13.01	
Zn_ppm	0.1	1.9	73.85	1.82	74.34	68.2	70
Zr_ppm	0.1	0.5	0.85	8.32	0.94	0.8	

Table 3. Aqua regia - ICPMS analysis of a quartz blank, duplicate internal TREK standard mean, percent RSD of the standard TREK duplicates, recommended TREK standard values (TREK Std. Rec.), CANMET TILL 1 standard value and CANMET recommended values (CANMET till rec.). IDL = instrument detection limit.

Analyte	IDL	Qtz. Blank	Mean TREK Std.	% RSD	CANMET TILL 1 Std.	CANMET Till 1Rec.
SiO2_pct	0.01	97.38	62.53	0.63	60.84	60.9
Al2O3_pct	0.01	0.06	16.03	0.31	13.42	13.7
Fe2O3_pct	0.04	-0.04	6.71	0.21	6.87	6.82
MgO_pct	0.01	-0.01	2.16	0.33	2.15	2.15
CaO_pct	0.01	0.04	1.23	0.00	2.65	2.72
Na2O_pct	0.01	0.01	1.72	0.41	2.76	2.71
K2O_pct	0.01	0.01	2.80	0.51	2.07	2.22
TiO2_pct	0.01	0.02	0.90	0.00	0.96	0.98
P2O5_pct	0.01	-0.01	0.18	7.86	0.21	0.22
MnO_pct	0.01	-0.01	0.07	0.00	0.19	0.18
Cr2O3_pct	0.002	-0.002	0.02	10.88	0.01	
Cu_ppm	5	-5	78.50	0.90	52	47
Ba_ppm	5	-5	611.00	0.69	667	702
Zn_ppm	5	-5	79.00	1.79	82	98
Ni_ppm	20	-20	40.50	5.24	26	24
Co_ppm	20	-20	-20.00	0.00	-20	18
Sr_ppm	2	5	219.00	0.00	296	291
Zr_ppm	5	79	385.00	4.04	513	502
Ce_ppm	30	-30	122.00	1.16	83	71
Y_ppm	3	-3	34.50	2.05	32	38
Nb_ppm	5	-5	20.00	35.36	14	10
Sc_ppm	1	-1	16.50	4.29	13	13
LOI_pct	-5.1	2.3	5.40	7.86	7.6	7.3
SUM_pct	0.01	99.93	99.88	0.00	99.92	
Total C_pct	0.02	-0.02	0.40	12.53	1.87	
Total S_pct	0.02	-0.02	-0.02	0.00	-0.02	
B_ppm_Na2O2	3	9		9.72	103	

Table 4. Lithium metaborate fusion - ICPES analysis of a quartz blank, duplicate internal TREK standard mean, percent RSD, recommended TREK standard values (TREK Std. Rec.), CANMET TILL 1 standard value and CANMET recommended values (CANMET till rec.). IDL = instrument detection limit.

Analyte	01 - 19 M	01 - 19 % RSD	20- 19 M	20 - 19 % RSD	41 - 52 M	41 - 52 % RSD	52- 53 M	52 - 53 % RSD
Ag_ppb	83.86	6.7	6.50	10.9	49.00	2.9	40.50	26.2
Al_pct	1.19	0.0	0.02	0.0	0.06	0.0	0.06	0.0
As_ppm	6.31	0.0	0.10	0.0	0.10	0.0	0.10	0.0
Au_ppb	6.66	31.8	0.20	0.0	0.25	28.3	0.25	28.3
B_ppm	5.29	53.5	52.00	24.5	20.00	0.0	20.00	0.0
Ba_ppm	43.59	1.3	115.05	3.4	122.95	6.0	127.90	0.3
Be_ppm	5.61	0.0	0.10	0.0	0.10	0.0	0.10	0.0
Bi_ppm	2.33	7.3	0.02	0.0	0.06	90.0	0.02	0.0
Ca_pct	3.43	7.6	17.29	19.2	23.81	0.2	24.01	1.0
Cd_ppm	2.54	0.6	0.02	70.7	0.23	22.0	0.28	7.7
Ce_ppm	21.24	0.3	0.20	0.0	0.55	12.9	0.65	10.9
Co_ppm	7.02	0.0	0.10	0.0	0.35	20.2	0.40	35.4
Cr_ppm	19.77	0.0	0.95	22.3	2.00	7.1	2.20	6.4
Cs_ppm	1.57	0.5	0.22	6.4	0.14	10.1	0.17	12.9
Cu_ppm	32.00	1.0	1.80	55.0	5.02	1.6	4.70	11.1
Fe_%	1.88	0.4	0.52	6.9	0.10	0.0	0.09	15.7
Ga_ppm	3.87	0.0	0.10	0.0	0.10	0.0	0.10	0.0
Ge_ppm	0.01	693.0	0.25	28.3	0.60	0.0	0.45	47.1
Hf_ppm	0.00	0.0	0.02	0.0	0.26	8.3	0.20	49.5
Hg_ppb	43.53	27.6	8.00	53.0	71.50	20.8	54.50	16.9
In_ppm	0.01	0.0	0.02	0.0	0.02	0.0	0.02	0.0
K_pct	2.61	0.0	0.02	0.0	0.02	0.0	0.02	47.1
La_ppm	8.47	0.0	0.50	0.0	0.50	0.0	0.50	0.0
Li_ppm	13.15	1.1	3.20	8.8	1.95	3.6	2.05	3.4
Mg_pct	0.73	1.0	0.77	2.8	0.67	4.2	0.64	3.3
Mn_ppm	384.83	0.7	390.50	31.3	83.00	6.8	134.00	49.6
Mo_ppm	1.70	1.7	1.10	64.3	0.10	7.4	0.08	35.4
Na_pct	2.90	0.0	0.18	14.5	0.05	2.9	0.04	29.0
Nb_ppm	3.22	0.0	0.07	32.6	0.24	3.0	0.18	39.3
Ni_ppm	16.40	1.3	2.35	33.1	147.70	2.4	128.65	18.2
P_pct	2.64	0.0	0.03	20.9	0.02	0.0	0.02	3.4
Pb_ppm	6.28	0.8	0.30	23.6	0.26	5.4	0.28	15.2
Pd_ppb	0.00	0.0	10.00	0.0	11.50	18.4	11.50	18.4
Pt_ppb	0.31	0.0	2.00	0.0	2.00	0.0	2.50	28.3
Rb_ppm	5.96	0.0	0.35	20.2	0.35	20.2	0.40	0.0
Re_ppm	0.43	165.0	2.50	28.3	1.00	0.0	1.00	0.0
S_pct	0.13	21.1	0.78	19.2	0.12	0.0	0.11	20.2
Sb_ppm	3.22	0.7	0.07	20.2	0.09	15.7	0.08	47.1
Sc_ppm	3.06	2.3	0.15	47.1	2.05	3.4	2.10	0.0
Se_ppm	0.61	35.0	2.90	39.0	0.65	10.9	0.45	47.1
Sn_ppm	0.22	0.0	0.10	0.0	0.10	0.0	0.10	0.0
Sr_ppm	507.65	25.2	3521.55	8.2	3579.90	7.2	3752.70	0.3
Ta_ppm	0.00	0.0	0.05	0.0	0.05	0.0	0.05	0.0
Te_ppm	3.79	3.5	0.42	18.7	0.22	51.4	0.28	12.9
Th_ppm	3.33	0.0	0.10	0.0	0.10	0.0	0.10	0.0
Ti_pct	0.50	0.0	0.00	47.1	0.01	0.0	0.01	10.9
Tl_ppm	0.04	0.0	0.02	0.0	0.04	0.0	0.04	0.0
U_ppm	4.41	0.0	0.10	0.0	0.10	0.0	0.10	0.0
V_ppm	27.49	0.0	7.00	40.4	2.00	0.0	2.00	0.0
W_ppm	0.06	0.0	0.10	0.0	0.10	0.0	0.10	0.0
Y_ppm	5.39	0.5	0.13	43.5	0.99	7.1	1.11	8.3
Zn_ppm	41.57	2.0	32.85	37.7	3.05	16.2	3.70	11.5
Zr_ppm	3.35	0.0	0.55	38.6	18.75	3.4	15.10	38.4

Table 5. Results of aqua regia - ICPMS analysis of analytical duplicates (01 :19; 41: 52) and field duplicate (19:20; 52:53). The table lists mean and percent relative standard deviation (%RSD) of the duplicate values. Full sample numbers are 139001, 129019, 139041, 139020, 139052 and 139053.

Sample No.	01 - 19 M	01 - 19 %RSD	20- 19 M	20 - 19 %RSD	41 - 52 M	41 - 52 %RSD	52- 53 M	52 - 53 %RSD
SiO2_pct	26.63	0.4	0.26	43.5	1.66	3.8	2.11	27.5
Al2O3_pct	6.29	0.0	0.09	25.0	0.32	4.4	0.41	26.2
Fe2O3_pct	3.10	0.7	0.88	12.1	0.19	3.8	0.21	17.2
MgO_pct	1.23	1.1	1.40	6.1	1.22	6.4	1.26	1.7
CaO_pct	4.27	10.3	28.25	27.9	36.64	0.2	37.99	5.2
Na2O_pct	1.20	0.0	0.22	6.4	0.12	6.1	0.14	15.7
K2O_pct	1.19	0.0	0.03	28.3	0.05	15.7	0.06	47.1
TiO2_pct	0.41	0.0	0.01	0.0	0.03	0.0	0.03	0.0
P2O5_pct	2.81	0.0	0.08	17.7	0.07	20.2	0.06	47.1
MnO_pct	0.07	10.5	0.06	38.6	0.01	0.0	0.02	47.1
Cr2O3_pct	4.38	0.0	0.00	0.0	0.00	0.0	0.00	0.0
Cu_ppm	27.34	25.9	13.00	87.0	15.00	66.0	14.50	73.1
Ba_ppm	299.70	0.5	124.50	16.5	125.00	6.8	135.00	4.2
Zn_ppm	44.39	0.0	43.00	9.9	25.00	113.1	25.00	113.1
Ni_ppm	12.18	0.0	-20.00	0.0	144.50	11.3	133.00	24.5
Co_ppm	-0.29	0.0	-20.00	0.0	20.00	0.0	20.00	0.0
Sr_ppm	608.57	8.0	3840.50	16.8	3606.00	3.5	3793.00	3.7
Zr_ppm	202.90	0.0	-5.00	0.0	36.00	3.9	32.50	19.6
Ce_ppm	35.74	0.0	-30.00	0.0	30.00	0.0	30.00	0.0
Y_ppm	15.31	0.0	-3.00	0.0	3.00	0.0	3.00	0.0
Nb_ppm	18.78	0.0	-5.00	0.0	5.00	0.0	5.00	0.0
Sc_ppm	7.51	0.0	-1.00	0.0	1.00	0.0	1.00	0.0
LOI_pct_IG	15.67	2.3	67.05	9.4	59.25	0.1	57.25	4.8
SUM_pct	49.55	0.1	98.79	1.7	99.98	0.0	99.98	0.0
C_pct_LECO	10.55	1.8	27.62	17.3	22.04	1.0	21.05	5.6
S_pct_LECO	0.15	53.6	0.67	19.0	0.04	0.0	0.04	20.2
B_ppm	43.22	21.3	77.00	5.5	18.50	11.5	14.50	24.4

Table 6. Results of Lithium metaborate fusion - ICPES analysis of analytical duplicates (01 :19; 41: 52) and field duplicate (19:20; 52:53). The table lists mean (M) and percent relative standard deviation (%RSD) of the duplicate values. Loss on ignition (LOI) at 550°C, total carbon and sulphur by Leco combustion _IR detection, Boron by sodium peroxide fusion-ICPMS. M = mean of duplicate values. Full sample numbers are 139001, 129019, 139041, 139020, 139052 and 139053.

Table 4 lists the result of analysing the quartz blank, the TREK standard in duplicate and CANMET TILL 1 for major oxides and minor elements by lithium metaborated - ICPES, LOI at 550°C, carbon and sulphur by Leco combustion and boron by sodium peroxide sinter-ICPMS. Only significant zirconium (79 ppm) was detected in the silica blank and only chromium (as Cr2O3), niobium and carbon have % RSD values more than 10 percent. These higher % RSD values reflect concentration of the minor elements in the TREK standard close to their instrumental detection limit. Table 4 also shows that major and minor element accuracy is

within 5 percent of the CANMET TILL 1 recommended values, but there are larger differences between reported and recommended minor element values, notably for barium and zirconium.

Table 5 and 6 list element means (M) and percent relative standard deviations (% RSD) for the analytical duplicate sample pairs (139001, 139019 and 139041, 1939052) and field duplicate sample pairs (139019, 139020 and 139052, 1939053). Each analytical duplicate samples pair is a routine sample split after preparation and inserted in to the sample sequence before analysis whereas a field duplicate sample pair represents two samples collected at the same sample site. Most element % RSD values for the analytical replicates are less than 10 percent. Exceptions are gold, boron, germanium, mercury, rhenium, selenium, strontium and sulphur in the 139001, 139019 duplicate pair and gold bismuth, cadmium, cobalt, mercury, palladium, rubidium, scandium. tellurium, zinc and potassium oxide in the 139041, 1939052 duplicate pair. More of the elements have larger % RSD values in the field duplicates and the variation appears greatest for trace elements (e.g. Cd, Co, Cu, Cr, Hg, Pb, Zn) rather than minor elements (e.g. Ba, Sr) and major oxides. Some of the variation may be caused by the small size of the field duplicate taken sampled with an auger or a large median grain size of material.

Tables 7 and 8 list instrument detection limits (IDL), element means (M) and percent relative standard deviations (% RSD) for one duplicate rock sample pairs (138002 and 138019), a quartz (SiO2) blank and reported values for CANMET standard STSD 1. Only strontium and barium are detectable above 1 ppm in the blank and values for both elements are less than 3 ppm. The % RSD values for most elements and oxides in the rock sample duplicate are less than 10 percent and those with large % RSD values have levels close to detection limit. Recommended CANMET values generally compare well with those reported by the laboratory analysis except for zirconium that has a CANMET recommended value of 502 ppm, a reported aqua regia-ICPMS analysis of 1 ppm and a reported lithium metaborate-ICPES value of 521 ppm.

Analyte	IDL	138002	138009	Mean	%RSD	SiO2	CANMET STSD 1	CANMET STSD 1 Rec.
Ag_ppb	2	4	3	3.5	20.2	4	229	200
Al_pct	0.01	-0.01	-0.01	-0.01	0.0	-0.01	1.69	
As_ppm	0.1	-0.1	0.2	0.05	424.3	0.4	16.1	13
Au_ppb	0.2	0.6	-0.2	0.2	282.8	-0.2	12.6	18
B_ppm	20	-20	21	0.5	5798.3	-20	-20	
Ba_ppm	0.5	297.3	304.7	301	1.7	2.7	83.6	84
Be_ppm	0.1	-0.1	-0.1	-0.1	0.0	-0.1	0.6	
Bi_ppm	0.02	-0.02	-0.02	-0.02	0.0	-0.02	1.93	-5
Ca_pct	0.01	35.92	32.04	33.98	8.1	0.02	0.28	
Cd_ppm	0.01	0.02	-0.01	0.005	424.3	-0.01	0.2	
Ce_ppm	0.1	-0.1	-0.1	-0.1	0.0	1	50.1	71
Co_ppm	0.1	0.7	-0.1	0.3	188.6	-0.1	11.6	12
Cr_ppm	0.5	0.8	-0.5	0.15	612.8	-0.5	23.5	30
Cs_ppm	0.02	-0.02	-0.02	-0.02	0.0	-0.02	0.51	1
Cu_ppm	0.01	0.41	0.28	0.345	26.6	0.41	45.34	48
Fe_%	0.01	0.03	0.04	0.035	20.2	0.01	3.16	3.1
Ga_ppm	0.1	-0.1	-0.1	-0.1	0.0	-0.1	5.5	
Ge_ppm	0.1	-0.1	-0.1	-0.1	0.0	-0.1	-0.1	
Hf_ppm	0.02	-0.02	-0.02	-0.02	0.0	-0.02	-0.02	13
Hg_ppb	5	-5	-5	-5	0.0	-5	94	92
In_ppm	0.02	-0.02	-0.02	-0.02	0.0	-0.02	0.05	
K_pct	0.01	0.01	-0.01	0	0.0	-0.01	0.05	
La_ppm	0.5	-0.5	-0.5	-0.5	0.0	-0.5	17.7	28
Li_ppm	0.1	5.3	5.3	5.3	0.0	0.1	8	15
Mg_pct	0.01	0.73	0.62	0.675	11.5	-0.01	0.54	
Mn_ppm	1	216	214	215	0.7	2	1069	950
Mo_ppm	0.01	0.02	-0.01	0.005	424.3	0.03	0.61	-2
Na_pct	0.001	0.148	0.129	0.1385	9.7	0.005	0.026	
Nb_ppm	0.02	-0.02	-0.02	-0.02	0.0	-0.02	0.83	10
Ni_ppm	0.1	2.3	1.1	1.7	49.9	0.5	16.1	18
P_pct	0.001	0.009	0.009	0.009	0.0	-0.001	0.082	
Pb_ppm	0.01	3.26	0.98	2.12	76.0	0.64	14.25	12
Rb_ppm	0.1	0.1	-0.1	0	0.0	-0.1	5.1	44
S_pct	0.02	0.05	0.05	0.05	0.0	-0.02	0.02	-0.05
Sb_ppm	0.02	0.04	-0.02	0.01	424.3	-0.02	4.18	7.8
Sc_ppm	0.1	0.3	0.2	0.25	28.3	-0.1	4	13
Se_ppm	0.1	0.2	-0.1	0.05	424.3	-0.1	-0.1	
Sr_ppm	0.5	10000	10000	10000	0.0	2.5	10.3	291
Ta_ppm	0.05	-0.05	-0.05	-0.05	0.0	-0.05	-0.05	0.7
Te_ppm	0.02	-0.02	1.41	0.695	145.5	0.04	-0.02	
Th_ppm	0.1	-0.1	-0.1	-0.1	0.0	0.2	2.1	5.6
Ti_pct	0.001	-0.001	-0.001	-0.001	0.0	-0.001	0.065	
Tl_ppm	0.02	-0.02	-0.02	-0.02	0.0	-0.02	0.09	
U_ppm	0.1	-0.1	-0.1	-0.1	0.0	-0.1	0.8	2.2
V_ppm	2	-2	-2	-2	0.0	-2	51	48
Y_ppm	0.01	0.07	0.03	0.05	56.6	0.81	11.35	38
Zn_ppm	0.1	1.1	1.1	1.1	0.0	1	57.9	70
Zr_ppm	0.1	0.5	0.4	0.45	15.7	0.6	1	502

Table 7. Aqua regia - ICPMS analysis of a quartz blank, duplicate rock samples, percent RSD duplicates, CANMET standard STSD 1 and CANMET recommended values (CANMET STSD Rec.). IDL = instrument detection limit.

Analyte	IDL	138002	138009	Mean	%RSD	SiO2	CANMET STSD 1	CANMET STSD 1 Rec.
SiO2_pct	0.01	0.03	0.04	0.035	20.2	98.77	60.46	60.9
Al2O3_pct	0.01	-0.01	-0.01	-0.01	0.0	0.06	13.75	13.7
Fe2O3_pct	0.04	-0.04	0.07	0.015	518.5	0.12	6.9	6.82
MgO_pct	0.01	1.18	1.18	1.18	0.0	0.04	2.16	2.15
CaO_pct	0.01	50.3	50.67	50.485	0.5	0.05	2.64	2.72
Na2O_pct	0.01	0.15	0.16	0.155	4.6	0.01	2.87	2.71
K2O_pct	0.01	-0.01	0.02	0.005	424.3	0.01	2.27	2.22
TiO2_pct	0.01	-0.01	-0.01	-0.01	0.0	0.02	0.97	0.98
P2O5_pct	0.01	0.02	0.02	0.02	0.0	0.03	0.22	0.22
MnO_pct	0.01	0.03	0.03	0.03	0.0	-0.01	0.19	0.18
Cr2O3_pct	0.002	-0.002	0.003	0.0005	707.1	-0.002	0.01	
Cu_ppm	5	-5	-5	-5	0.0	-5	46	47
Ba_ppm	5	324	323	323.5	0.2	-5	679	702
Zn_ppm	5	-5	-5	-5	0.0	-5	86	98
Ni_ppm	20	-20	-20	-20	0.0	-20	-20	24
Co_ppm	20	-20	-20	-20	0.0	-20	24	18
Sr_ppm	2	14304	14147	14225.5	0.8	6	304	291
Zr_ppm	5	-5	-5	-5	0.0	82	521	502
Ce_ppm	30	-30	-30	-30	0.0	-30	83	71
Y_ppm	3	-3	-3	-3	0.0	-3	34	38
Nb_ppm	5	-5	-5	-5	0.0	-5	9	10
Sc_ppm	1	-1	-1	-1	0.0	-1	13	13
LOI_pct_IG	-5.1	46.5	46.1	46.3	0.6	0.8	7.3	7.3
SUM_pct	0.01	99.99	99.97	99.98	0.0	99.96	99.94	
C_pct_LECO	0.02	13.28	13.19	13.235	0.5	-0.02	2.01	
S_pct_LECO	0.02	0.02	0.02	0.02	0.0	-0.02	0.02	
B_ppm_Na2O2	3	13	18	15.5	22.8	7	104	

Table 8. Results of Lithium metaborate fusion - ICPES analysis of a duplicates rock sample, quartz blank (SiO2) and CANMET standard STSD 1. The table lists mean (M) and percent relative standard deviation (%RSD) of the duplicate values. Loss on ignition (LOI) at 1100°C, total carbon and sulphur by Leco combustion _IR detection, Boron by sodium peroxide fusion-ICPMS.

Ground and Surface Water geochemistry

Figures 9 and 10 are box plots that compare range (maximum, minimum), median and third quartile statistics for elements, anions and parameters measured in ground water and surface (combined bog and stream), water samples. Because graph log scale cannot clearly display median pH, the pH range and temperature statistics these are listed below:

Ground water median pH 6.53, Range = 5.85-7.03. Median Temp. 13.5^{o}C, Range = 5.6-15.3^{o}C

Surface water median pH 7.76, Range = 6.58-9.06. Median Temp. 14.5^{o}C, Range = 7.2-23°C

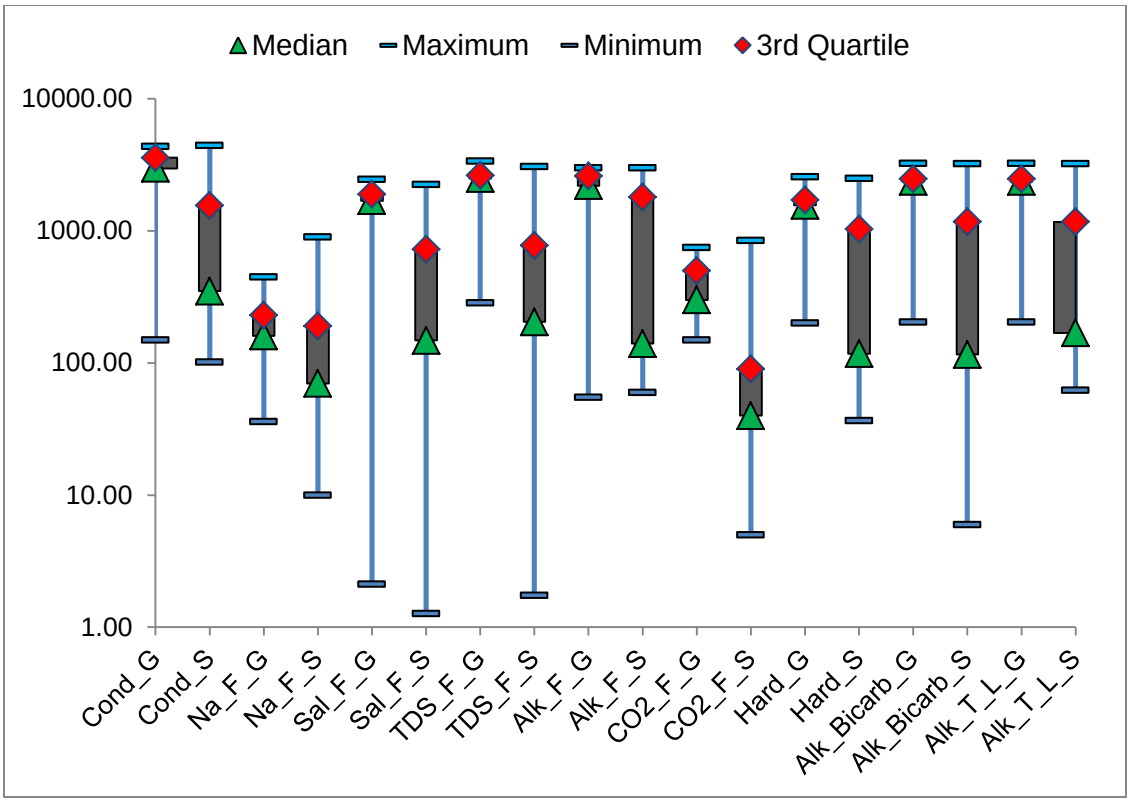

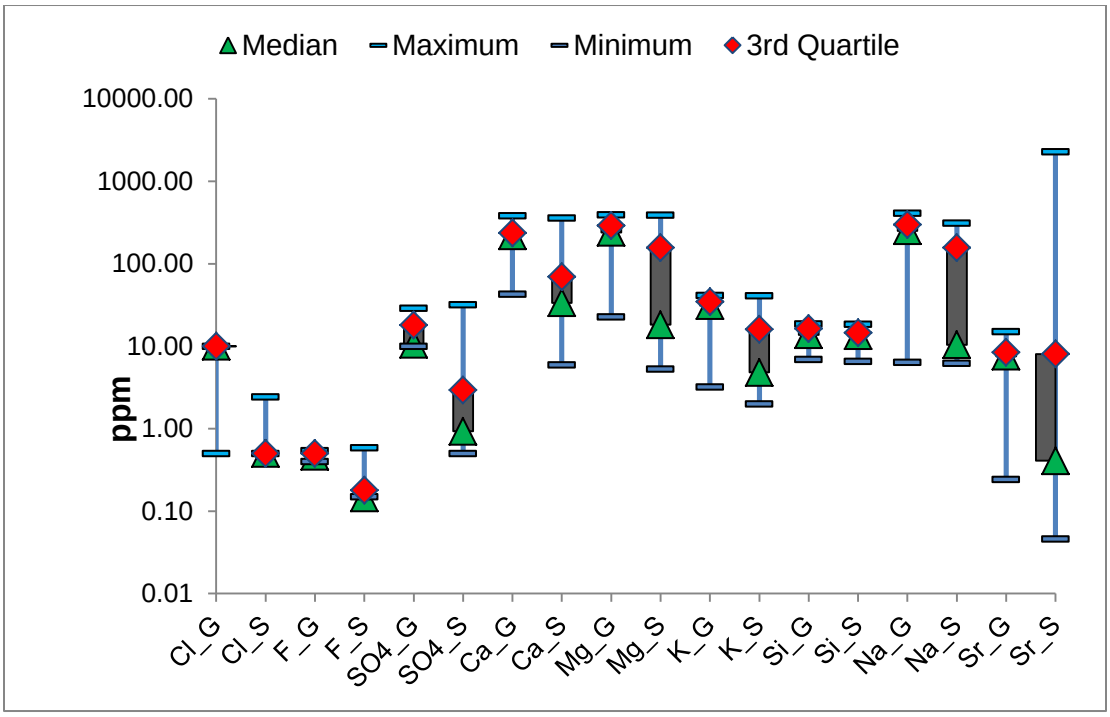

Figure 9 Median, 3rd quartile and range for elements anions by ion chromatography and cation by ICP-ES in parts per million (ppm) for 13 ground and 21 surface water samples. Alkalinity in mg $CaCO_3$ L-1. Field measured parameter identified as_ F; G – ground water sample; S – surface water sample.

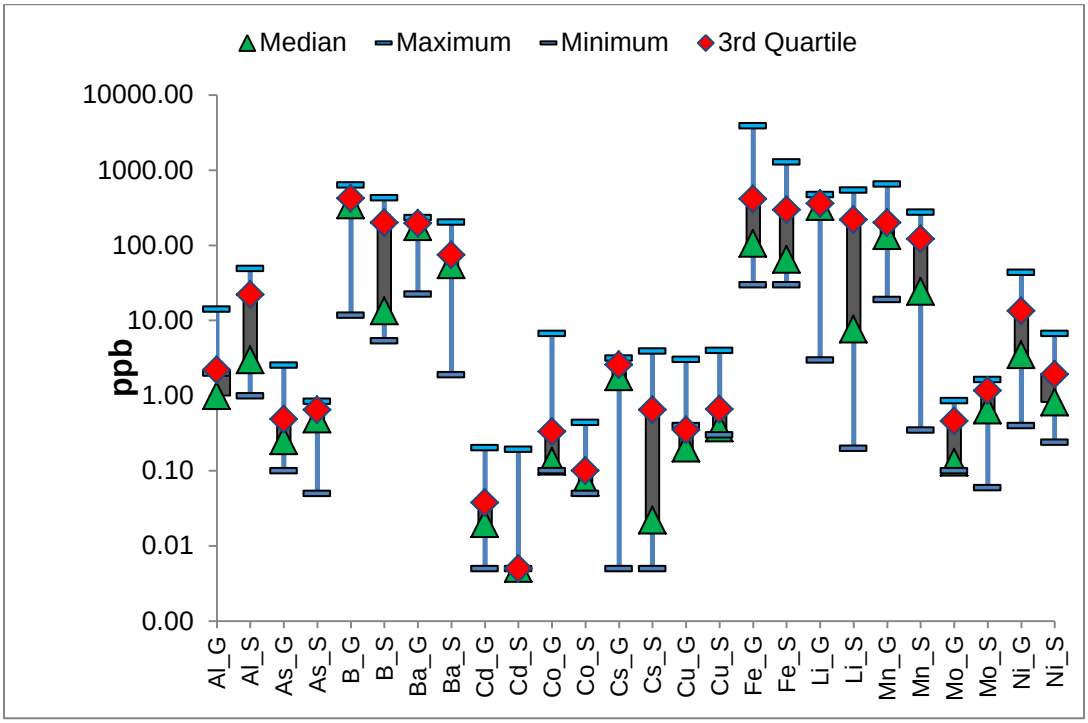

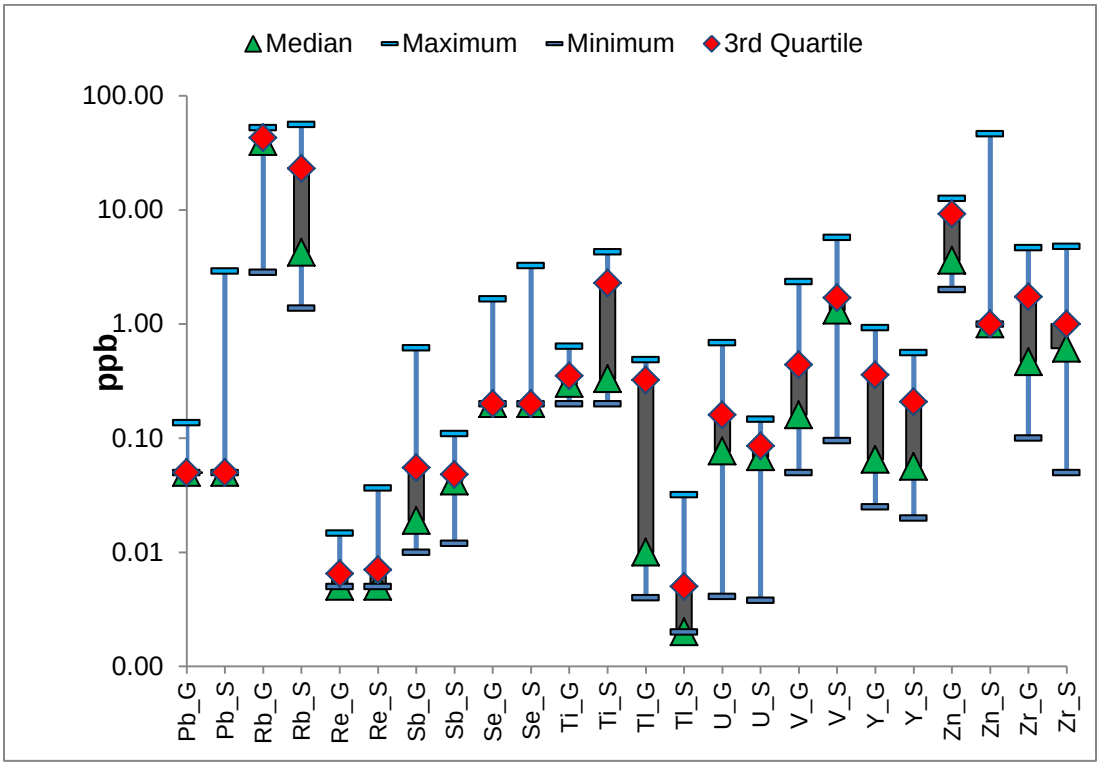

Figure 10 Median, third quartile and range of elements in parts per billion (ppb) for 13 ground water and 21 surface water samples. Tin, silver, phosphorus, gallium, tungsten, thorium and bismuth are not included because most values are below detection limit.

Median, range and 3rd quartile statistics show that the ground water sampled from pits and the travertine cone seepage has a lower pH and temperature than surface water. The lowest temperature of 5.9^{o}C measured in water that had accumulated in the bottom of the travertine cone-carbon dioxide seeps near the North Bog also has the highest arsenic and nickel detected in all of the ground and surface water, although maximum arsenic measured (2.6 ppb) is well below the recommended BC Ministry of Environment level for aquatic life (5 ppb) and for safe drinking water (25 ppb). Lake water is the most alkaline (pH 9.6) water and has the highest measured temperature of 23°C. Figure 9 reveals that sulphate, conductivity, salinity, alkalinity, dissolved CO_2 , magnesium and calcium are higher in ground water compared to surface water, but median and maximum silica concentrations are similar for both water types. Although the ground water strontium median is higher than that of surface water, the maximum strontium was measured in a surface water sample. Statistics for trace elements (parts per billion range) in ground water are compared with surface water in Figure 10 showing that many of the trace elements such as boron, barium, cesium, lithium, manganese, nickel, iron, yttrium and zirconium are higher in ground water, while only vanadium and selenium are higher in surface water. Concentrations of geothermal pathfinder elements such as boron, lithium and arsenic are typically higher in the ground water samples.

Variation of the geothermal pathfinder and other elements in stream water, stream sediment and lake-bottom sediment from the area surrounding the North and South Bogs are compared in the following figures. Figure 11 shows the location of the stream and lake water samples and stream sediment samples collected during the TREK Geothermal study and also lake-bottom samples sampled as part of a TREK regional geochemical survey (Jackaman, 2014). Not all of the TREK Geothermal project stream water sites have a corresponding sediment sample. Figure 12 shows that stream water pH increases from 7.25 in steams above the bogs to more than 9 in the lake water close to where the stream flows into Fishpot Lake. Stream water temperature (Figure 13) clearly increases from below 8°C in stream water flowing into the bogs to 23°C in the lake water.

Variation of stream water calcium in Figure 14 can be explained by the influence of bedrock geology on water chemistry. The stream flowing into the North Bog from the east drains an area where there are basalt outcrops with calcite-coated vesicles along the stream channel. Calcite solution will increase dissolved calcium in the stream water. Lower calcium in the stream flowing into the South Bog from the south suggests an absence of calcite in bedrock although the pH is alkaline. Variation of dissolved calcium in the streams as they flow through the bogs likely reflects changes in calcium carbonate solubility with higher dissolved carbon dioxide in the water. The highest calcium detected in stream and lake sediment is from the site where the stream flows past the calcite-coated basalt outcrop (Figure 15).

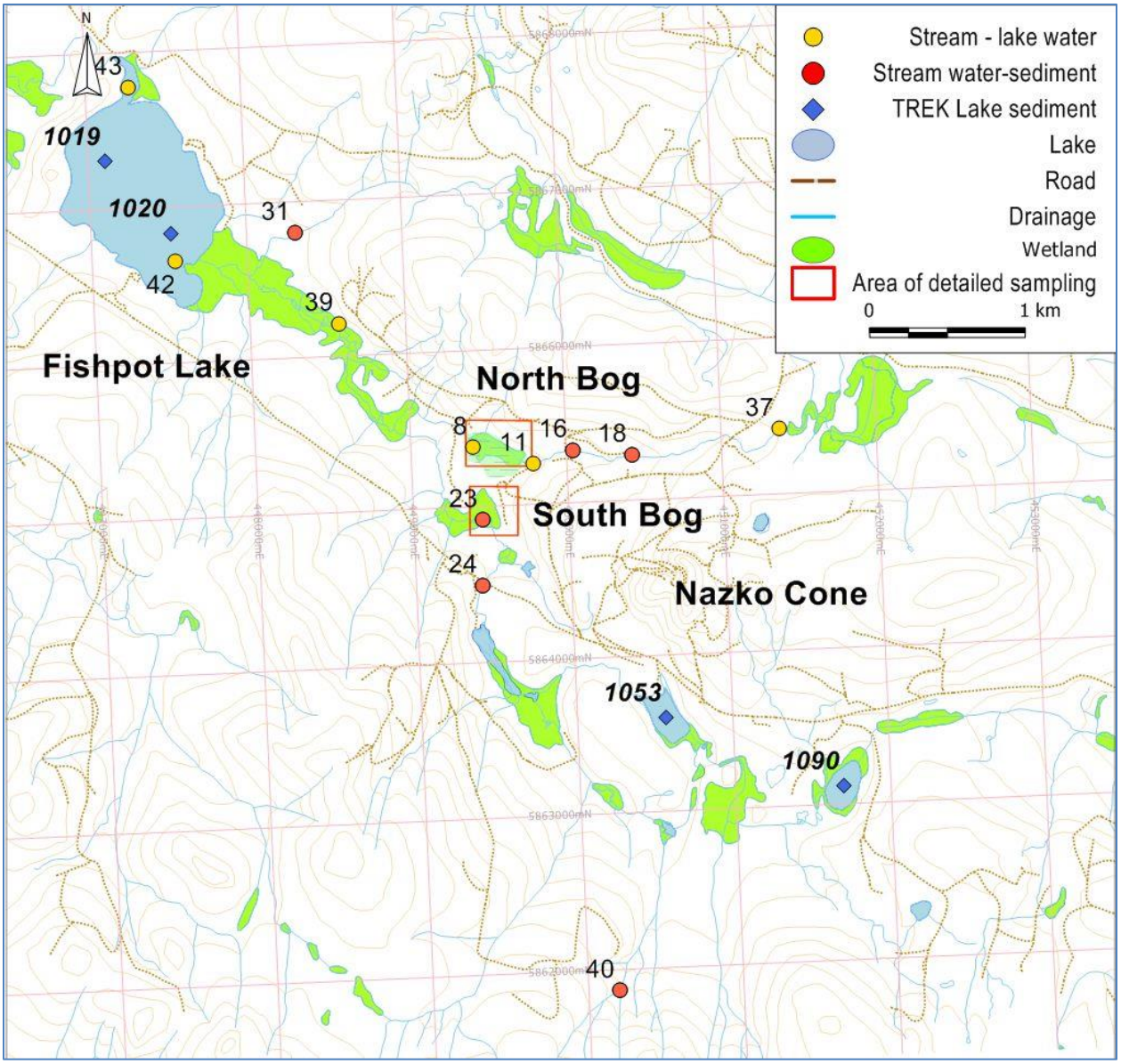

Figure 11 TREK Geothermal Project stream and lake water sample, stream sediment samples and TREK regional lake sediment survey samples. The TREK Geothermal Project sample numbers are prefixed 201393B and the TREK lake sample numbers are prefixed LAKE 093B13.

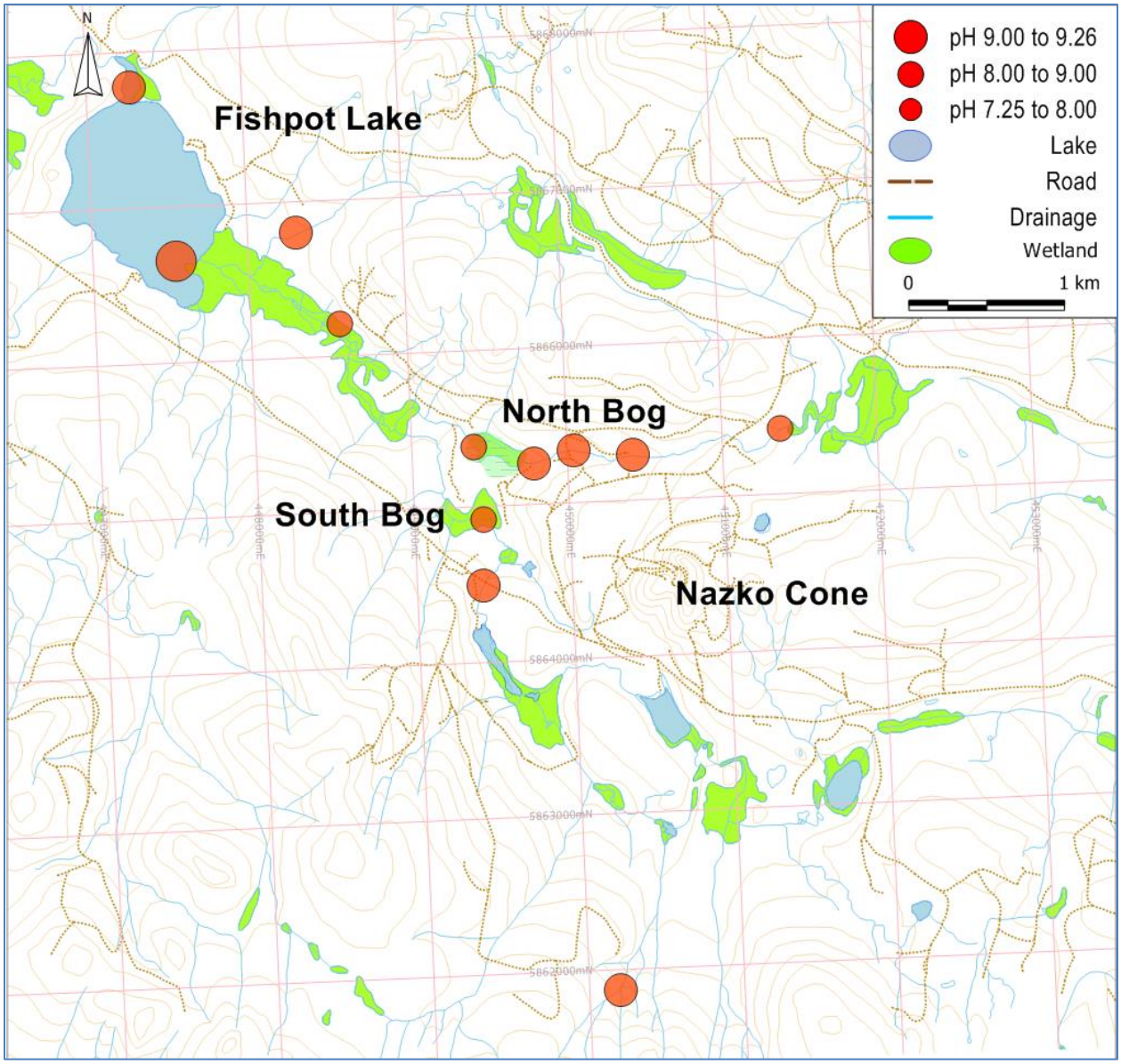

Figure 12 TREK Geothermal project stream water pH.

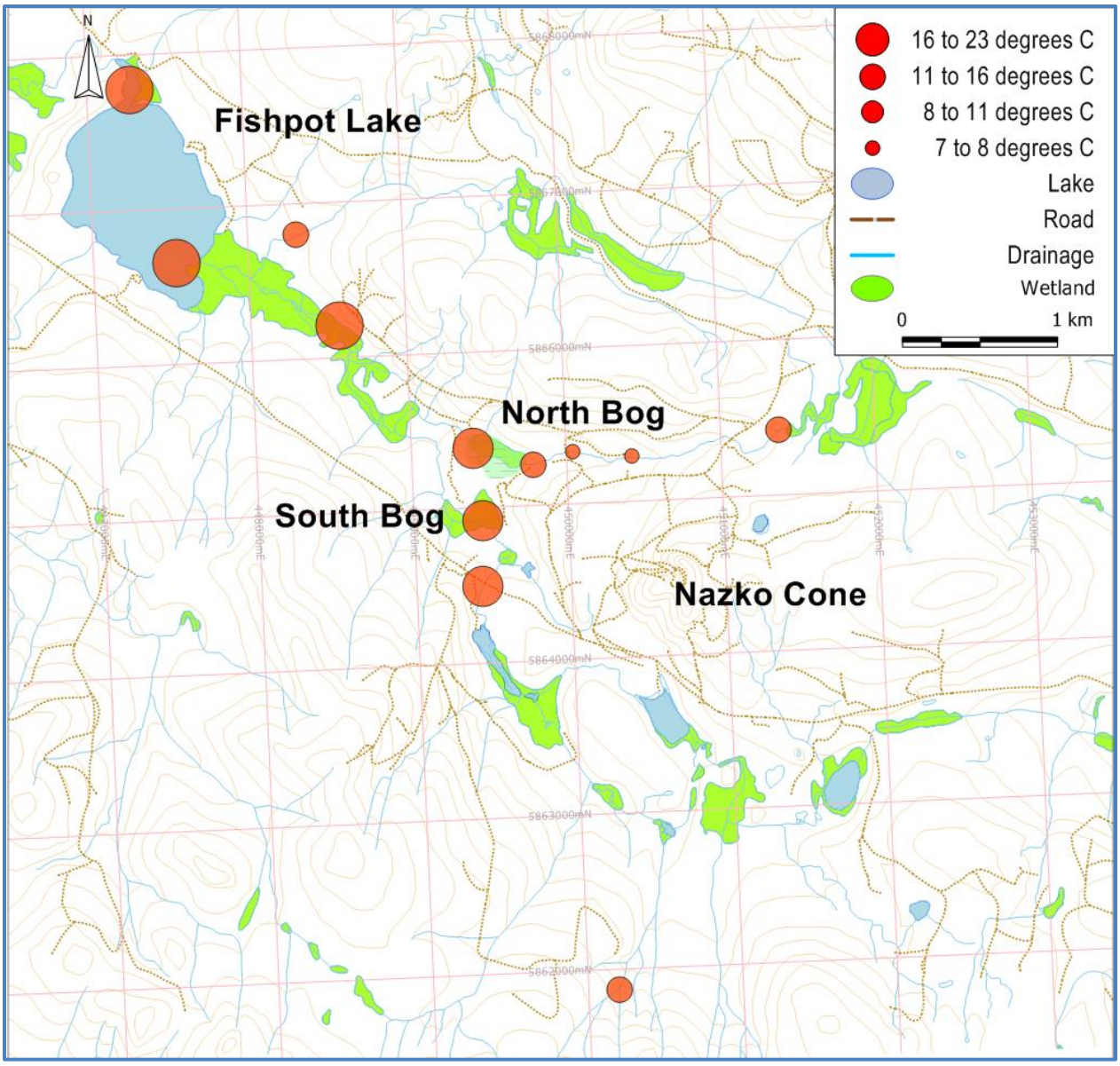

Figure 13 TREK Geothermal project stream water temperature.

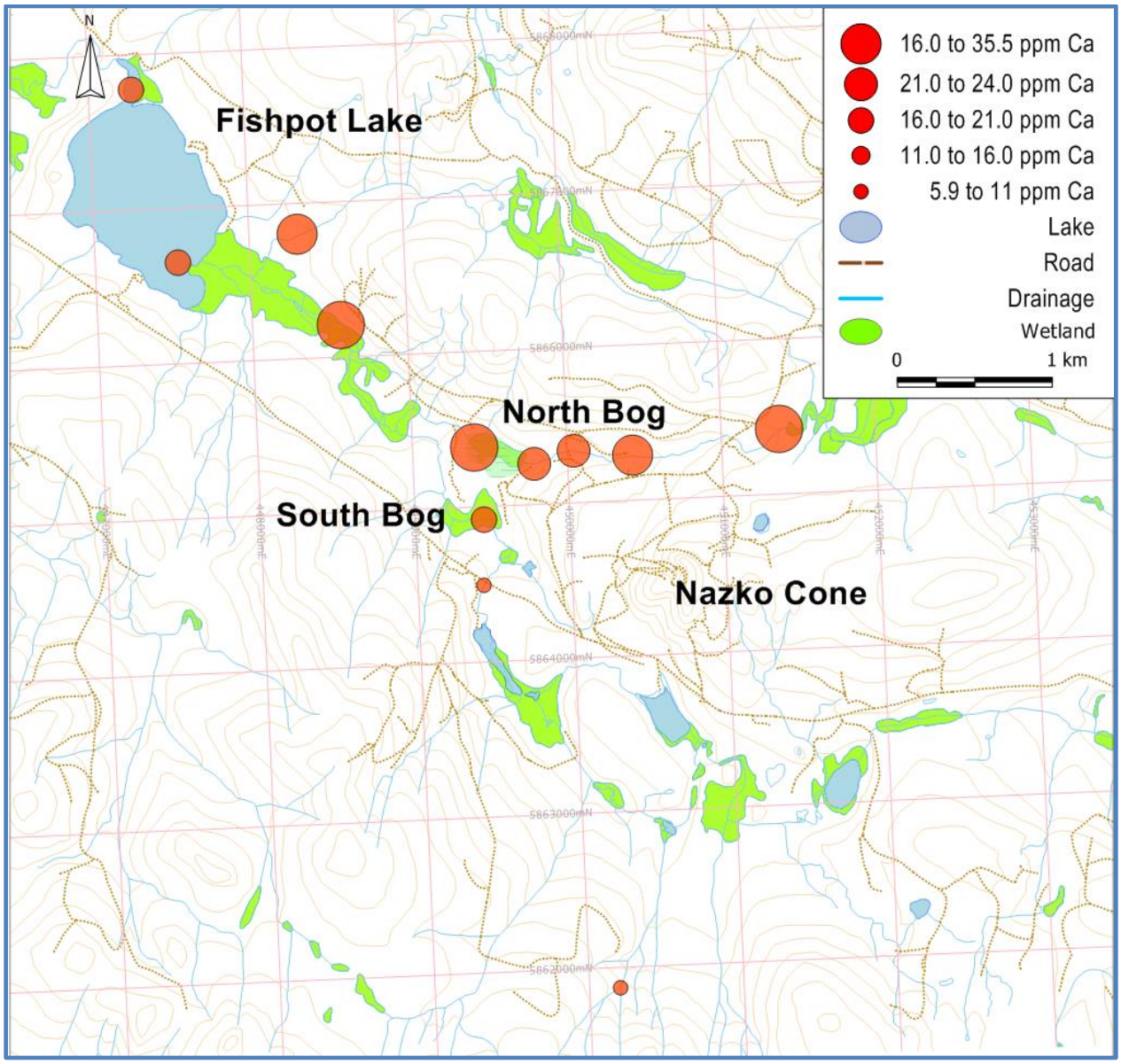

Figure 14 TREK Geothermal project stream water calcium in parts per million.

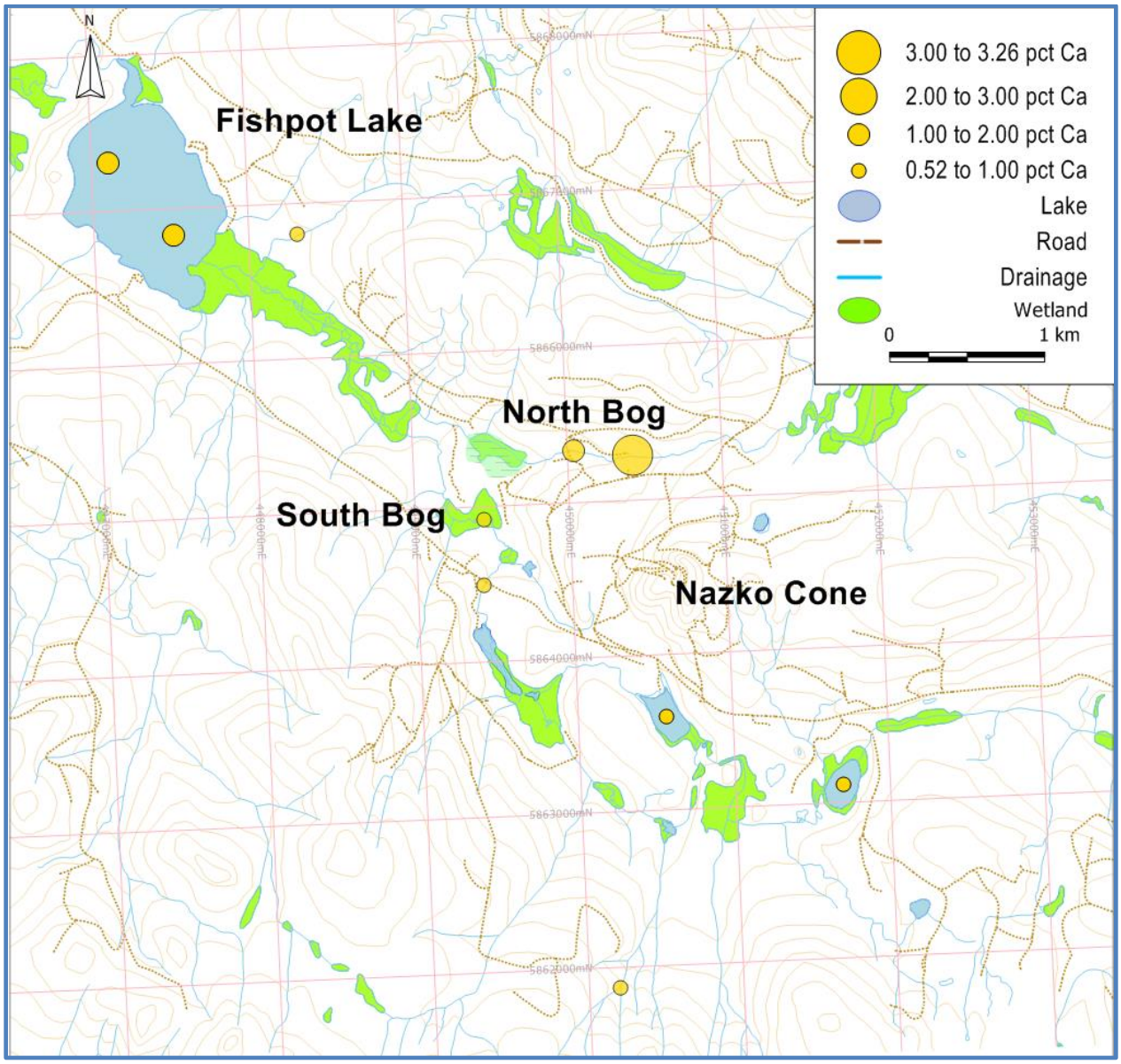

Figure 15 TREK Geothermal project stream sediment calcium and TREK regional lake sediment survey calcium in percent (pct).

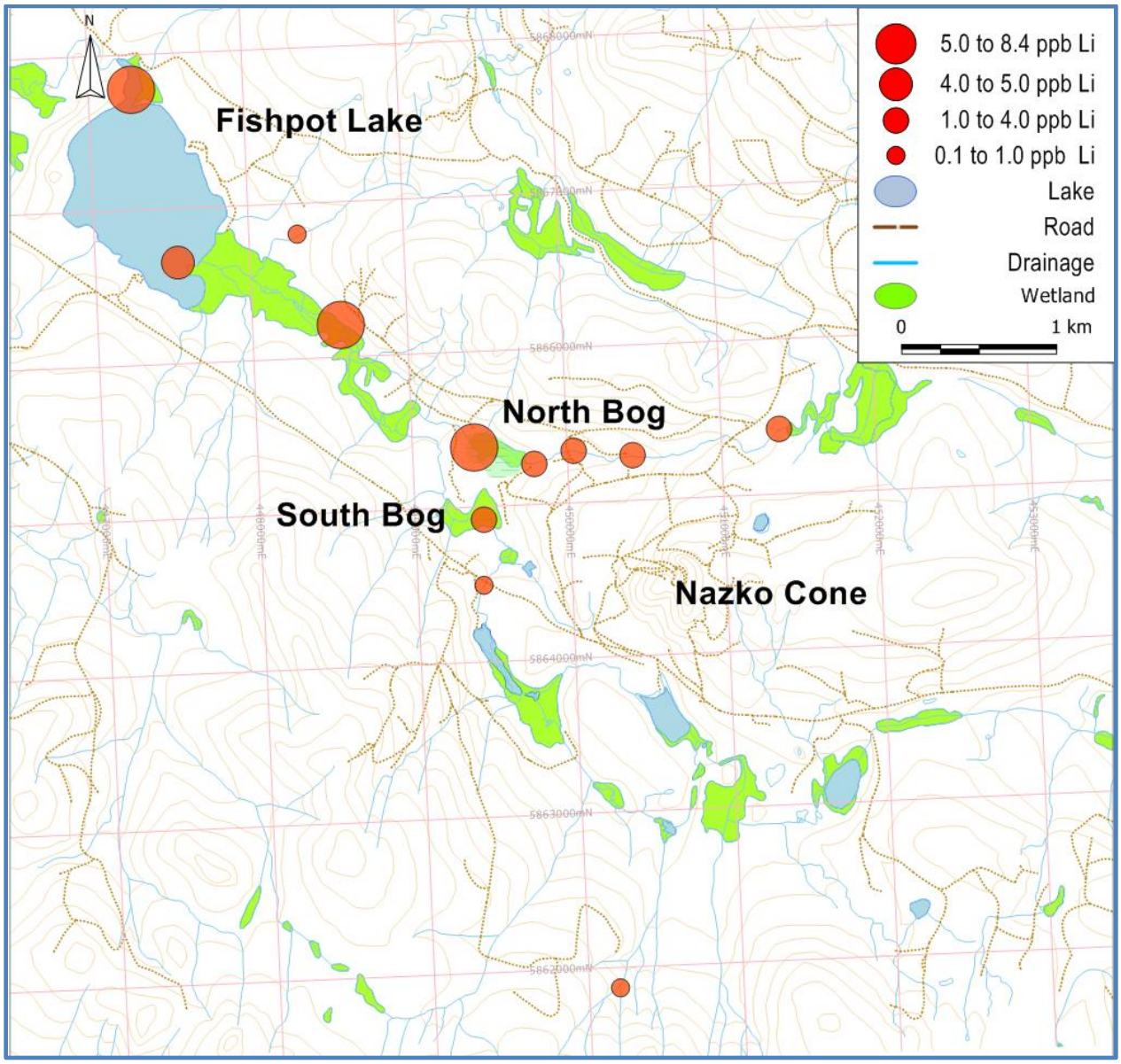

Figure 16 TREK Geothermal project stream water lithium in parts per billion.

Figure 16 shows a sharp increase in stream water lithium where the stream leaves the North Bog suggesting a lithium source in or beneath the bog. The more alkaline lake water likely increases the solubility of lithium carbonate meaning more dissolved lithium in the water. Variation of boron (Figure 17) in stream water is similar to that of lithium although higher boron concentrations persist in the bog streams. Higher dissolved boron can be explained by the greater stability of borate complexes and a possible boron source in the eastern part of the North Bog. Silicon (Figure 18) variation in stream water is small and values range from 12.5 and

16 ppm. The high silicon values are found in streams flowing through wetland and into wetland. In the stream and lake sediments lithium, boron and silicon variations are minor and values for both elements are less than 11 ppm. Figure 19 shows a similar stream water barium variation to calcium suggesting a common source for elements such as weathering of feldspar in the basalt.

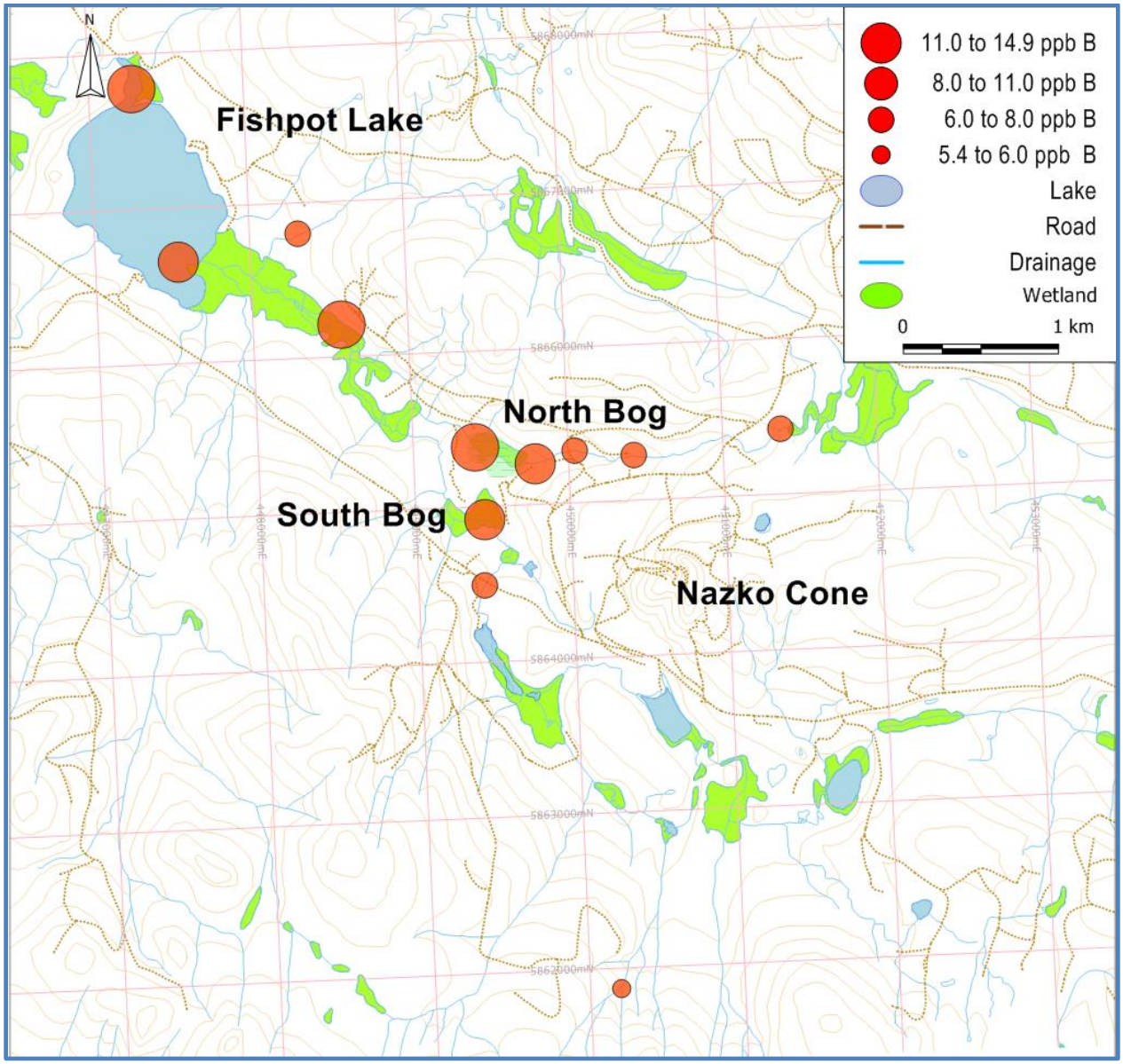

Figure 17 TREK Geothermal project stream water boron in parts per billion.

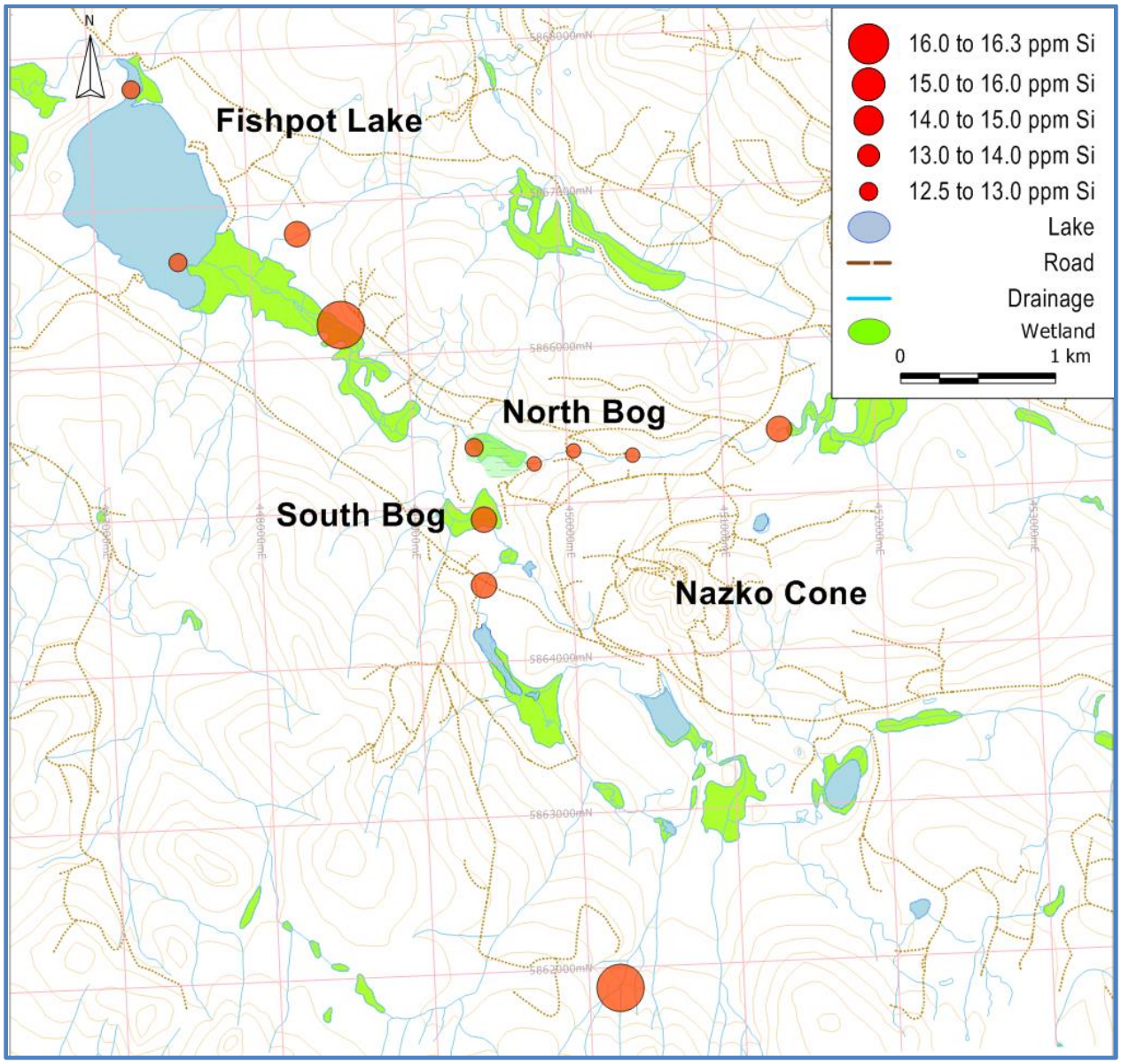

Figure 18 TREK Geothermal project stream water silica in parts per million.

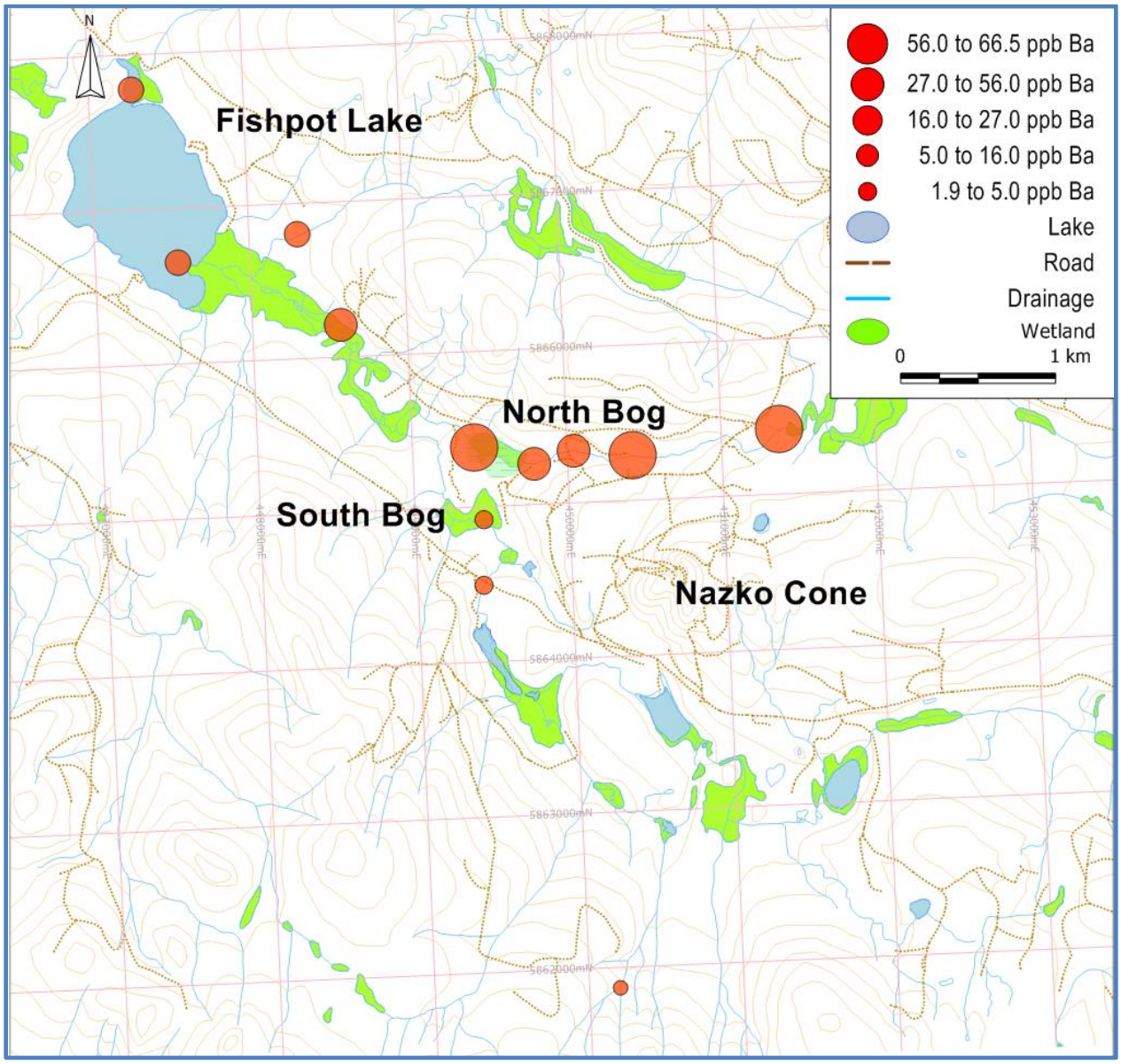

Figure 19 TREK Geothermal project stream water barium in parts per billion

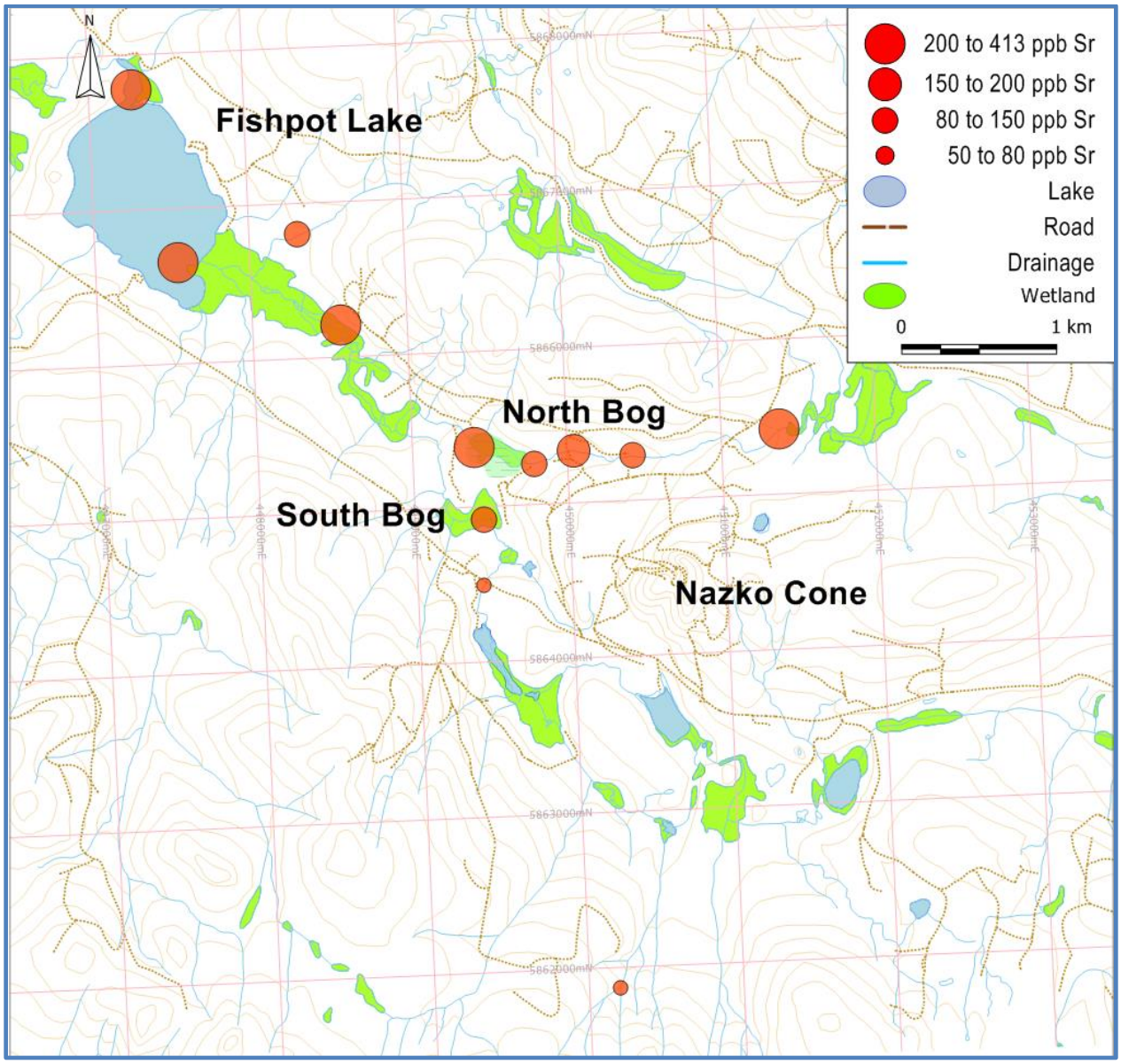

Figure 20 TREK Geothermal project stream water strontium in parts per billion.

Figure 20 shows that the stream water strontium variation is also similar to calcium with levels above 200 ppb in the stream east of the wetlands, the North Bog and in Fishpot Lake. Figure 21 shows that the sediment sampled from the stream east of the North Bog has up to 400 ppm strontium and this level may reflect bedrock chemistry.

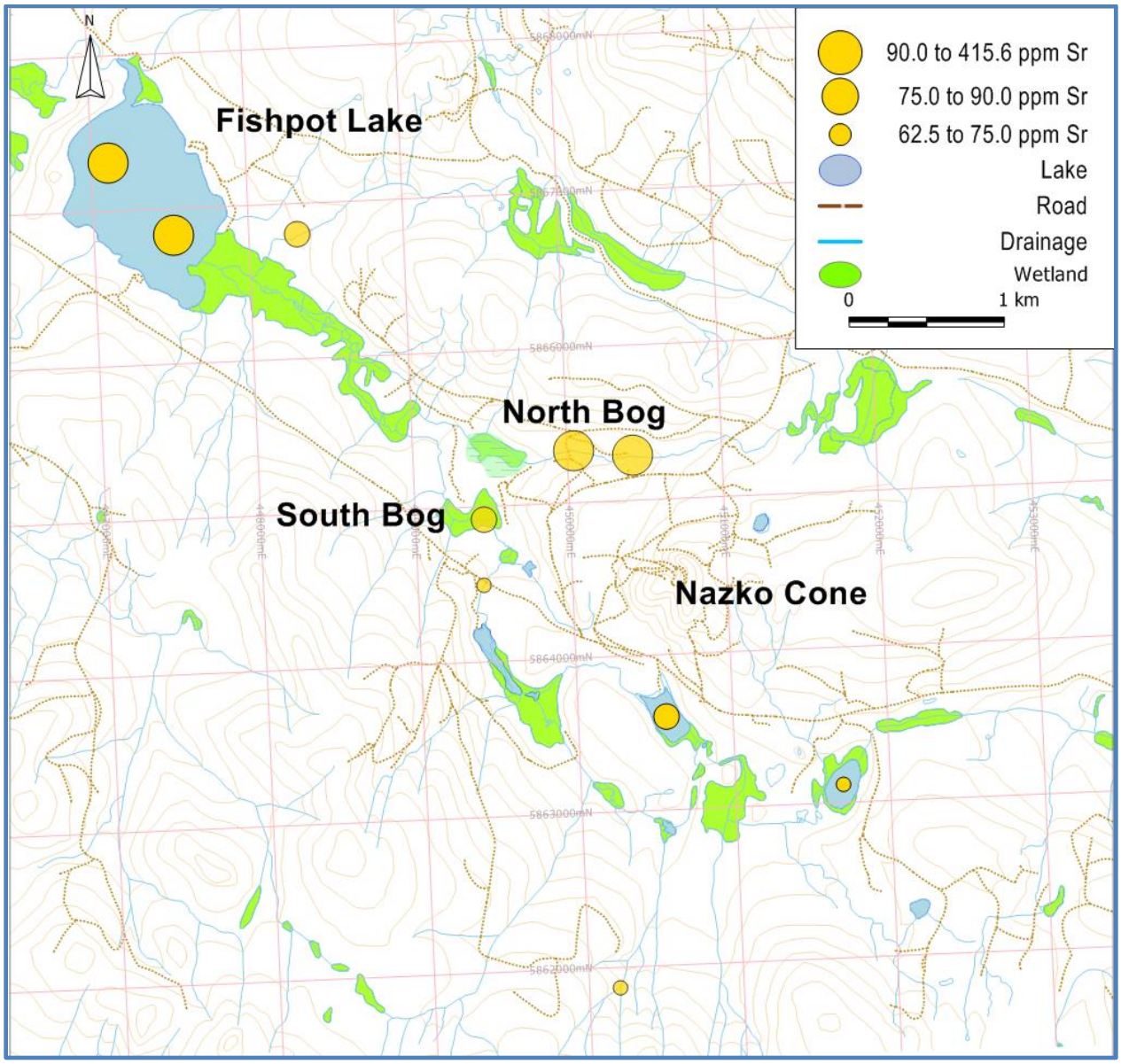

Figure 21 TREK Geothermal project stream sediment and TREK lake sediment survey strontium in parts per million.

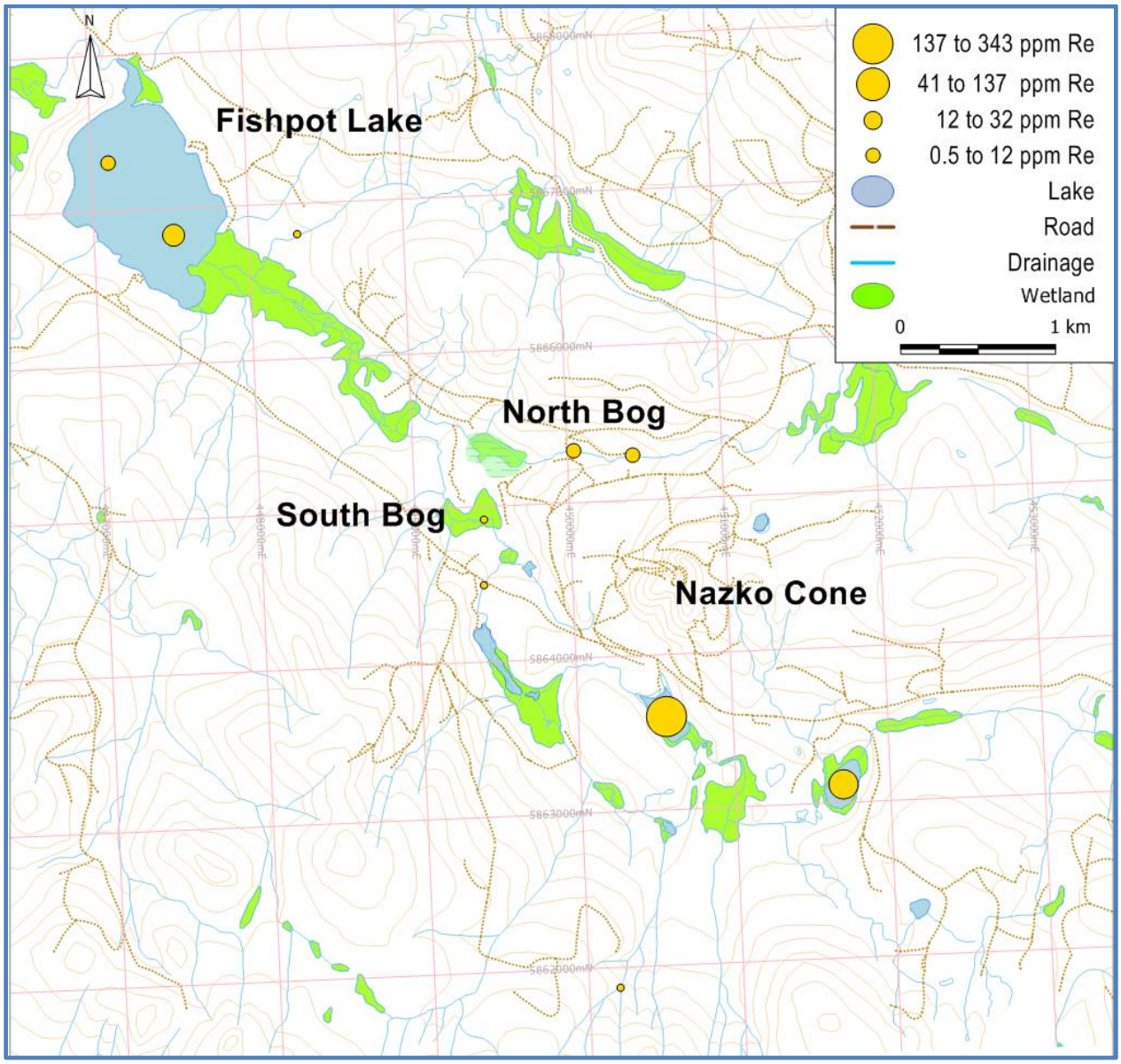

Figure 22 TREK Geothermal project stream sediment and TREK lake sediment survey rhenium in part per million

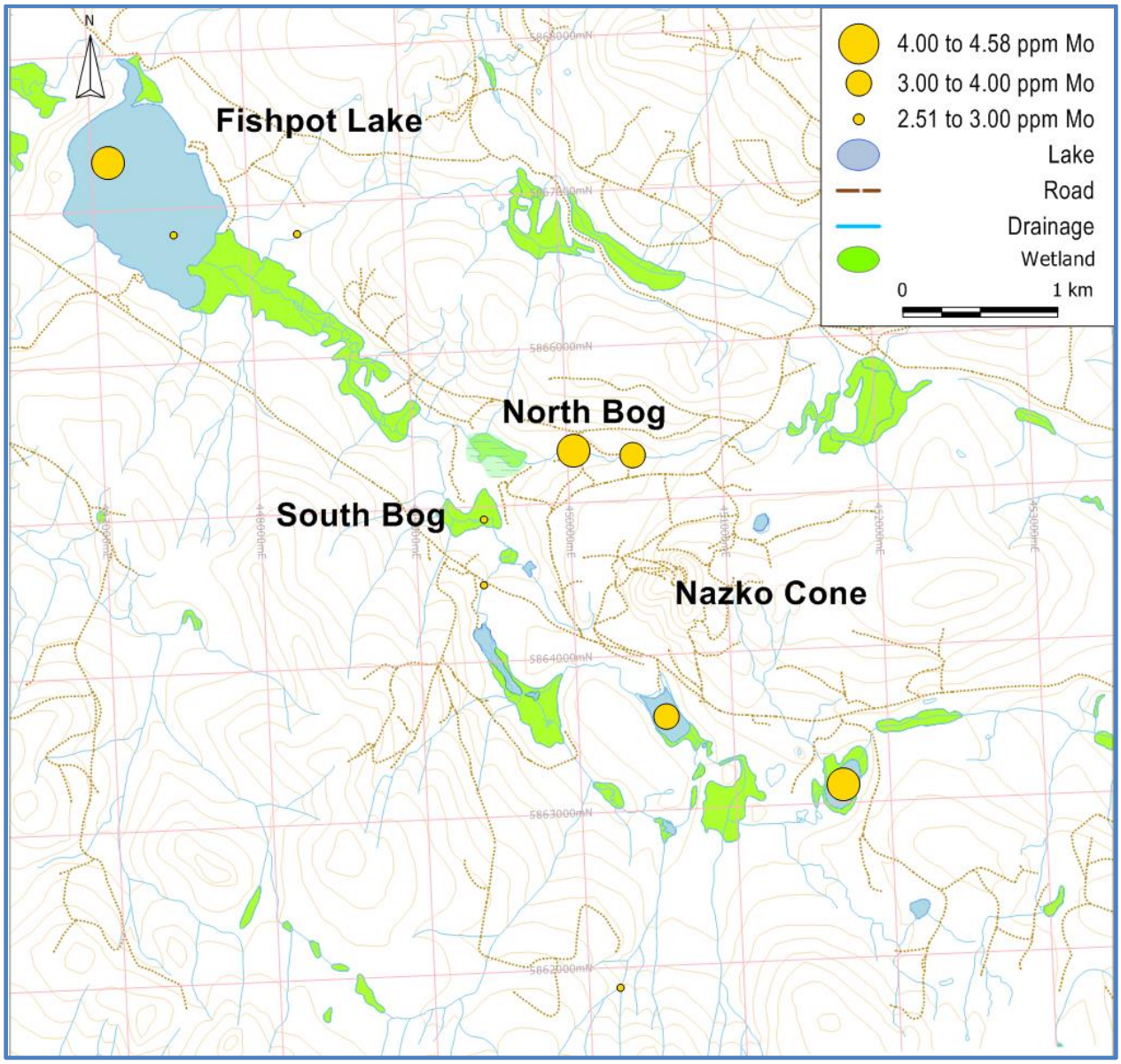

Figure 23 TREK Geothermal project stream sediment and TREK lake sediment survey molybdenum in part per million.

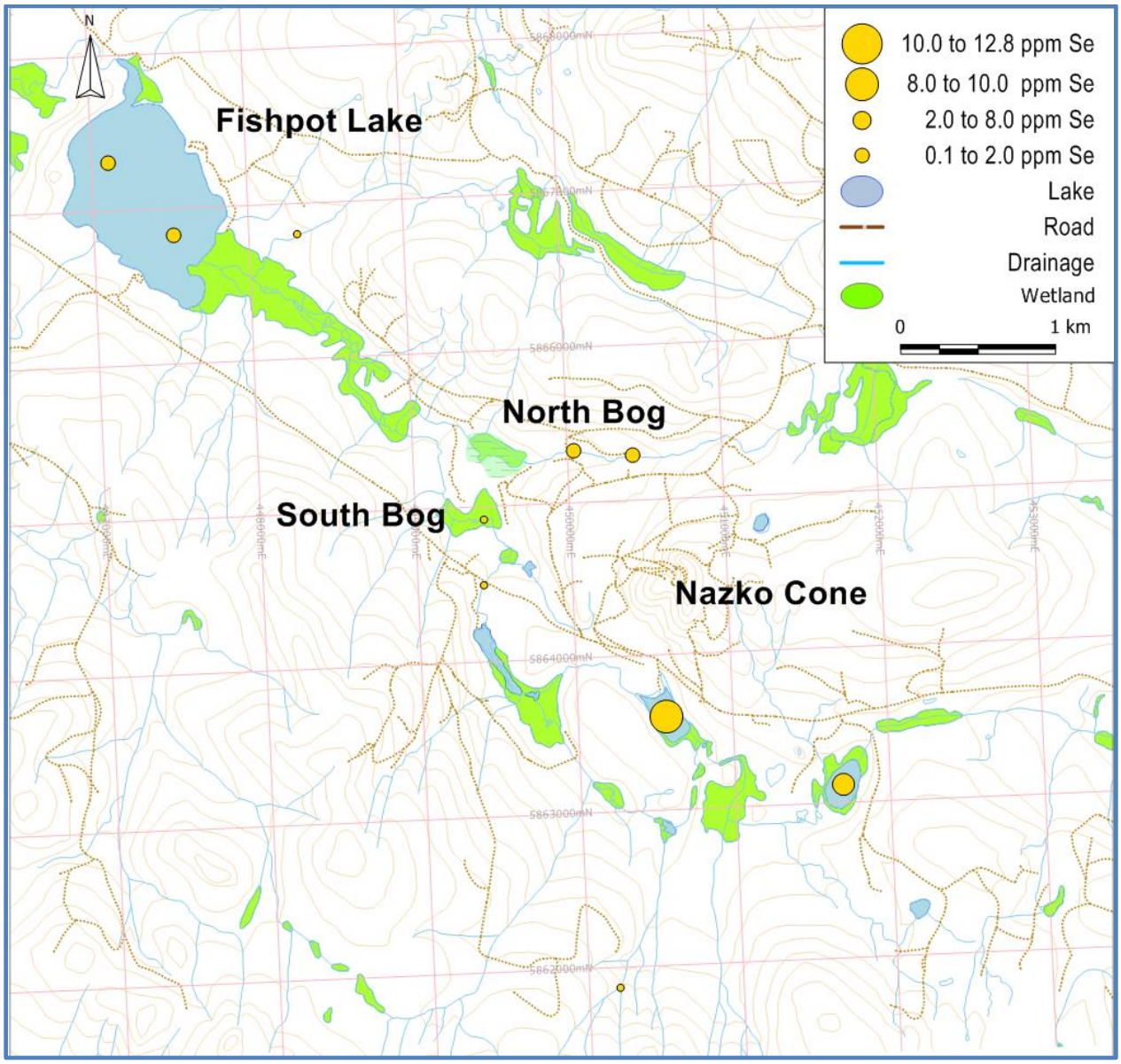

Figure 24 TREK Geothermal project stream sediment and TREK lake sediment survey selenium in parts per million.

Common geothermal pathfinder elements lithium, boron and arsenic are less than 11 ppm in stream and lake sediment. However, levels of other trace elements such as rhenium, selenium, molybdenum, mercury and palladium are elevated in the stream and especially in the lake sediment. Two lakes south of the Nazko Cone have up to 343 ppm rhenium (Figure 22), over 4 ppm molybdenum (Figure 23) and up to 12.8 ppm selenium (Figure 24). In contrast to the lake sediment geochemistry, streams flowing into the North and South Bogs have up to 370

ppb mercury (Figure 25) and 43 ppb palladium (Figure 26). Sediment from the same stream reach east of the North Bog also has up to 128 ppm nickel (Figure 27) in addition to high palladium. These elements are more common pathfinders for sulphide mineralization.

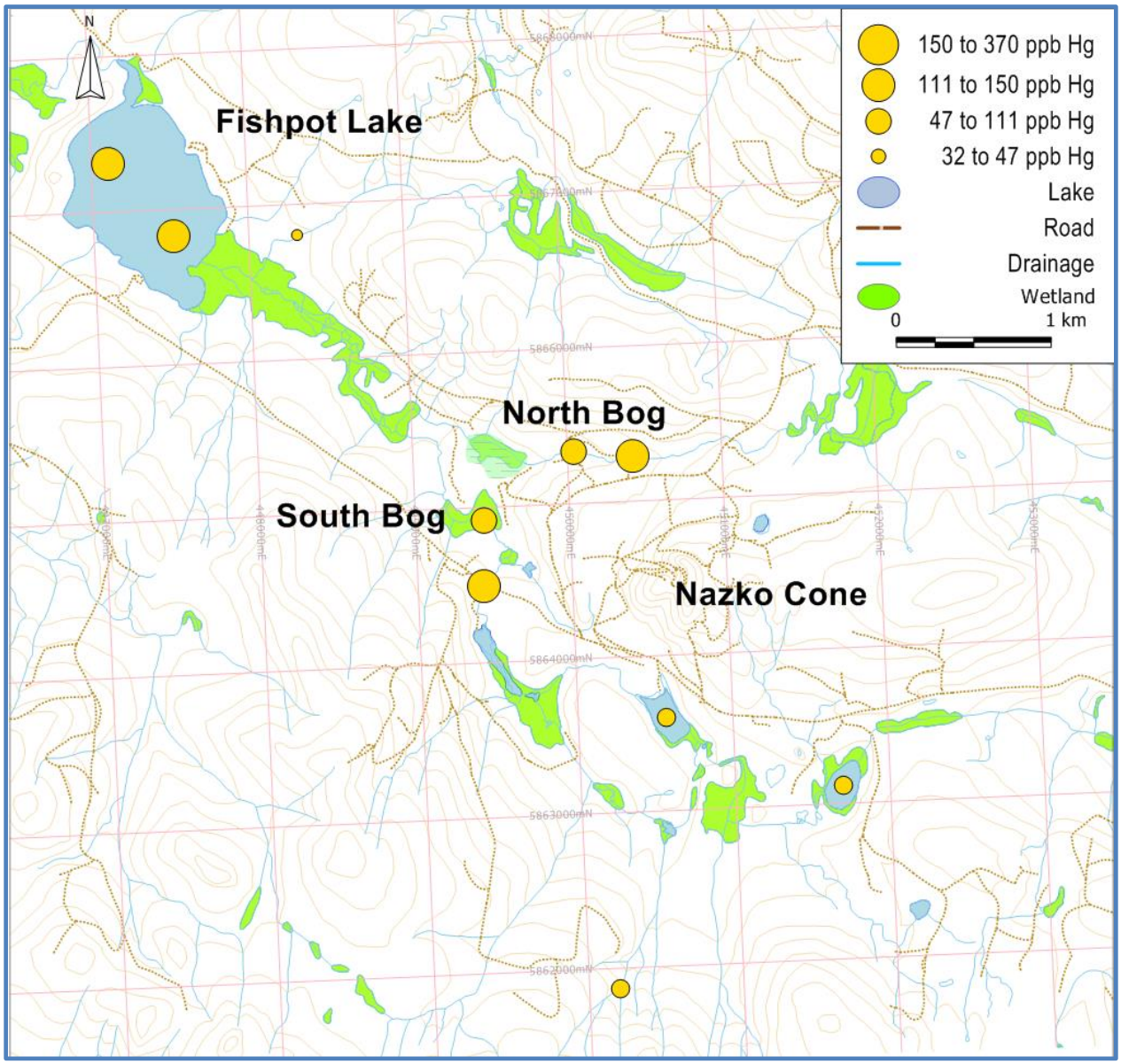

Figure 25 TREK Geothermal project stream sediment and TREK lake sediment survey mercury in part per billion.

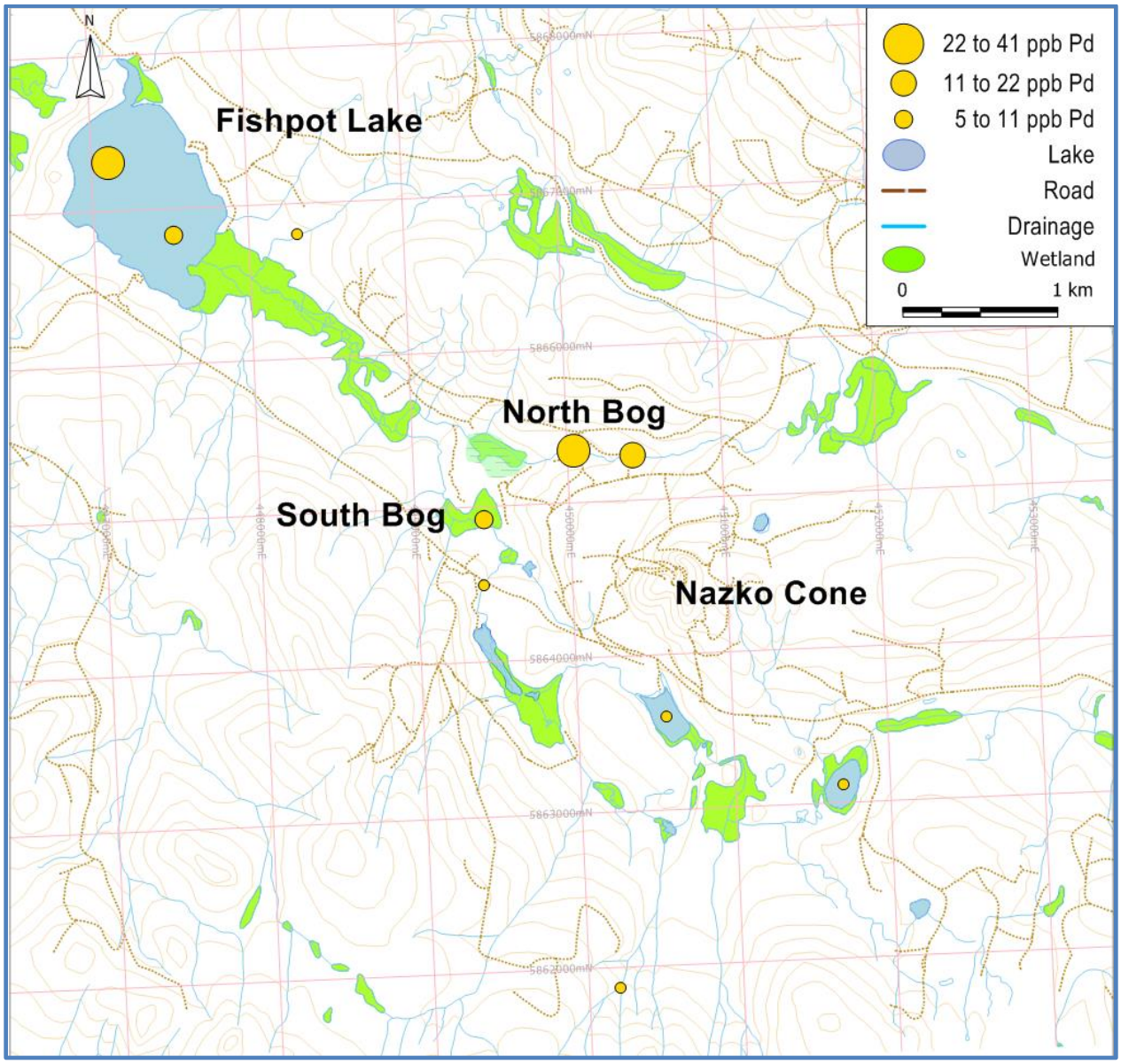

Figure 26 TREK Geothermal project stream sediment and TREK lake sediment survey palladium in part per billion

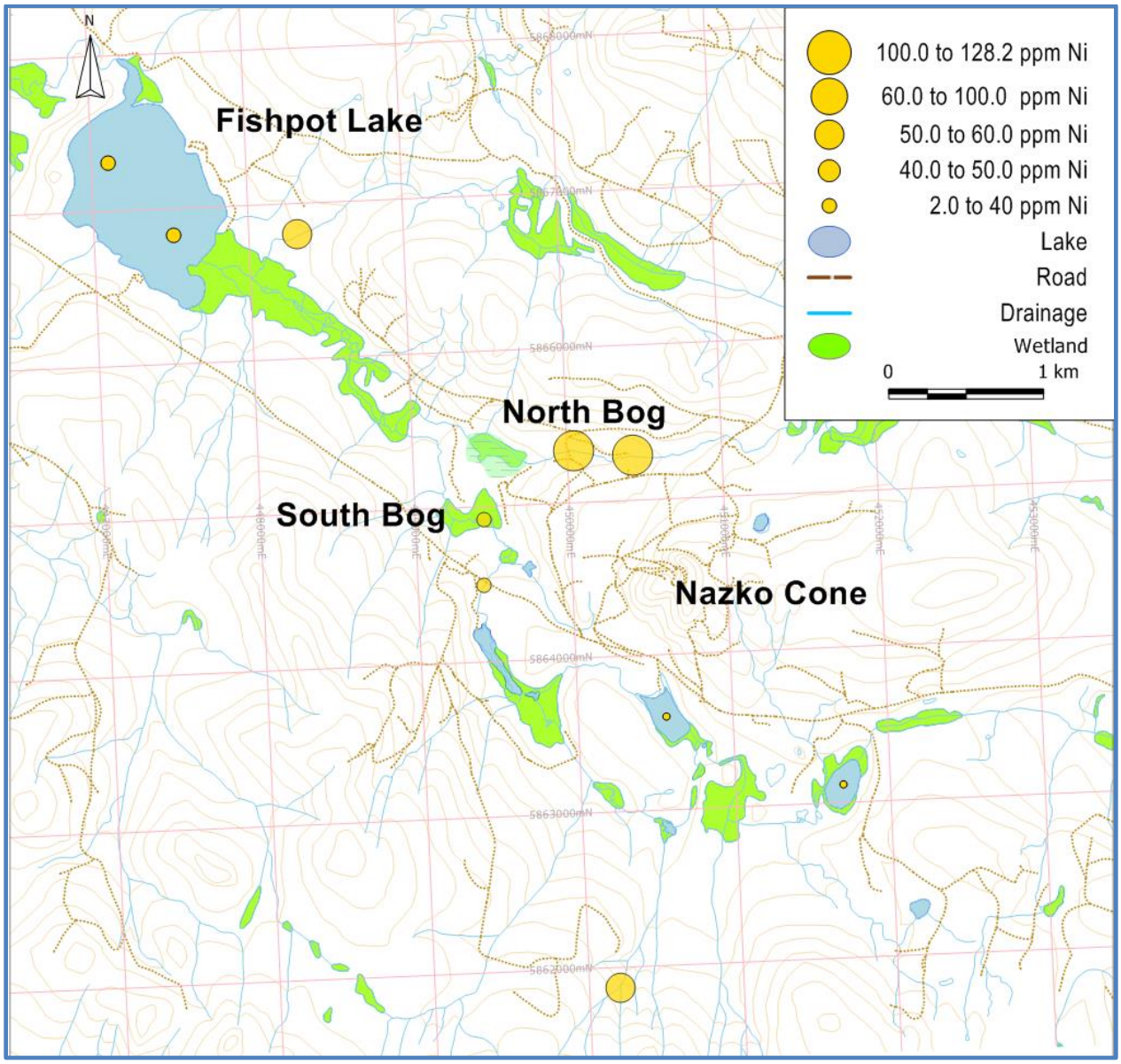

Figure 27 TREK Geothermal project stream and TREK lake sediment survey nickel in parts per million.

Figure 28 shows the location of North Bog ground and surface water samples. The lowest temperature (5.9^{o} C) recorded in the North Bog is in the water from the travertine cone - carbon dioxide vent (Figure 29), but surrounding ground and surface water samples have a temperature up to 20°C. The pH of the travertine cone carbon dioxide vent water is also lower than that of the nearby ground and surface water (Figure 30). Most ground and surface waters in the North Bog have a high dissolved carbon dioxide content caused by the carbon dioxide seeping to the surface of bog pools (Figure 31). Ground and surface waters have up to 637 ppb boron and 397 ppb lithium and concentrations increase towards the centre of the bog (Figures 32 and 33).

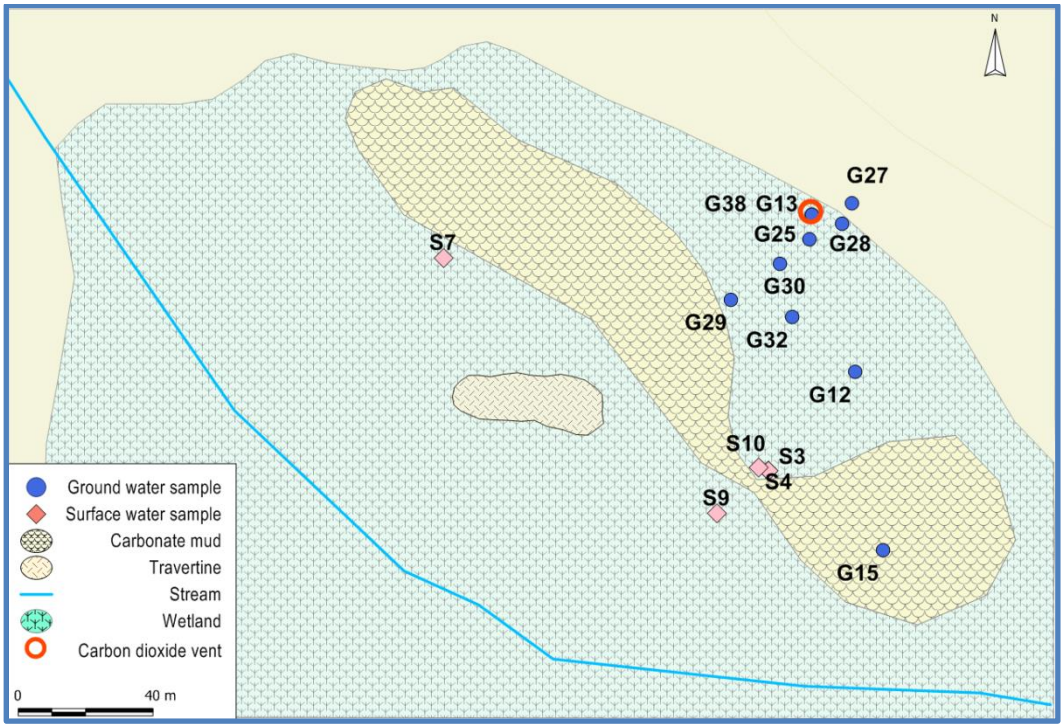

Figure 28 TREK Geothermal Project North Bog surface (S) and ground (G) water samples. The sample number identification is prefixed 201393B.

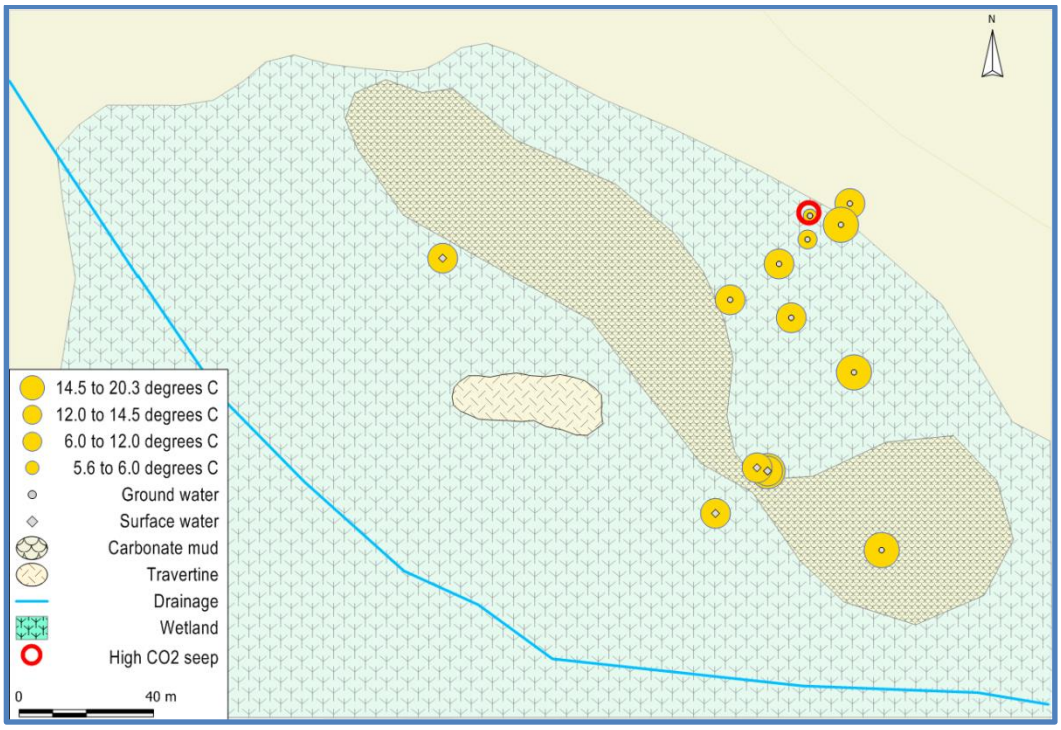

Figure 29 TREK Geothermal Project North Bog surface and ground water temperature.

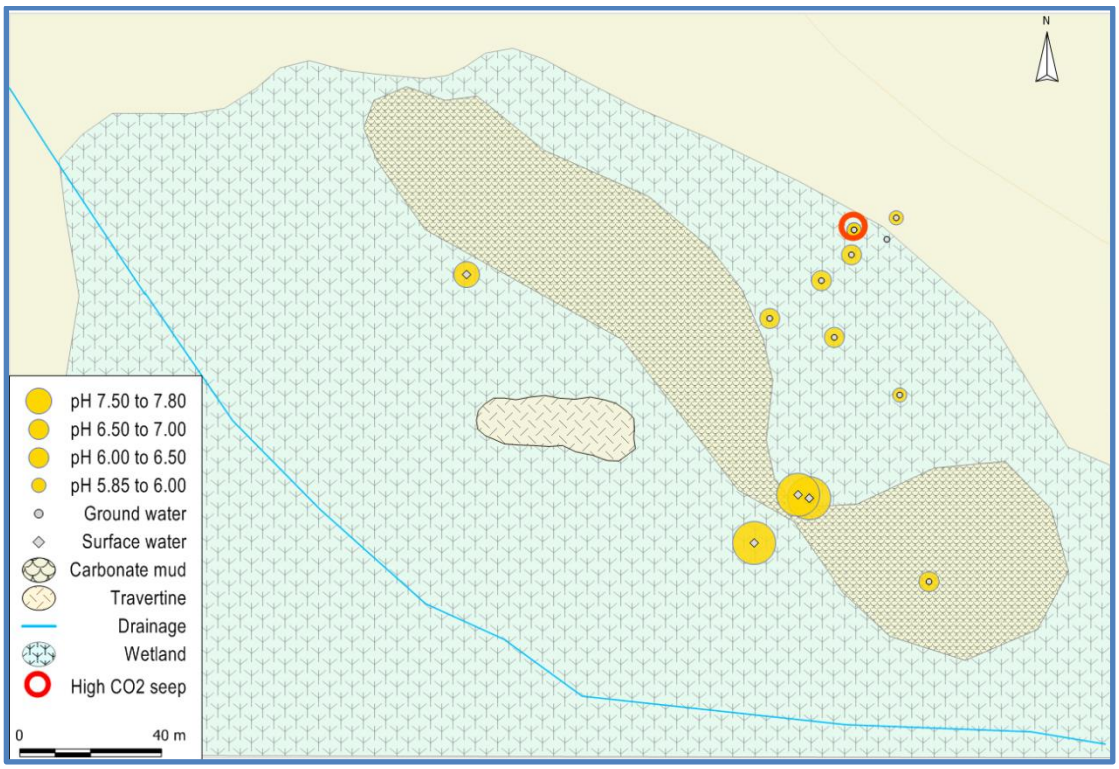

Figure 30 TREK Geothermal Project North Bog surface and ground water pH.

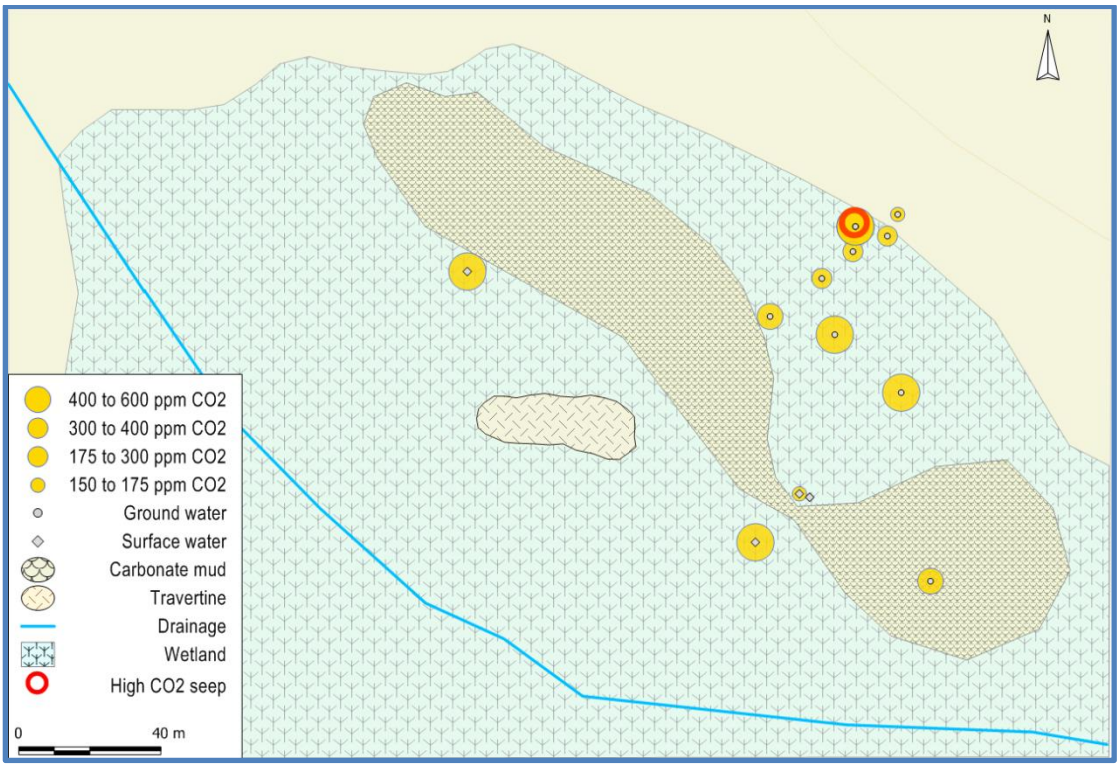

Figure 31 TREK Geothermal project North Bog surface and ground water dissolved carbon dioxide.

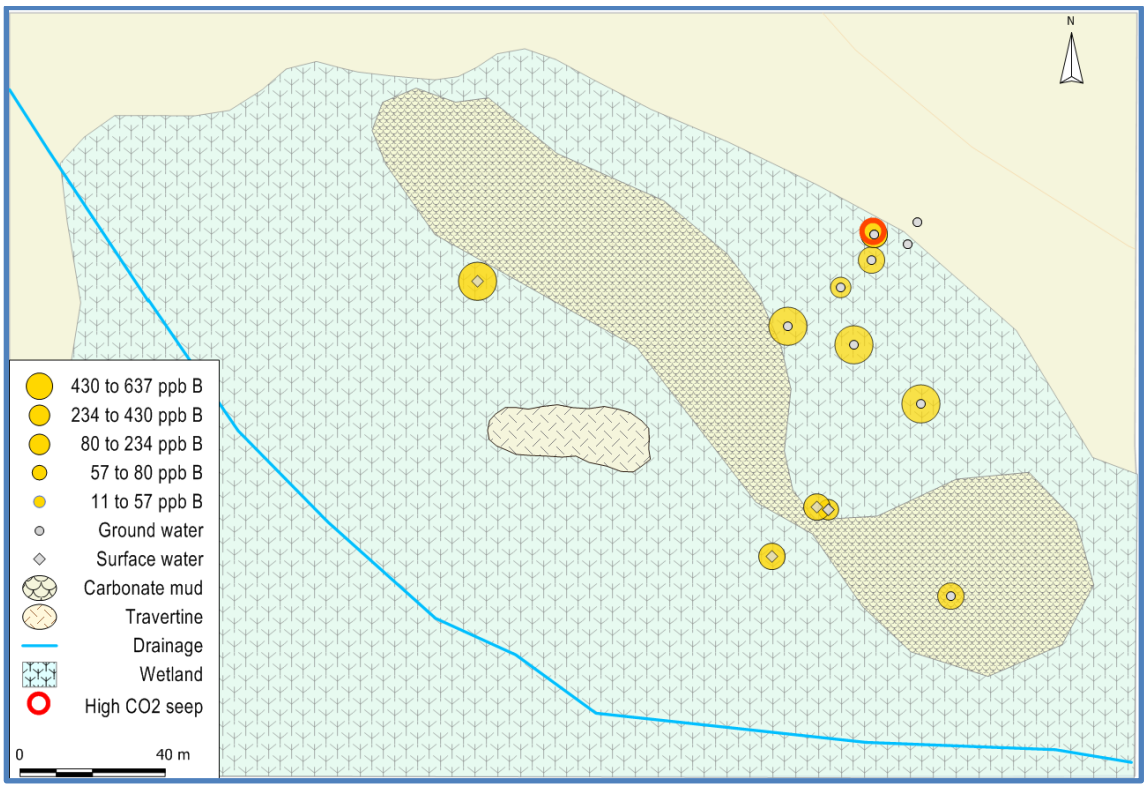

Figure 32 TREK Geothermal project North Bog surface and ground water boron

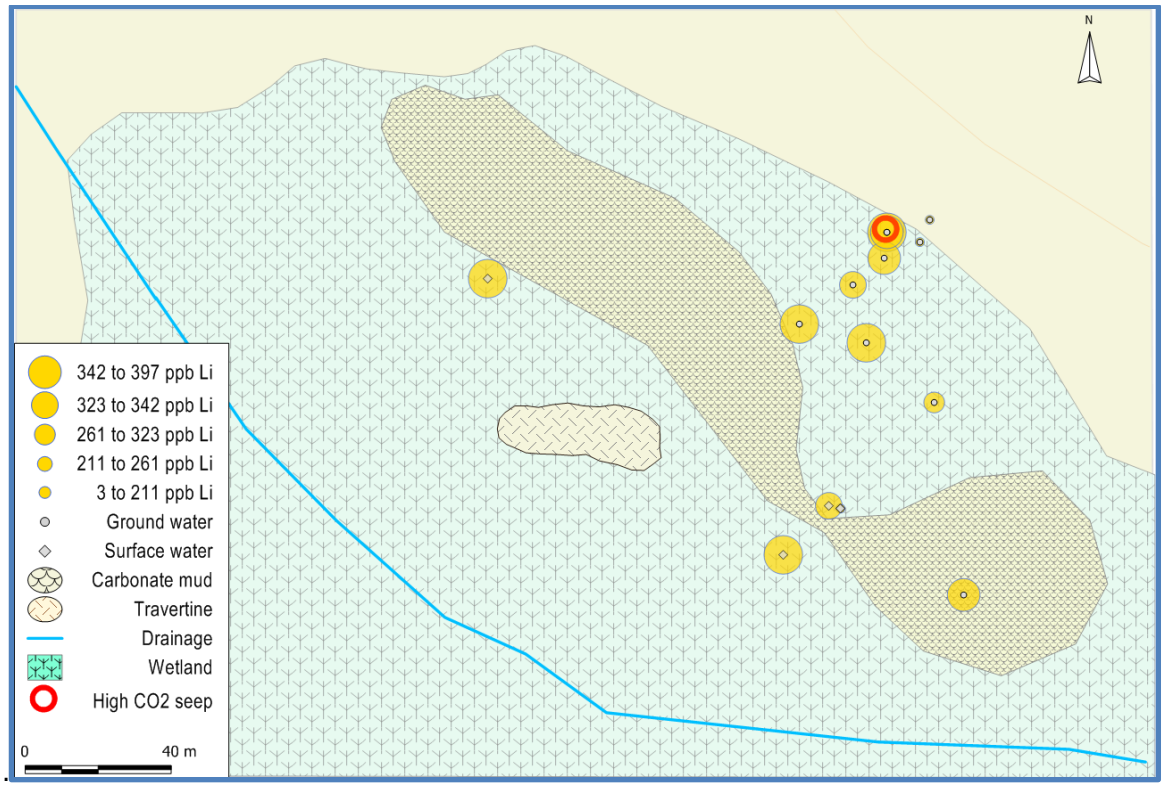

Figure 33 TREK Geothermal North Bog stream, surface and ground water lithium.

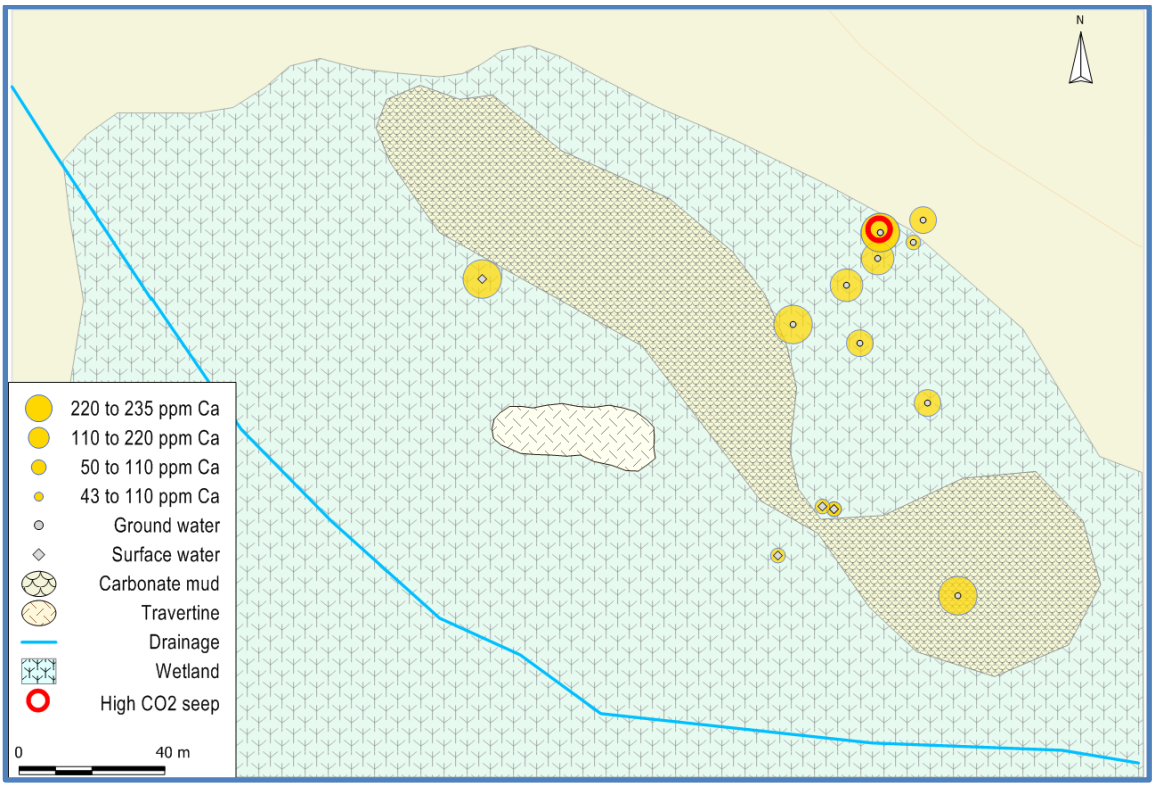

Figure 34 TREK Geothermal project North Bog surface and ground water calcium.

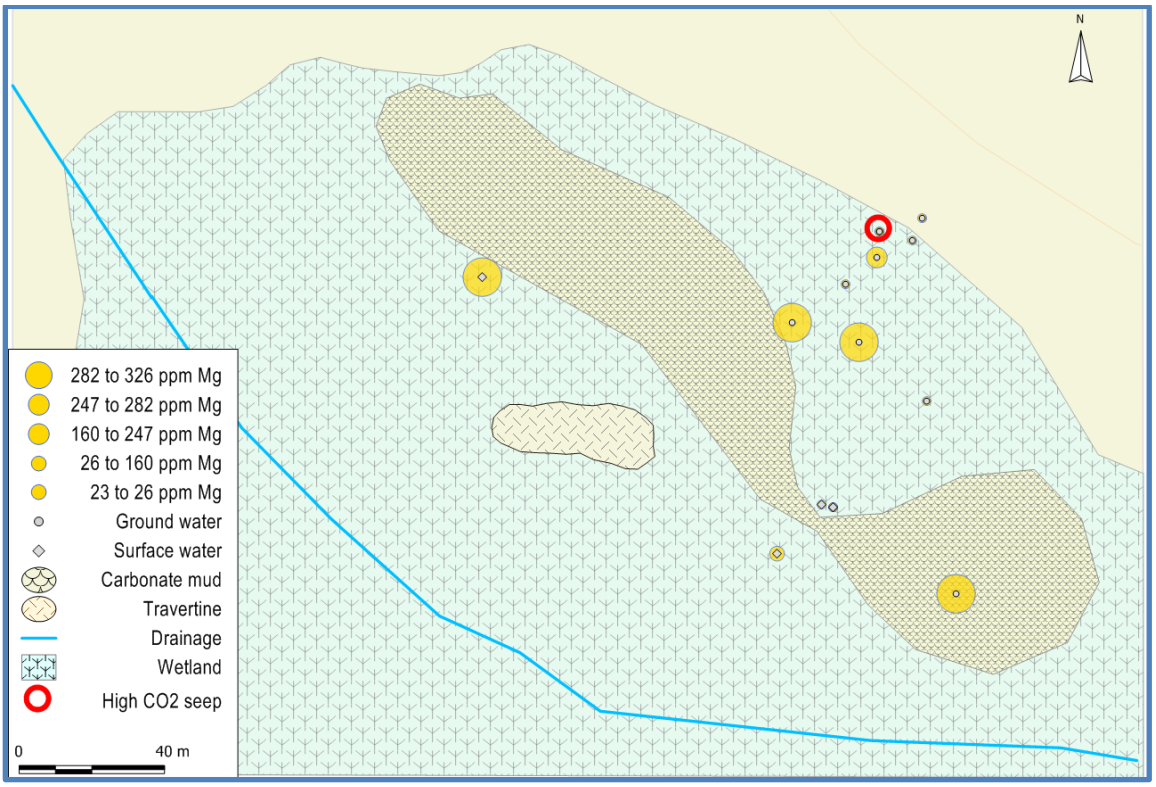

Figure 35 TREK Geothermal project North Bog stream, surface, and ground water magnesium.

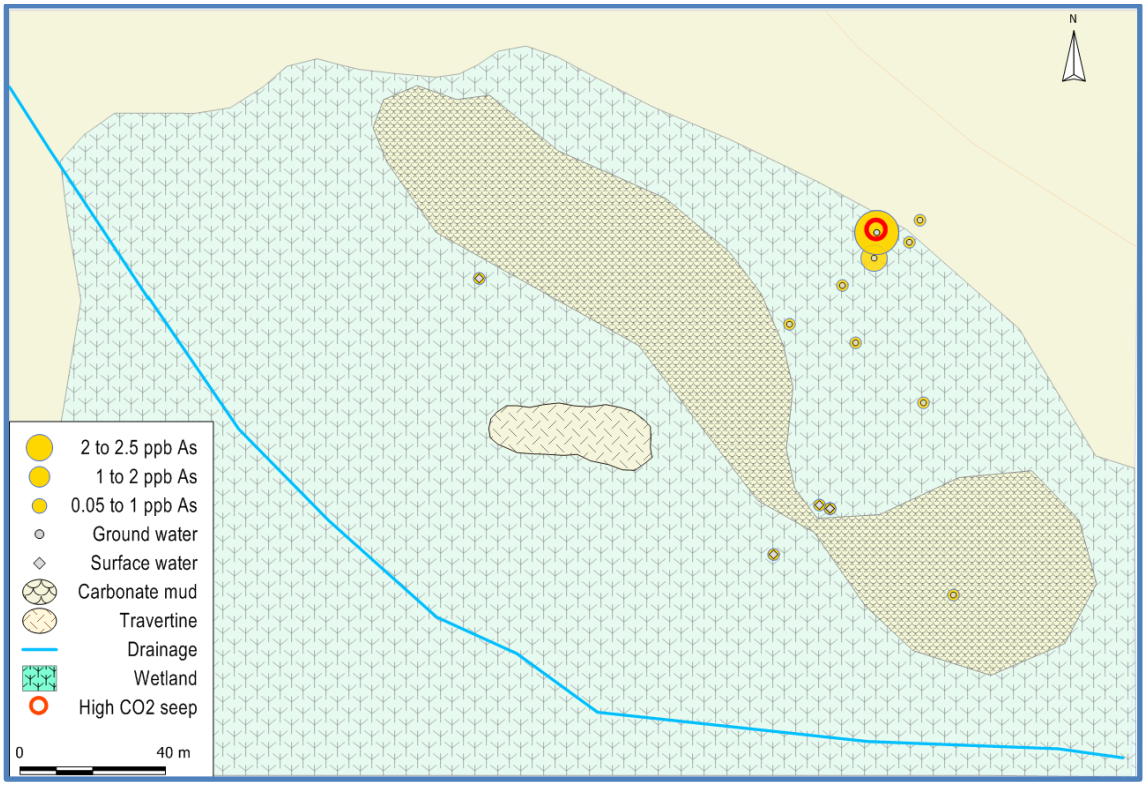

Figure 36 TREK Geothermal project North Bog surface and ground water arsenic.

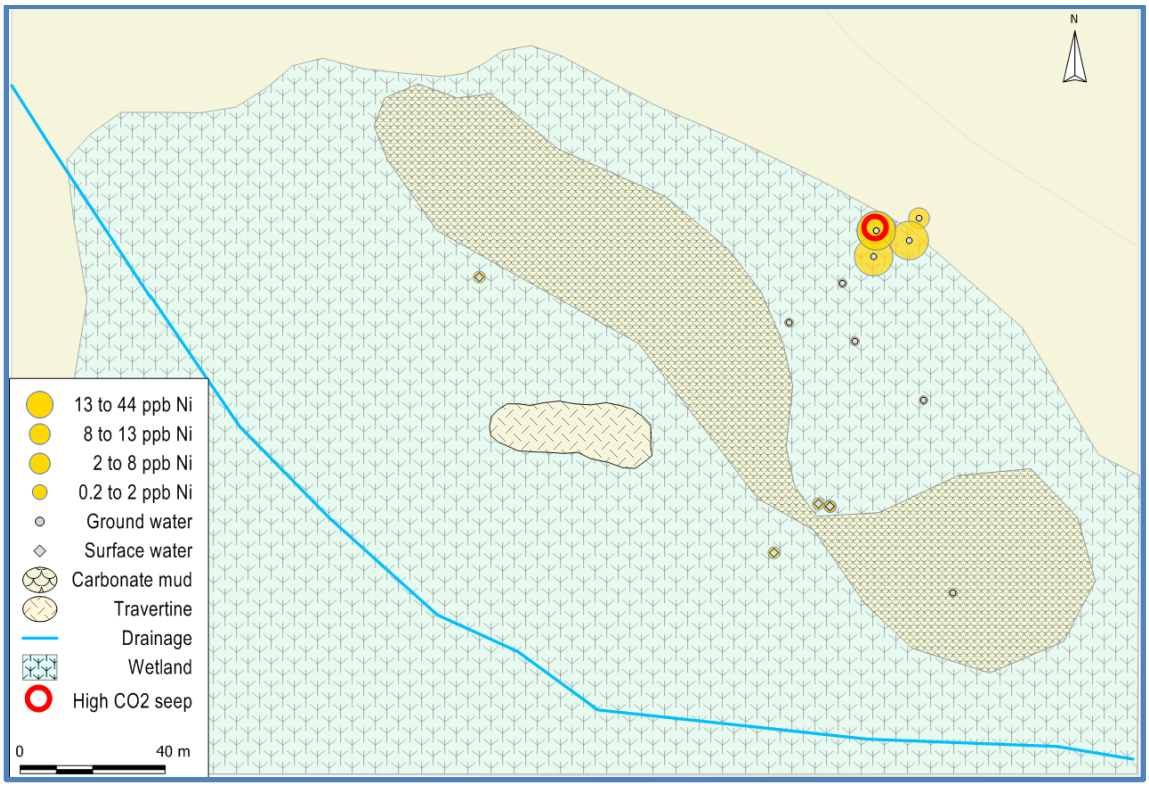

Figure 37 TREK Geothermal project North Bog stream, surface, and ground water nickel.

Figures 34 and 35 reveal increased calcium and magnesium levels in the ground and surface water from the margin towards the middle of North Bog. These elements and dissolved carbon dioxide in surface water also appear to increase towards the west of the bog although the sample density in not sufficient to confirm this concentration variation. The travertine cone – carbon dioxide vent water has 2.5 ppb arsenic and 44 ppb nickel and there are lower levels of these elements in the ground water sampled in the pits near the vent (Figures 36 and 37). The travertine cone water also has up to 3 ppm iron with cobalt and copper levels ranging from 1 to 3 ppb. Samples taken from the travertine cone – carbon dioxide vent water on two different days recorded very similar trace concentrations of all traced elements except iron suggesting a uniform ground water chemistry source.

Ground and surface waters in the South Bog have lower trace element concentrations compared than in the North Bog. Most ground water sample sites shown in Figure 38 are from the surface of travertine where this is a small carbon dioxide seep (Figure 39) and from pits around the deposit.

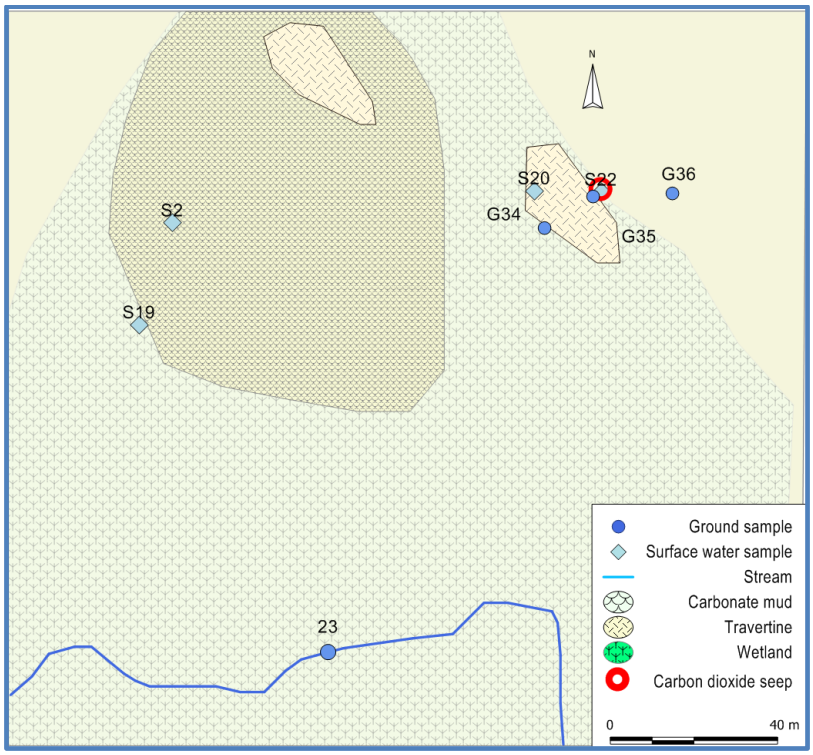

Figure 38 TREK Geothermal Project South Bog surface (S) and ground(G) water samples. The sample numbers are prefixed 201393B.

Figure 39 TREK Geothermal project South Bog travertine water and carbon dioxide seepage. The area of rusty travertine is about 2 m by 1 m.

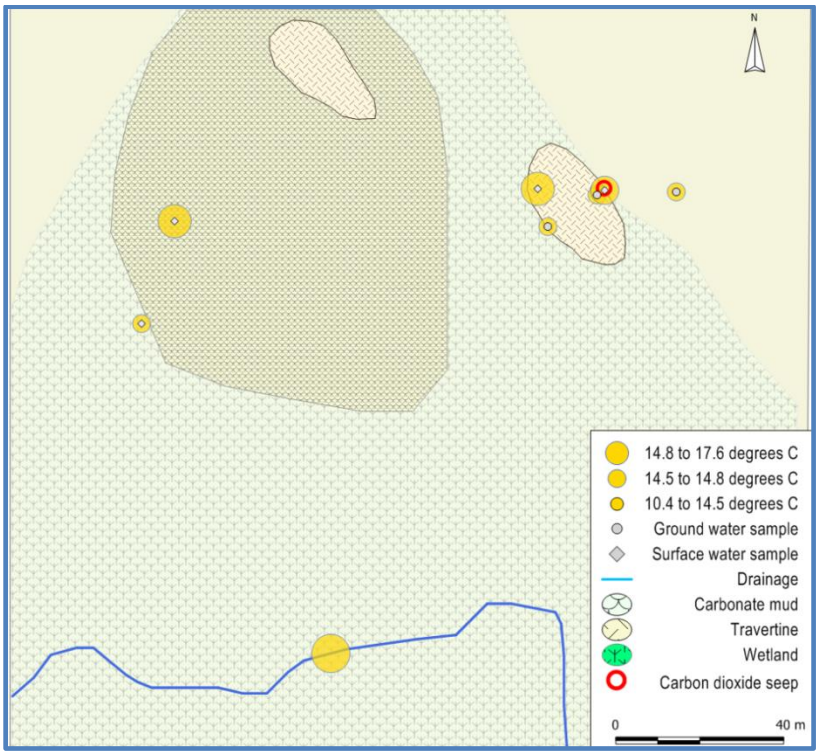

Figure 40 TREK Geothermal project South Bog surface and ground water temperature

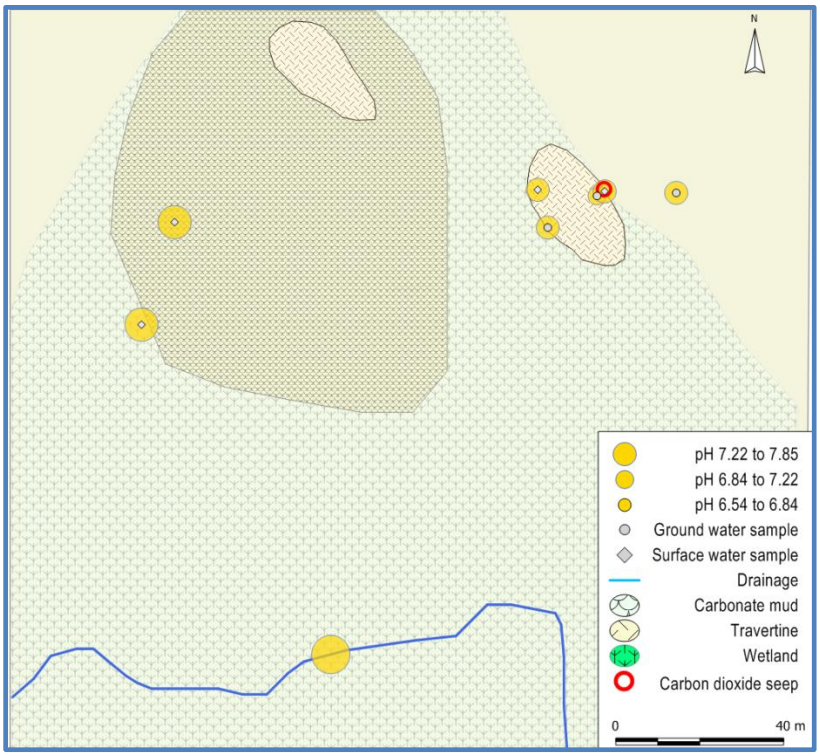

Figure 41 TREK Geothermal project South Bog surface and ground water pH

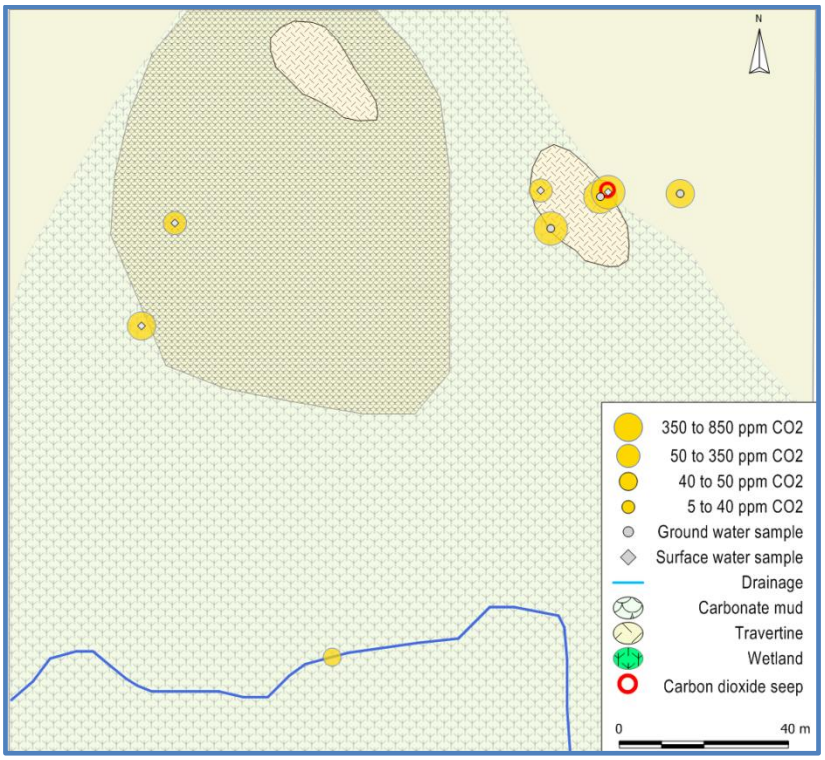

Figure 42 TREK Geothermal project South Bog surface and ground water dissolved carbon dioxide.

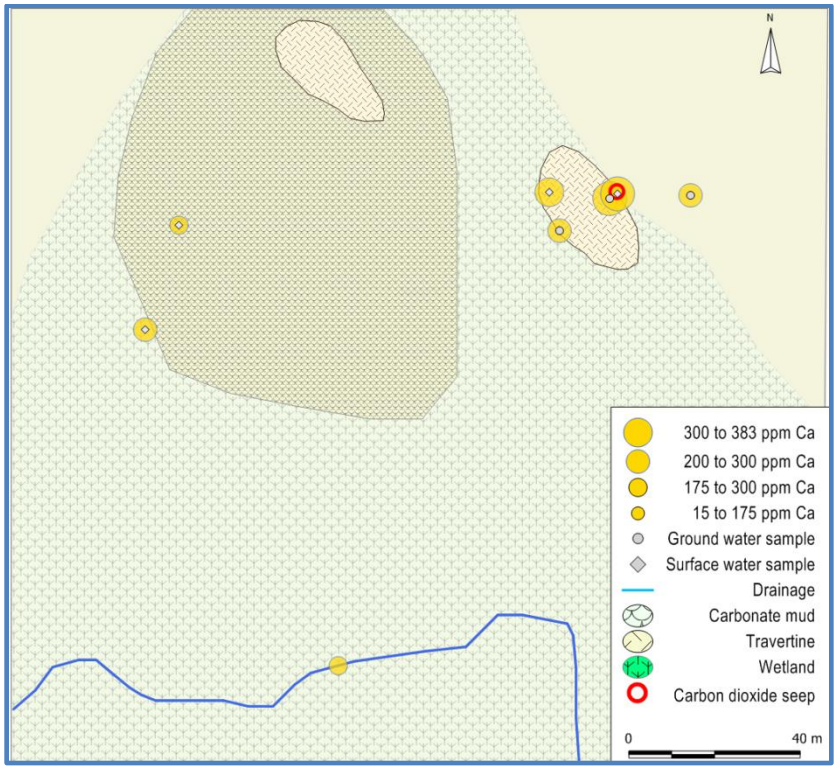

Figure 43 TREK Geothermal project South Bog surface and ground water calcium

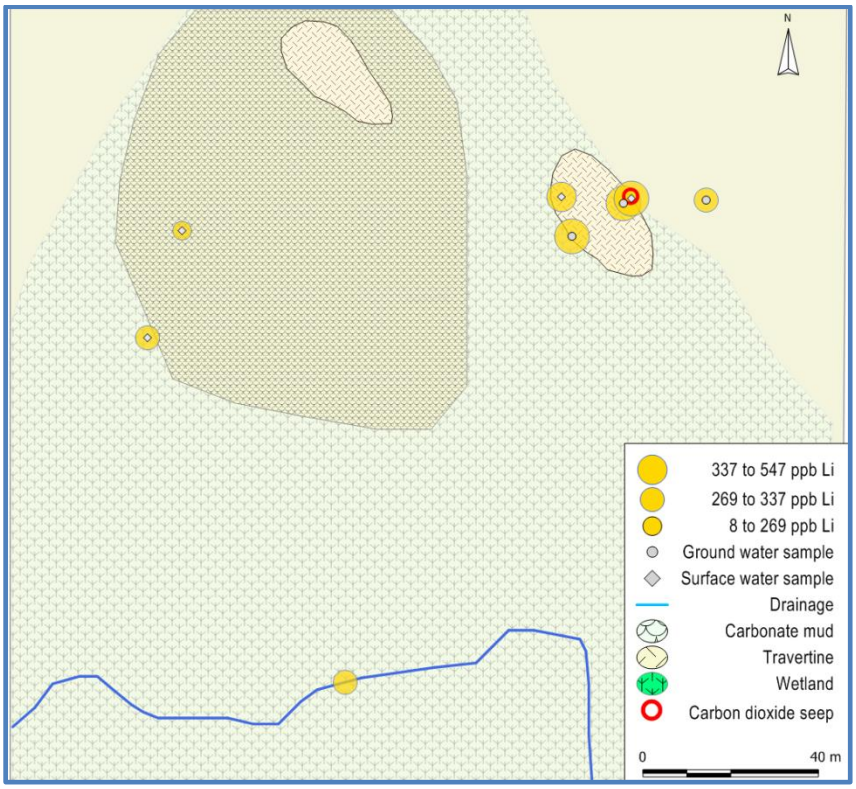

Figure 44 TREK Geothermal project South Bog surface and ground water lithium

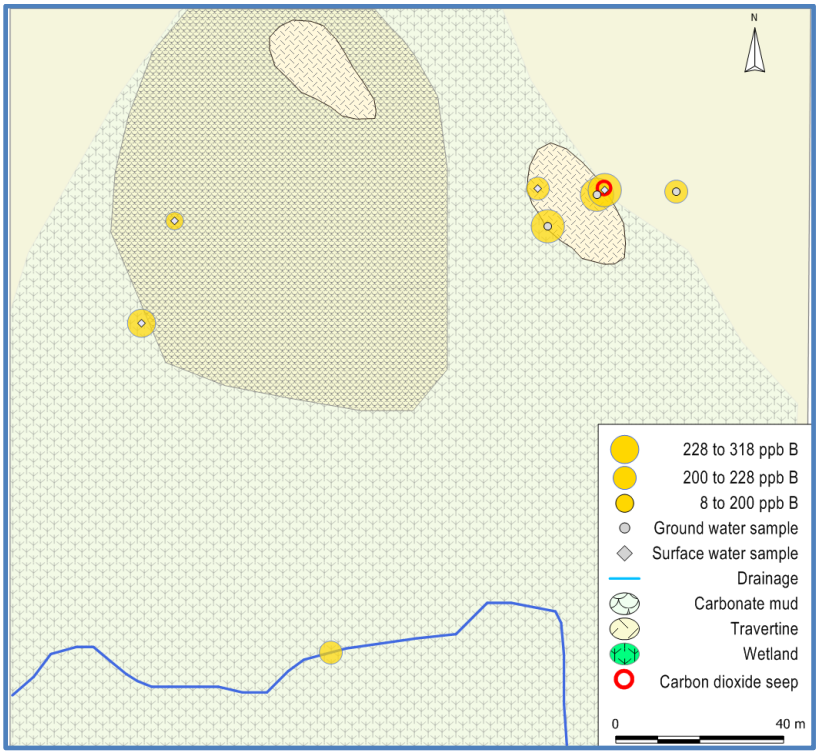

Figure 45 TREK Geothermal project South Bog surface and ground water boron.

Figure 40 shows that South Bog water temperature varies between 10.4 to 17.2^{o} C and that ground water from the travertine carbon dioxide seep has the lowest pH recorded in the bog of 6.54 (Figure 41) This water has the highest dissolved carbon dioxide and dissolved calcium (Figure 42, 43) and there are numerous carbon dioxide seeps to the surface of the South Bog pools as shown in Figure 2. Figures 44 and 45 reveal that maximum boron levels in the ground water (318 ppb) and lower than in the North Bog (637 ppb), but lithium is higher (547 ppb). The concentrations of other potential geothermal pathfinders such as arsenic in the South Bog waters are less than one ppb. The travertine, close association with carbon dioxide slow degassing and numerous seeps into surface pools are all evidence for geothermal activity, but the ground water chemistry does not indicate a significant thermal source for the water.

Soil Geochemistry

The median, third quartile and range for major oxides, minor elements by lithium metaborate (LMB)-ICPMS and trace elements by aqua regia-ICPMS in mineral and bog soils are compared by box plots in Figures 46 to 48. Calcium oxide is higher in bog soils and the bog soil median LMB-ICPMS calcium oxide is similar to the bog soil aqua regia-ICPMS calcium oxide median value indicating that calcium is mainly present as acid soluble calcium carbonate. Median magnesium oxide, total carbon and total sulphur are also higher in bog soils owing to a greater content of organic matter and carbonate minerals. By contrast, the mineral soil has higher median values of LMB-ICPMS silica, aluminum oxide, iron oxide, chromium, nickel, niobium, yttrium and zirconium whereas bog soil has higher boron, zinc and strontium median values. The LMB-ICPMS strontium and aqua regia strontium median values are similar suggesting that strontium is mainly present as strontianite. Among trace elements by aqua regia-ICPMS the medians and third quartiles for cerium, chromium, copper, arsenic, lead, lithium, iron, nickel, mercury, manganese, molybdenum, vanadium, rubidium, yttrium and zinc populations are higher in the mineral soil whereas rhenium, selenium, boron and barium are higher in the bog soils.

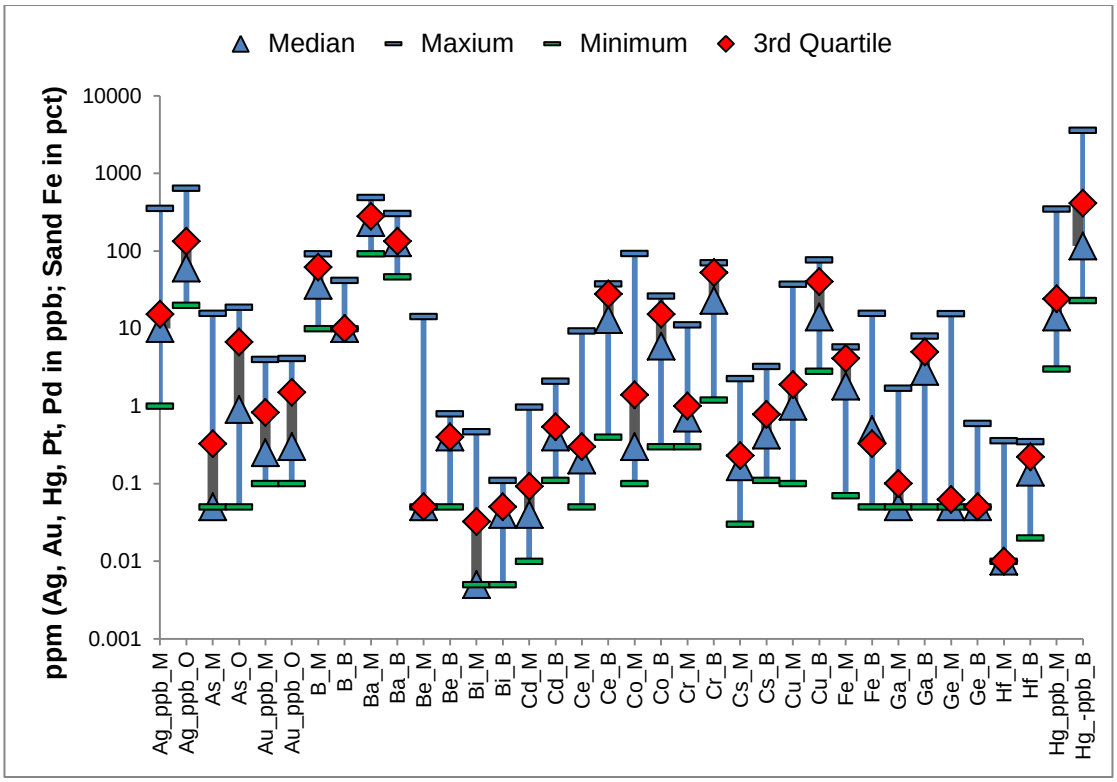

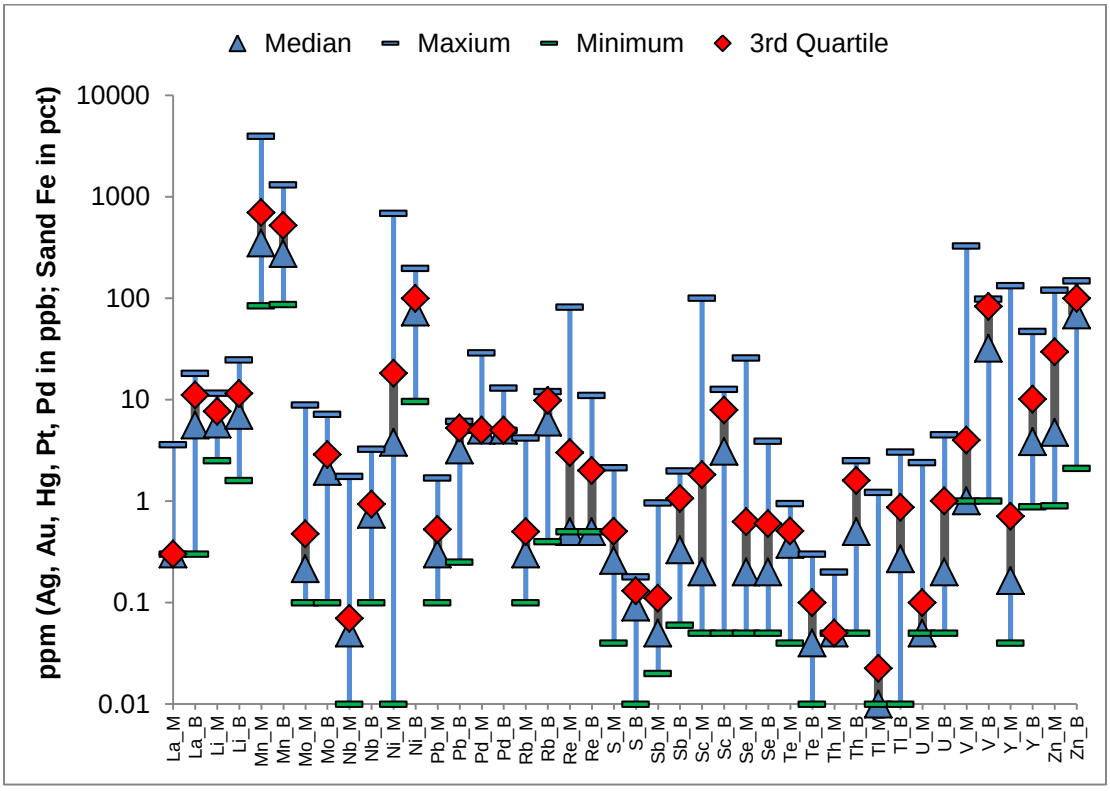

Figure 46 TREK Geothermal project trace element medians, third quartiles and range for 40 bog (B) and 13 mineral (M) soil samples by aqua regia-ICPMS. Platinum and tungsten are not included because most values are below detection limit.

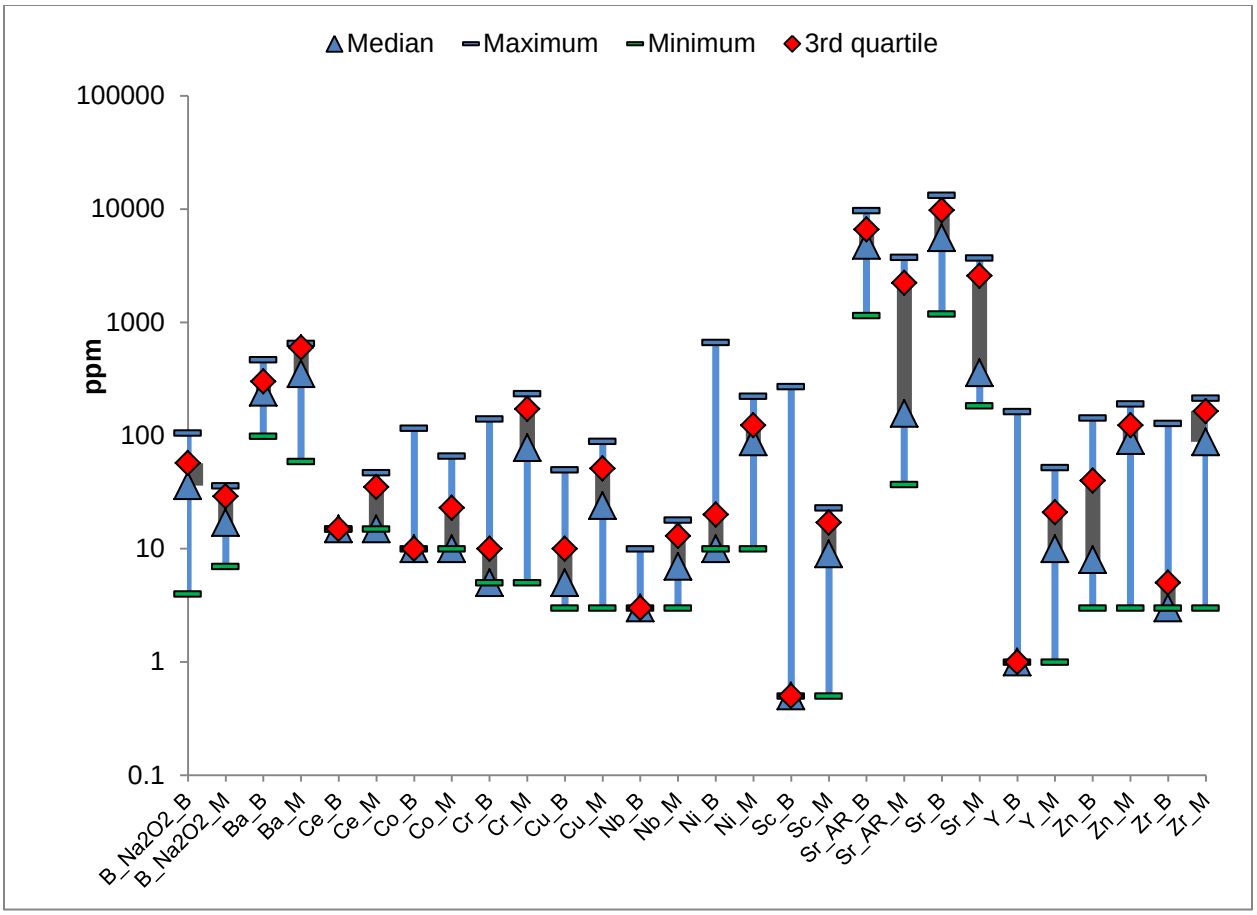

Figure 47 TREK Geothermal project trace and minor element medians, third quartiles and range for 40 bog (B) and 13 mineral (M)soil samples by lithium metaborate-ICPES and by sodium peroxide sinter - ICPMS (boron). Strontium statistics by aqua regia-ICPMS are shown for comparison.

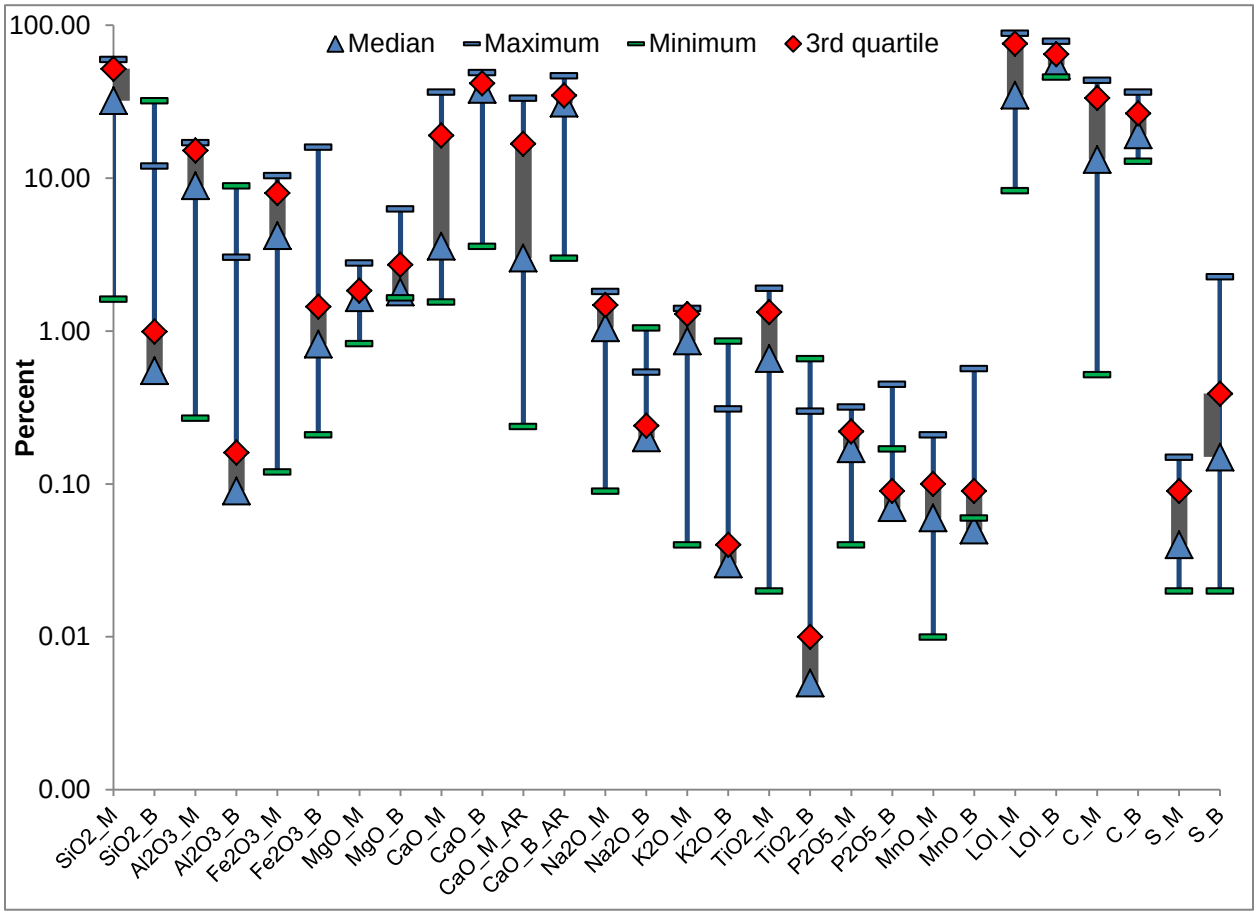

Figure 48 TREK Geothermal project medians, third quartiles and range for major oxides in 40 bog (B) and 13 mineral (M) soil samples by lithium metaborate-ICPMS, aqua regia-ICPMS, loss on ignition (LOI) carbon and sulphur by Leco combustion.

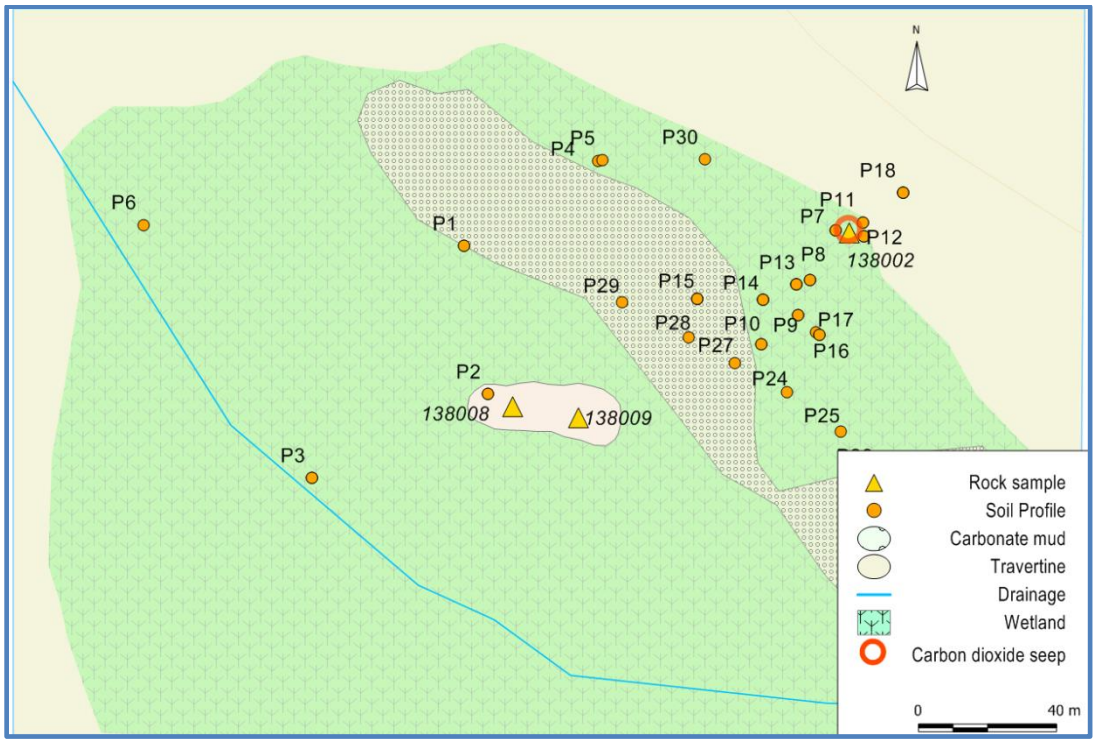

Figure 49 TREK Geothermal project North Bog soil and rock sample locations. Samples corresponding to the profile numbers (P) are listed in Appendix B**.**

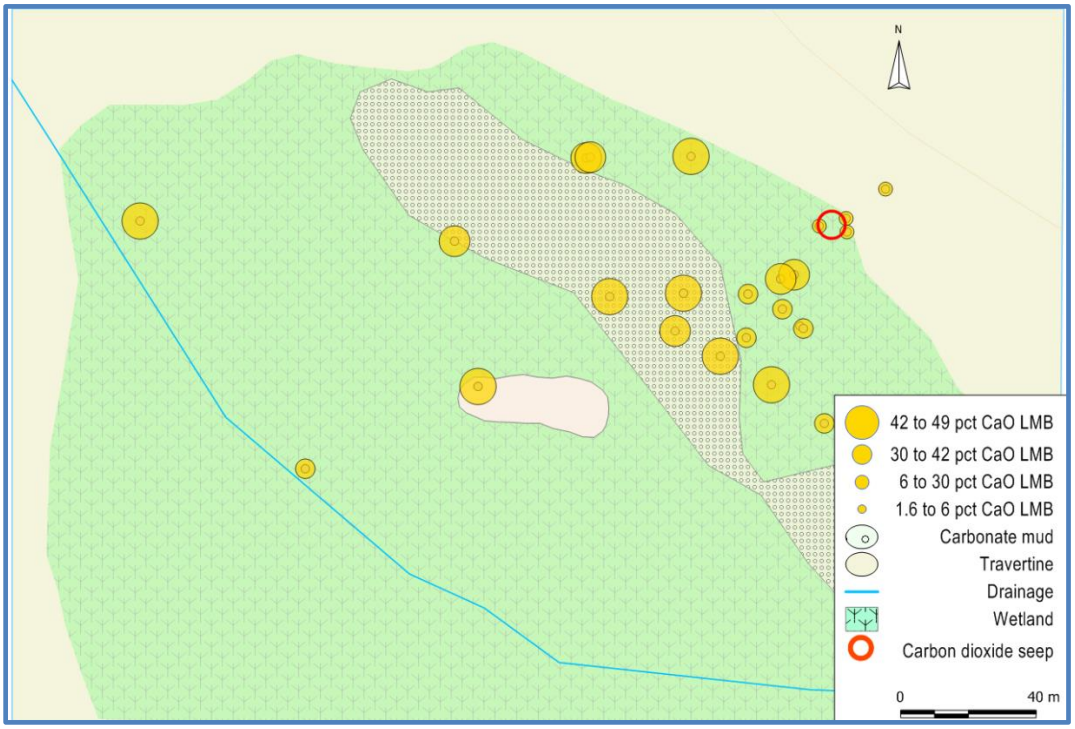

Figure 50 TREK Geothermal project calcium oxide in North Bog mineral C horizon soil samples and deeper bog soils samples by LMB fusion-ICPMS.

Figure 49 shows location of the North Bog soil profiles (P) rather than the individual sample identifications to simplify the map. Soil profiles, their component samples, sample descriptions and the chemistry area listed in Appendix B. The map also shows the location of travertine samples analysed for major oxides and trace elements. In Figure 50 the deeper bog samples typically has more than 30 percent LMB calcium oxide compared to less than 6 percent in the mineral soil C soil horizon. Figure 51 shows an inverse relationship between silica and calcium oxide with up to 56 percent silica in the mineral soil of profiles around the travertine cone, but less than 6 percent silica in the deeper bog soil. Magnesium oxide patterns (Figure 52) differ from calcium oxide and silica because most values in the mineral and bog soil are less than 2 percent and only reach 4 percent northern part of the bog.

In Figure 53, total carbon (by Leco combustion) variation through the bog and surrounding area reflect differences in both soil carbonate and soil organic matter content. For example, higher carbon values close to the travertine cone-carbon dioxide vent along the bog margin indicate a mainly organic soil, but values further in the bog reflect a more carbonate-rich matrix of the soil. Figure 4 shows that deeper bog soil samples with more than 2 percent total sulphur cluster 20 metres south west of the travertine cone. These samples also have higher aqua regia-ICPMS iron content (Figure 55) suggesting that the iron may have formed iron sulphides.

Since the boron and lithium water can indicate geothermal activity these elements might be also expected to be higher in the bog soil if there is a thermal source. Figures 56 and 57 show that the boron levels (by sodium peroxide sinter-ICPMS) in the deeper bog soil horizon reach 84 ppm with lithium values to 11.7 ppm. Samples with most boron and lithium are also from the bog margin near travertine cone-carbon dioxide vent. Samples with higher lithium are also from other bog profiles to the west in an area covered by carbonate mud.

Mercury shown in Figure 58 is over 3000 ppb in water-saturated, organic soil sampled 20 metres away from the travertine cone-carbon dioxide vent. The mercury content of the soil increases from 1528 ppb at 5 to 10 centimetres depth to 3600 ppb at 35 to 40 centimetres depth. Nickel, silver, molybdenum, selenium and rhenium show a concomitant increase with the higher mercury, but values decrease with depth rather than increase. An analysis of a field duplicate sample of the deeper soil found 3515 ppm mercury and reanalysis of this sample detected 3312 ppb. Mercury levels in a brunsolic soil profile 90 metres up slope from the travertine cone-carbon dioxide vent ranged from 116 ppb in the Ah horizon to 405 in glacial sediment (till) at 50 cm depth.

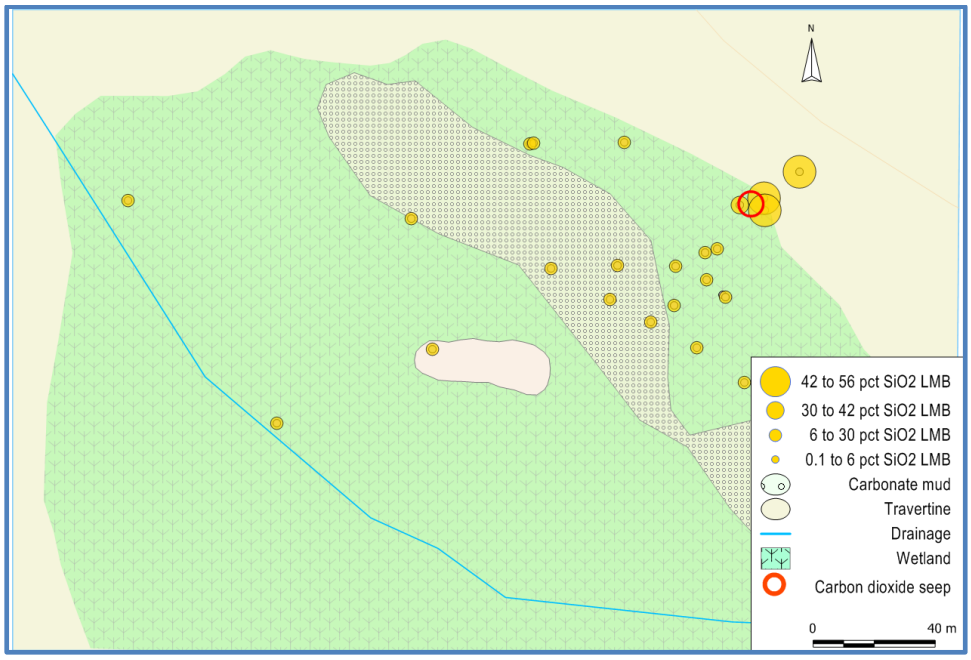

Figure 51 TREK Geothermal project silica in North Bog mineral soil C horizon and deeper bog samples by LMB fusion-ICPMS.

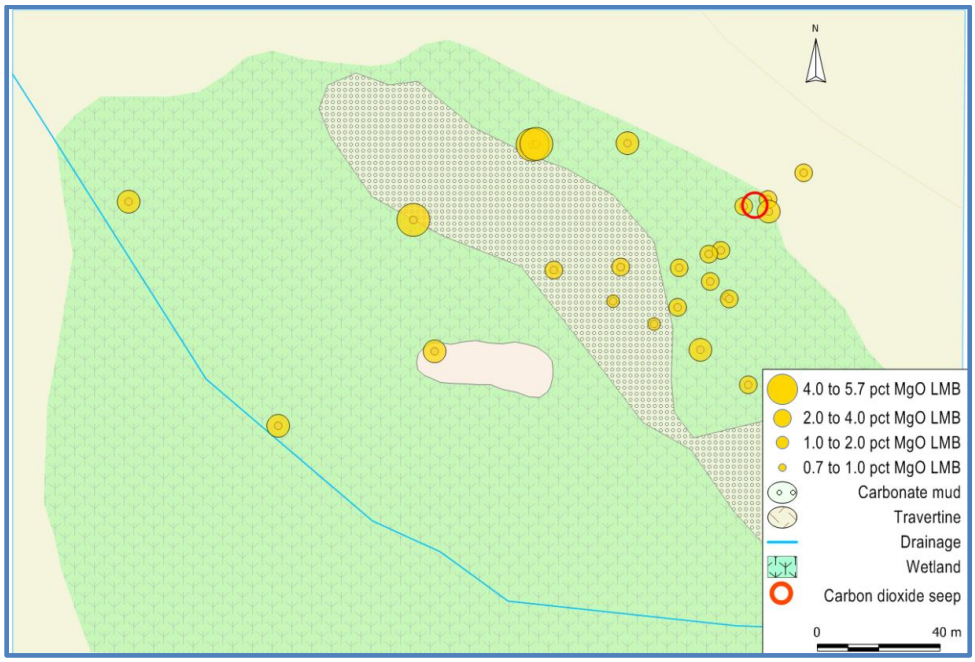

Figure 52 TREK Geothermal project magnesium oxide in North Bog mineral soil C horizon and deeper bog samples by LMB fusion-ICPMS.

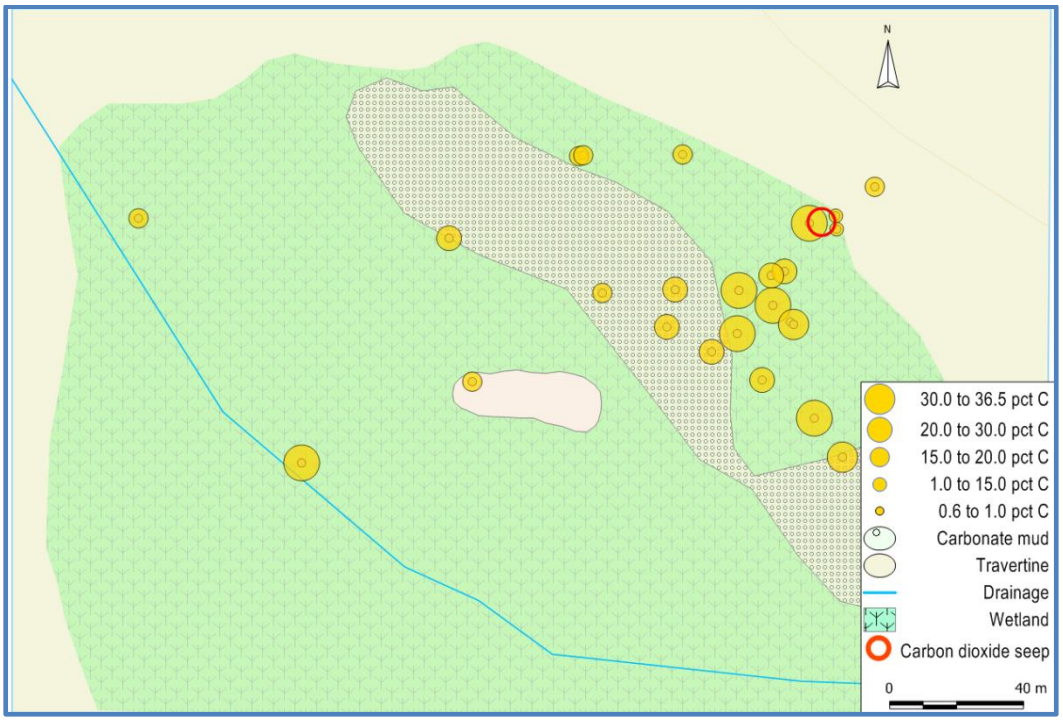

Figure 53 TREK Geothermal project carbon in North Bog mineral soil C horizon and deeper bog samples by Leco combustion**.**

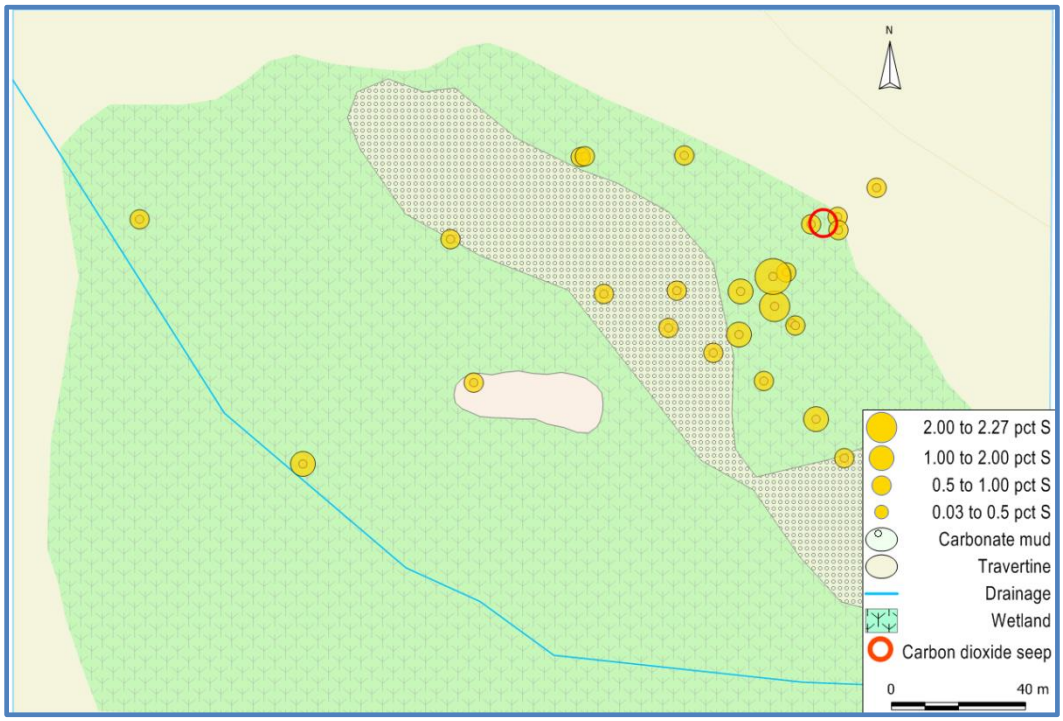

Figure 54 TREK Geothermal project sulphur in North Bog in mineral C horizon and deeper bog soil samples by Leco combustion.

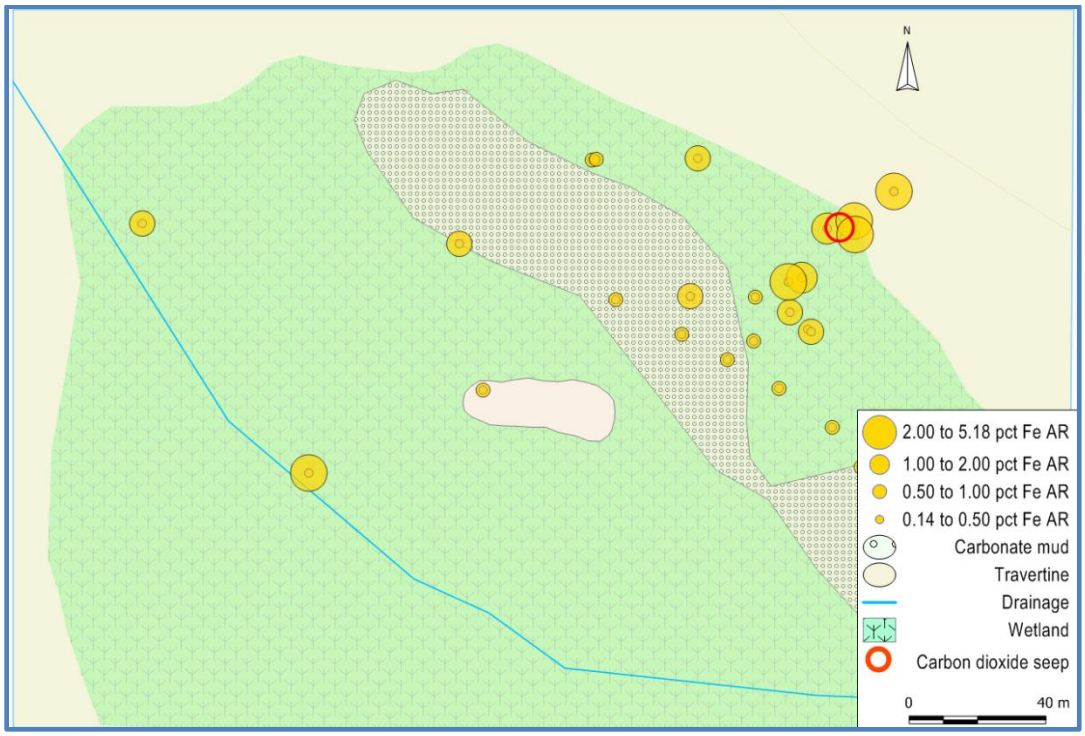

Figure 55 TREK Geothermal project iron in North Bog C soil samples by aqua regia-ICPMS.

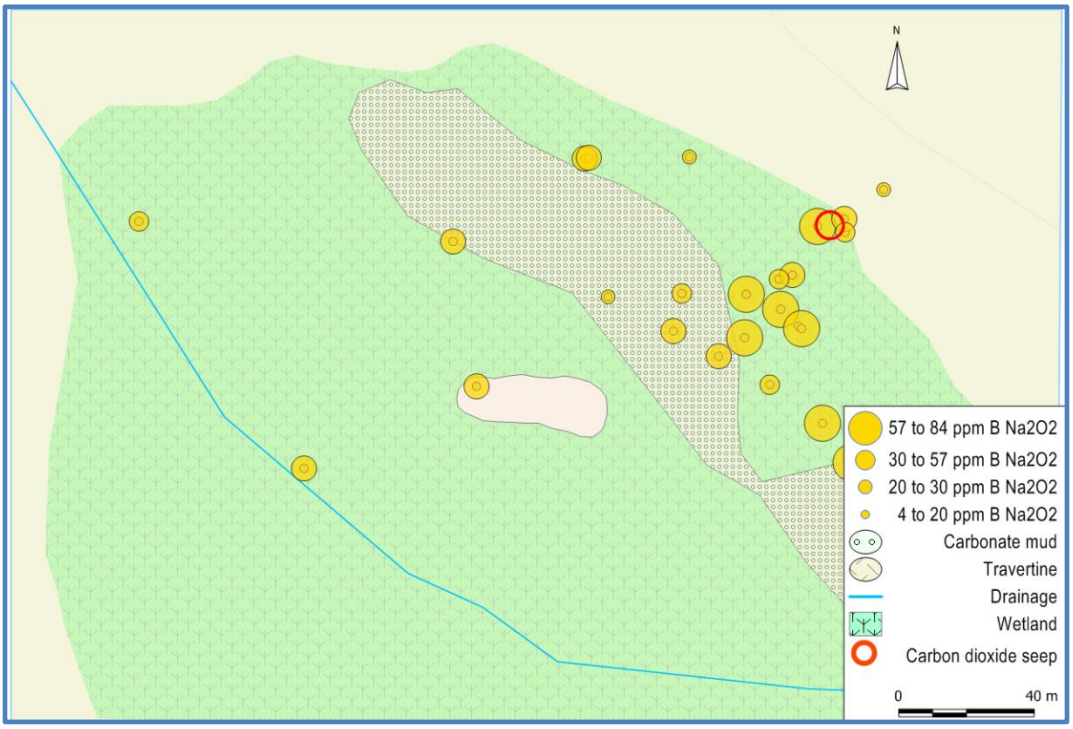

Figure 56 .TREK Geothermal project boron in North Bog C soil horizon samples by sodium peroxide-ICPMS

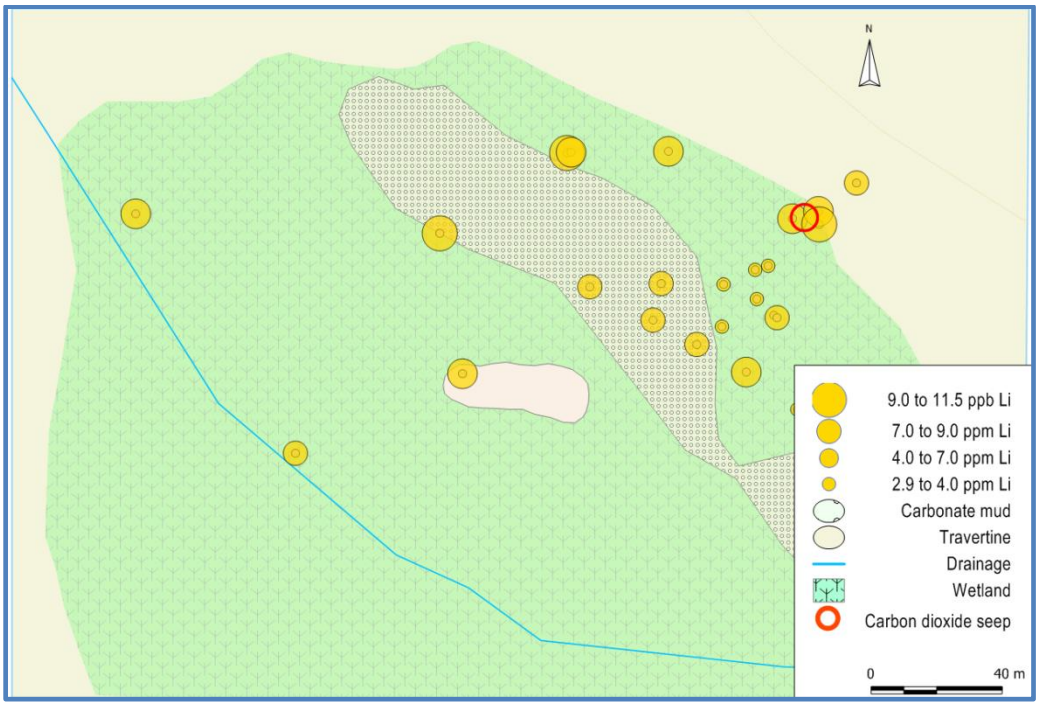

Figure 57 TREK Geothermal project lithium in North Bog C soil horizon samples by aqua regia-ICPMS.

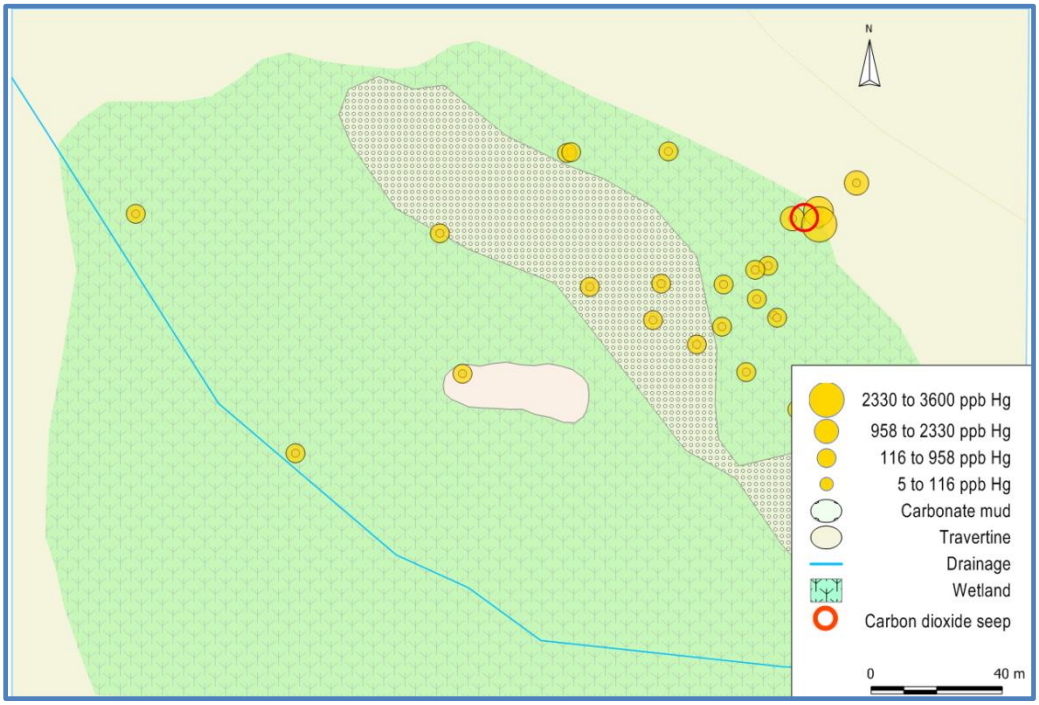

Figure 58 TREK Geothermal project mercury in North Bog C soil horizon samples by aqua regia-ICPMS.

The relationship between chemistry of different soil horizons can be compared in line graphs that show element variation along a traverse beginning in the brunisolic soil on the hill side above the North Bog, through organic soil in the poorly drained bog margin and extending into the area of the bog covered by surface carbonate mud. Depths indicated on the graphs are the average of an individual sample depth measured in each sample profile. The location of the travertine cone-carbon dioxide seep near the edge of the bog is shown on the graph. While the better drained B and C bruinisolic soil horizons can be easily identified in the field it is more difficult to visibly distinguish individual bog soil horizons. Hence, in the graphs organic soil depth rather than horizon is shown. Figure 59 displays a similar mercury pattern for both organic soil depths with the peak mercury value in the deeper, water saturated organic soil 20 metres from the travertine cone-carbon dioxide vent. Mercury values then fall sharply in the organic soil towards the center of the bog. Also, the more shallow bog soil has a higher mercury content than the deeper soil. The soil sample density is not sufficient to allow an estimate of the mercury anomaly size, but since that there are lower mercury values in a brunisolic soil profile 90 west and upslope from the vent and in organic soil to the east the anomaly is probably less than 100 metres wide.

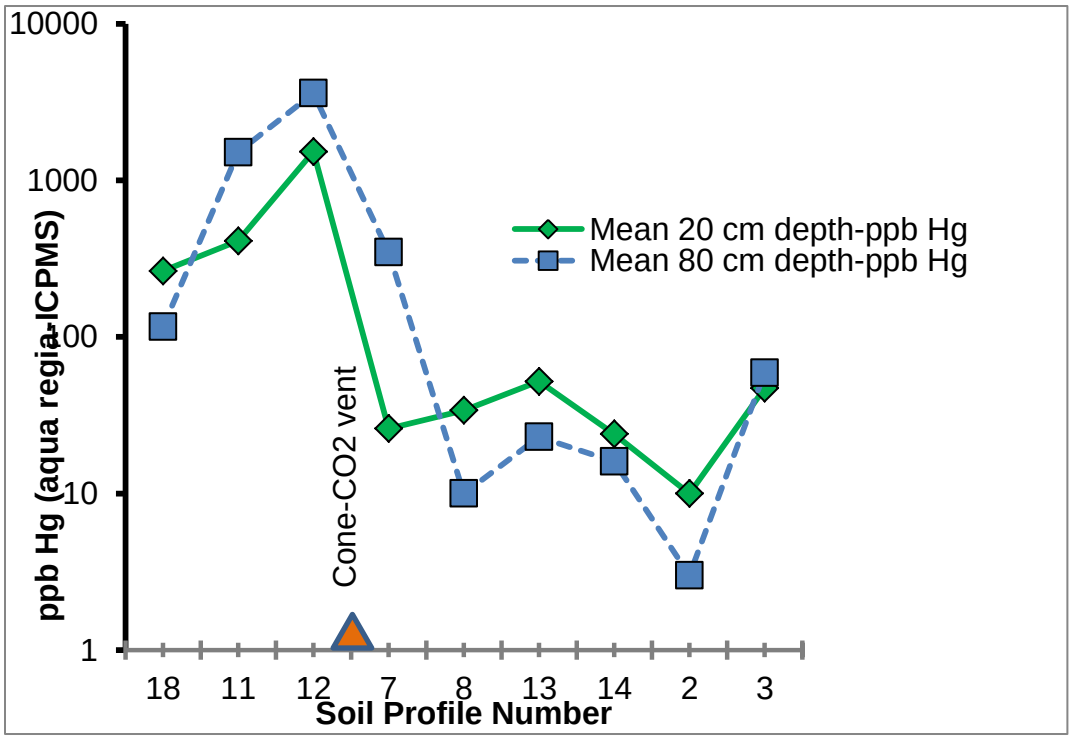

Figure 59 TREK Geothermal project mercury patterns in North Bog soil. Horizontal distance is not to scale.

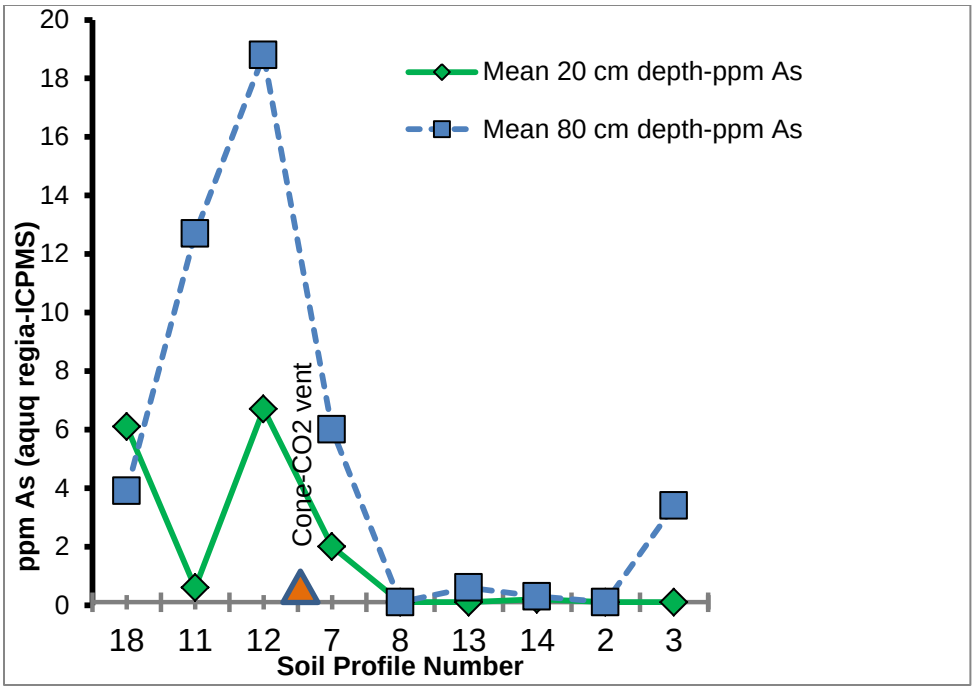

Figure 60 TREK Geothermal project arsenic patterns in North Bog soil.

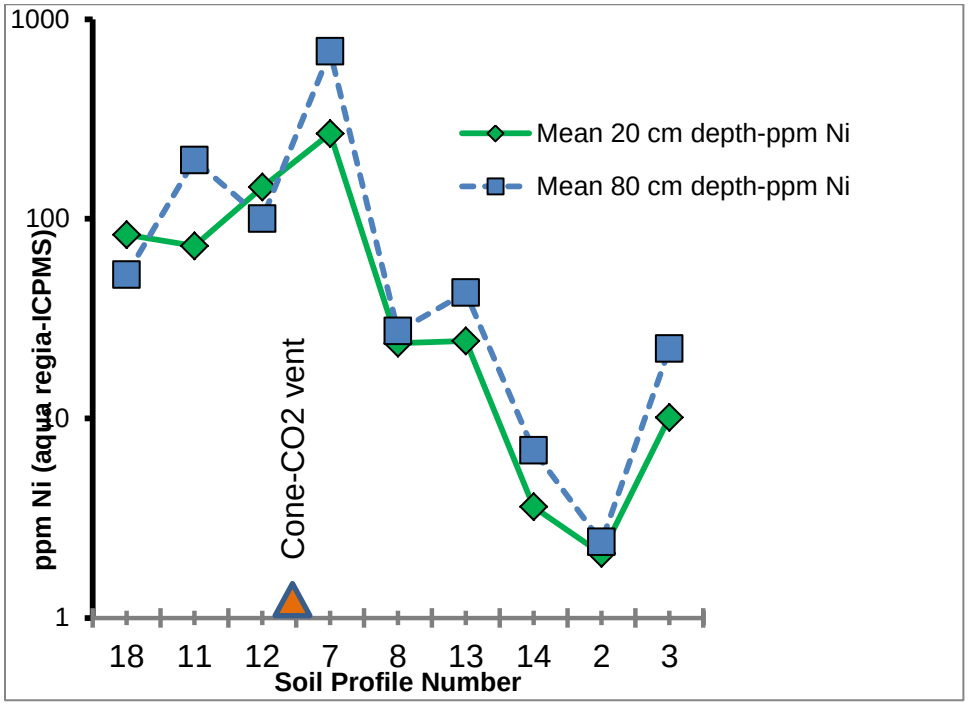

Figure 61 TREK Geothermal project nickel patterns in North Bog soil.

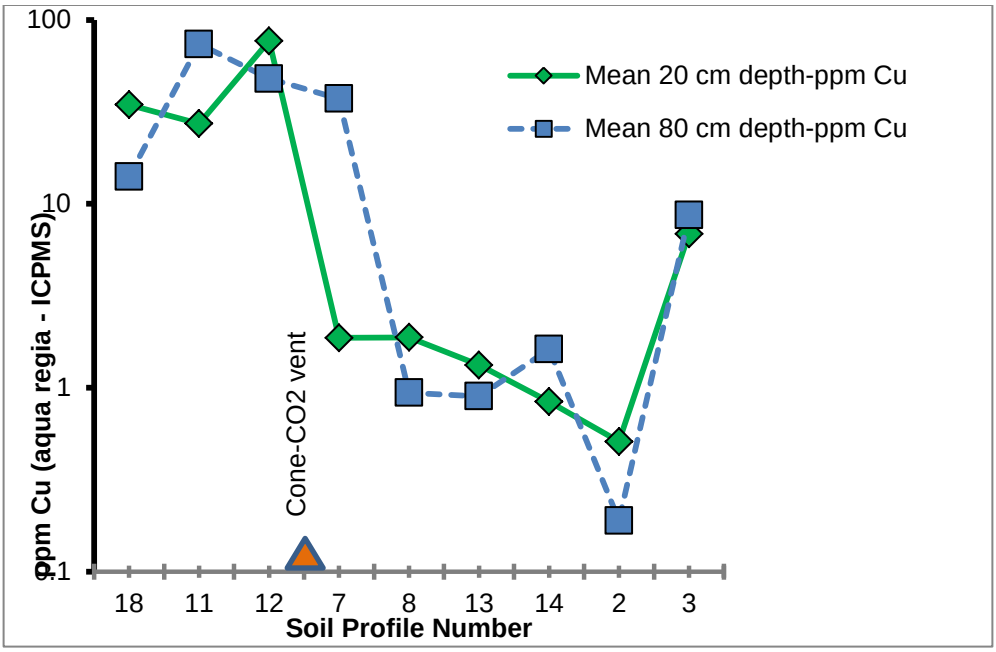

Figure 62 TREK Geothermal project copper patterns in North Bog soil.

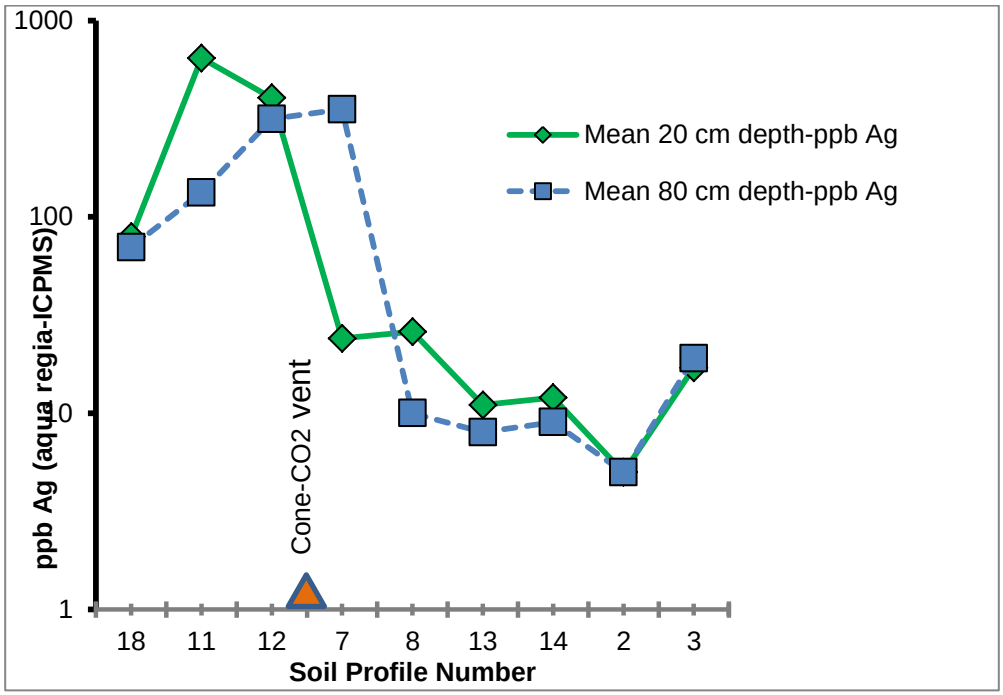

Figure 63 TREK Geothermal project silver patterns in North Bog soil.

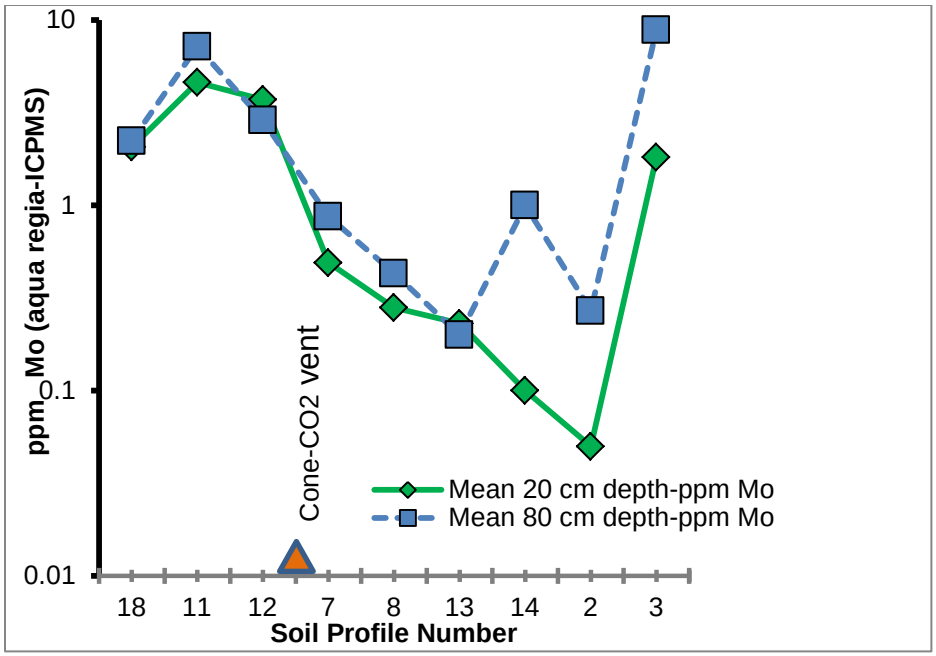

Figure 64 TREK Geothermal project molybdenum patterns in North Bog soil.

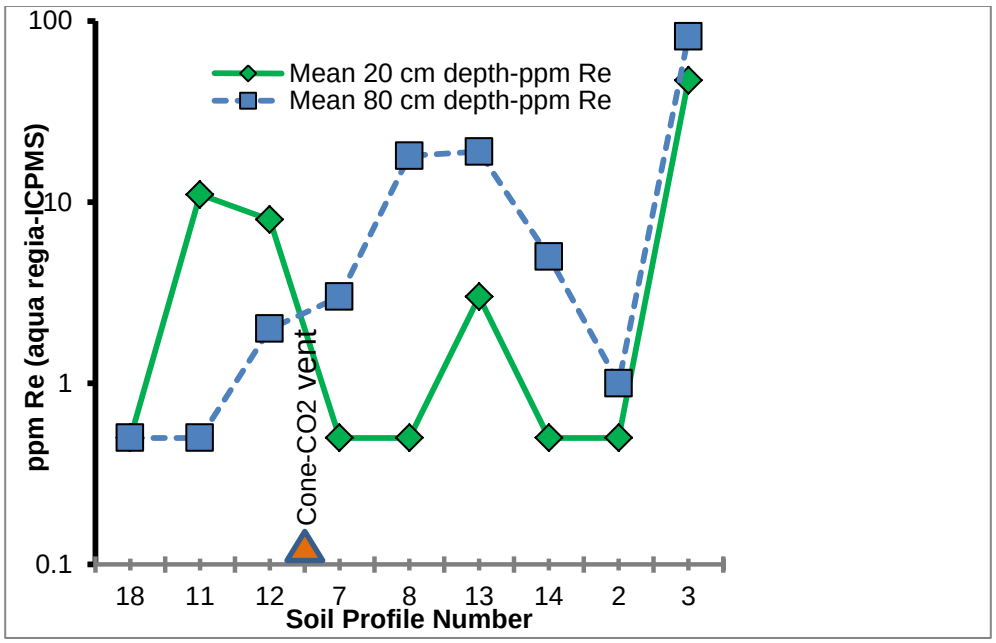

Figure 65 TREK Geothermal project rhenium patterns in North Bog soil.

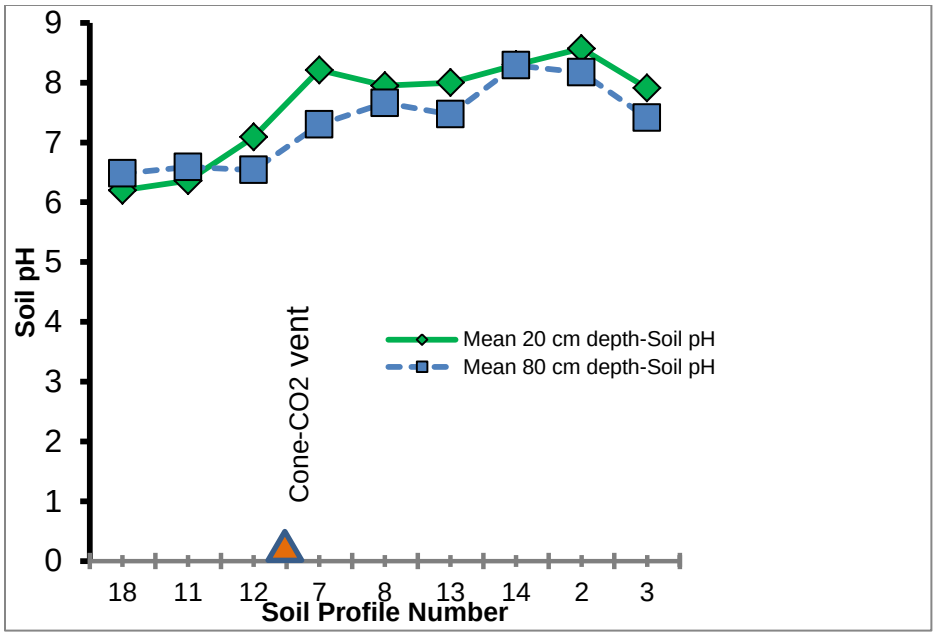

Figure 66 TREK Geothermal project North Bog soil pH patterns.

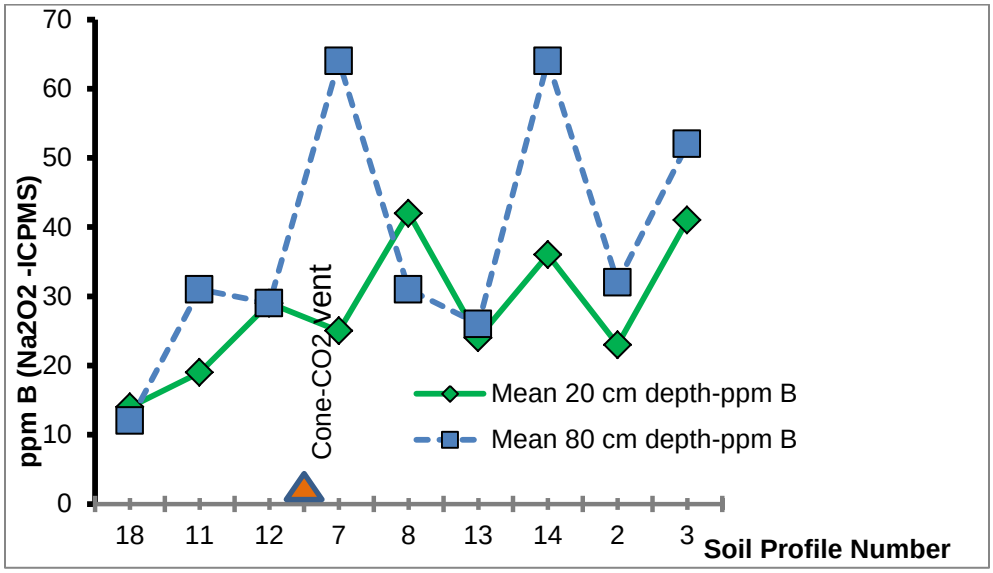

Figure 67 TREK Geothermal project boron patterns in North Bog soil.

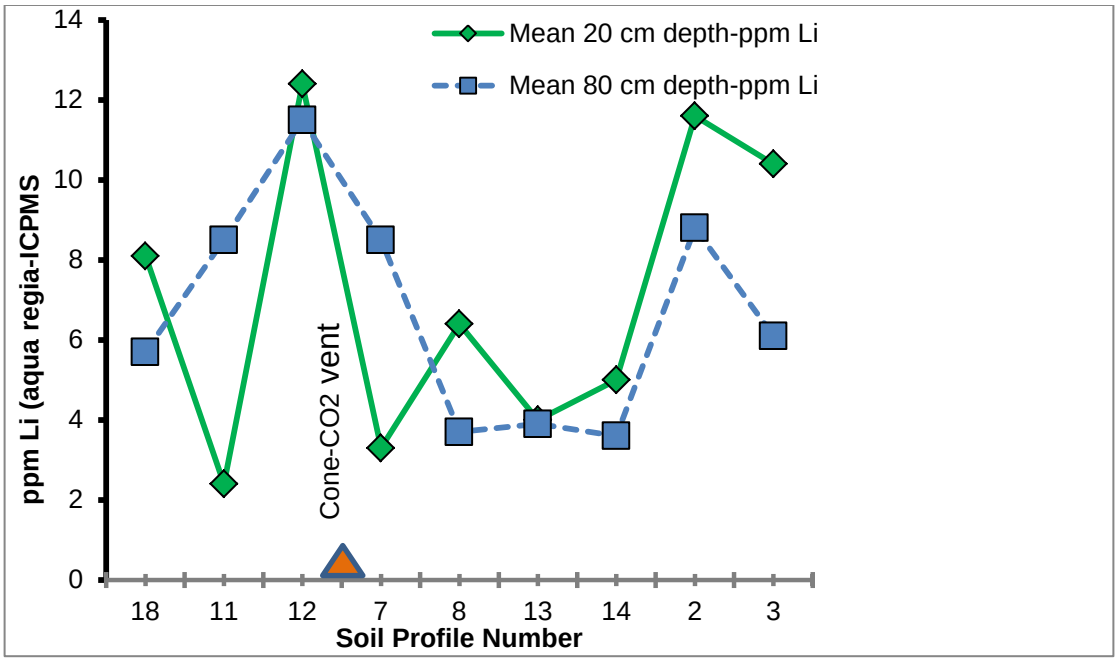

Figure 68 TREK Geothermal project lithium patterns in North Bog soil.

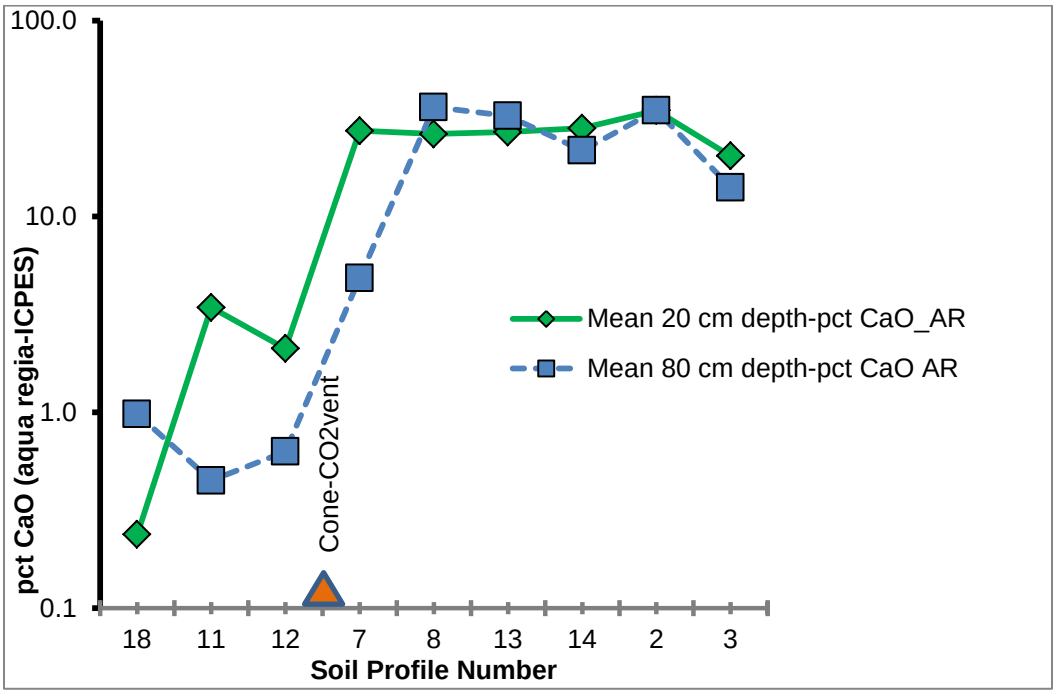

Figure 69 TREK Geothermal project calcium patterns in North Bog soil.

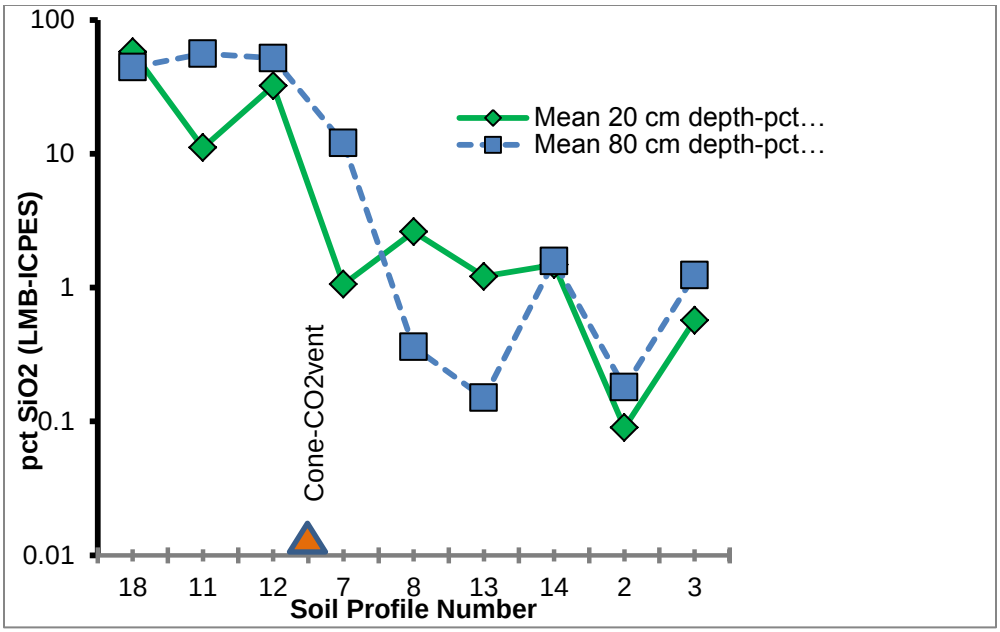

Figure 70 TREK Geothermal project silica patterns in North Bog soil.

Arsenic in Figure 60, nickel in Figure 61, copper in Figure 62, silver in Figure 63, molybdenum in Figure 64 and rhenium in Figure 65 all show a similar pattern with a high value corresponding to the water saturated organic soil near the travertine cone-carbon dioxide vent. Element contents in the organic soil then decreases where the surface is covered by carbonate mud, but then increase again in the more central part of the bog. This pattern is especially marked for the concomitant molybdenum and rhenium increase and the higher values may, in part, reflect a change in the pH of the bog soils shown in Figure 66. Boron in Figure 67 and lithium in Figure 68 also show higher values for the deeper organic soil close to the bog margin and in the middle of the bog. Patterns for calcium in Figure 69 and silica in Figure 70 differ from other trace elements in that calcium sharply increases from the better drained soil into the bog whereas silica decreases. Only the shallow soil variation in the two oxides increases to a peak in the water saturated, organic soil along the bog margin.

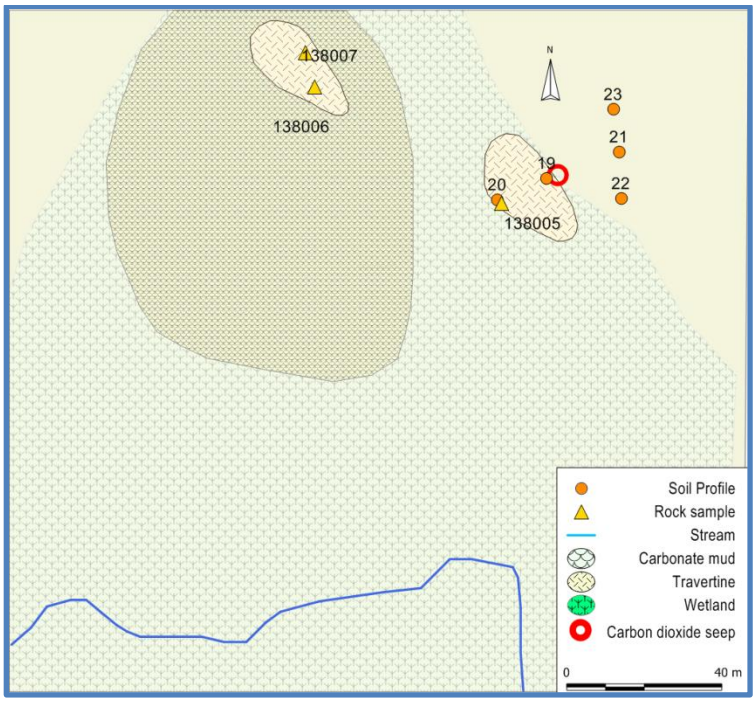

Figure 71 TREK Geothermal project South Bog soil profile locations.

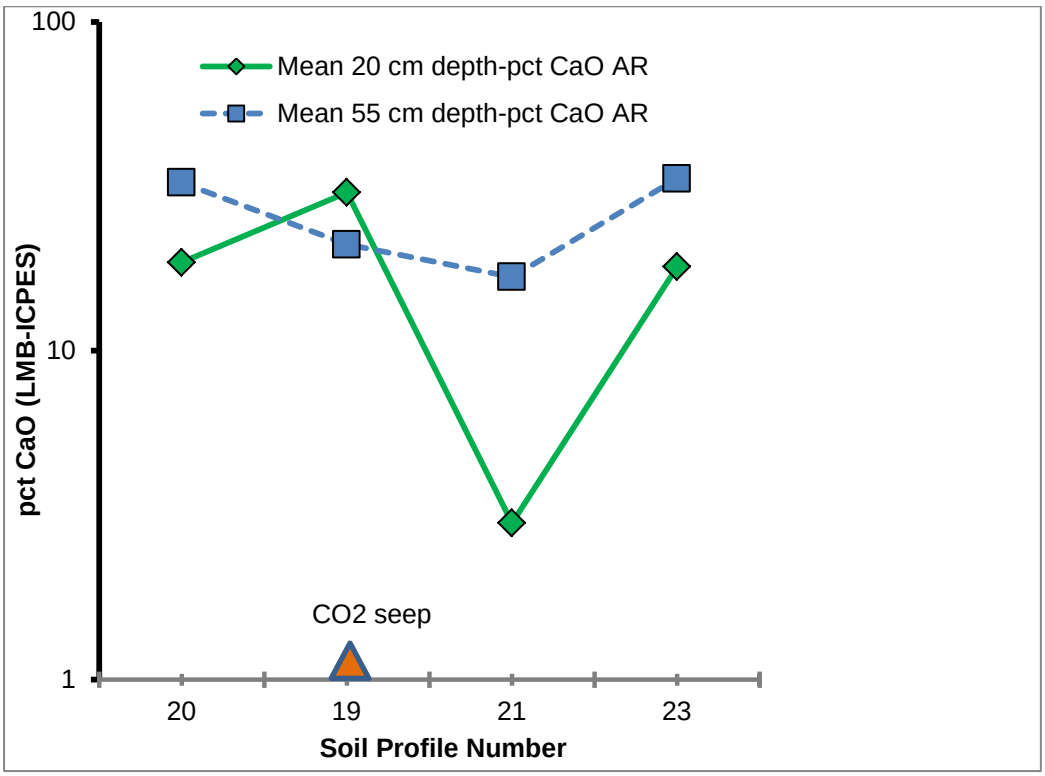

Figure 72 TREK Geothermal project calcium profiles in South Bog soil. Horizontal distance not to scale

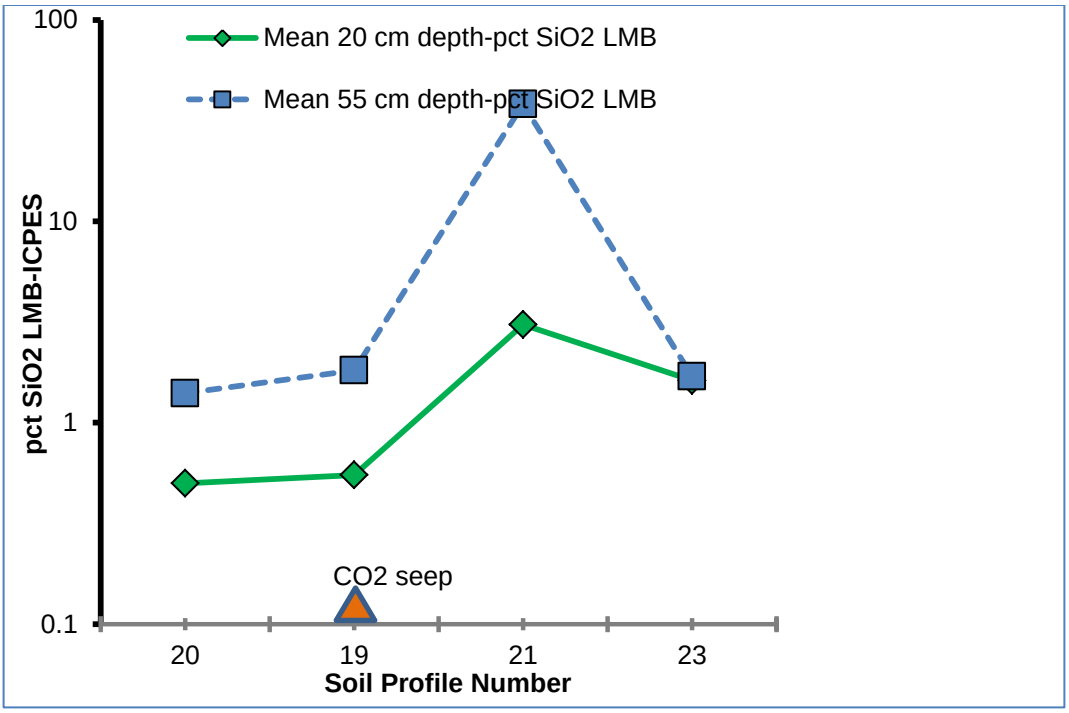

Figure 73 TREK Geothermal project silica profiles in South Bog soil.

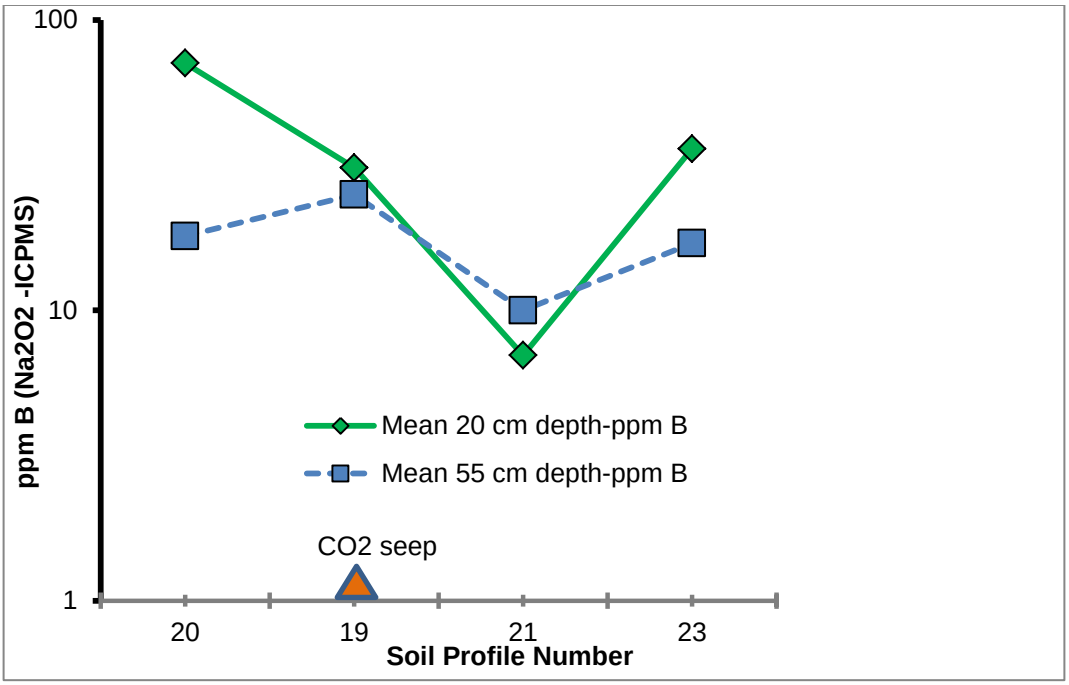

Figure 74 TREK Geothermal boron profiles in South Bog soil.

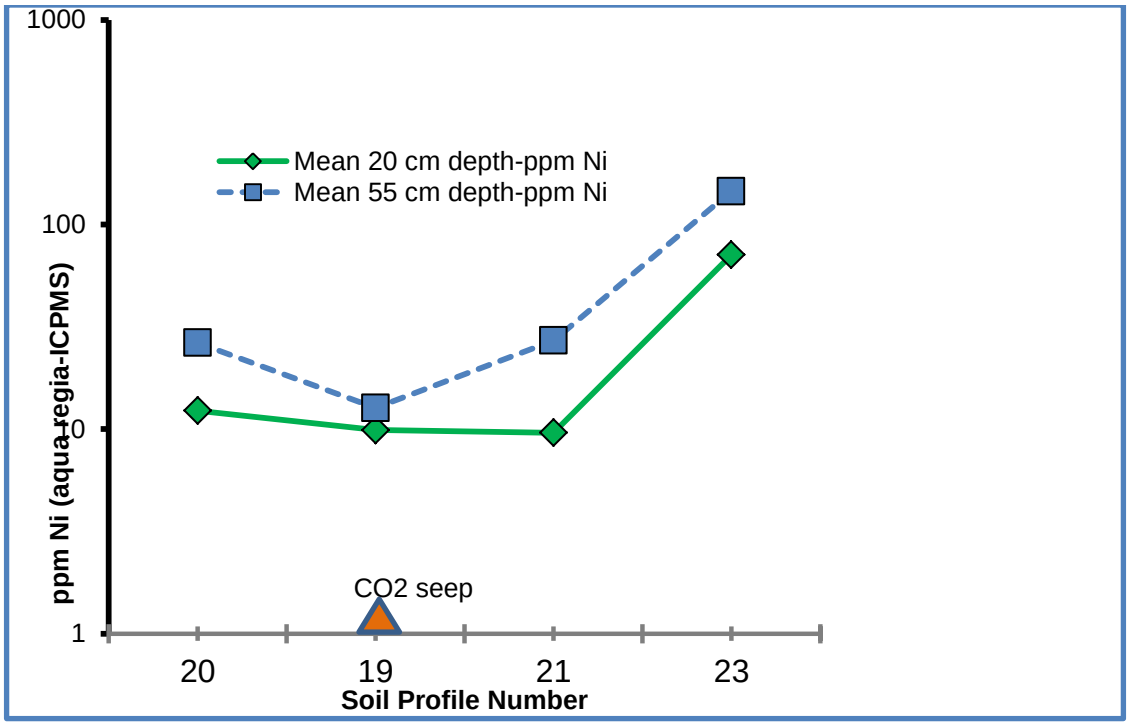

Figure 75 TREK Geothermal project nickel in South Bog soil.

Figure 71 shows location of soil profiles in the South Bog. Unlike trace element patterns in the North Bog, most elements in the South Bog soil do not increase in poorly drained organic soil near a carbon dioxide seep in a travertine deposit. Calcium oxide in Figure 72 and boron in Figure 73 increase from the organic soil into the travertine covered area whereas silica in Figure 74 and nickel in Figure 75 decreases. Both calcium and silicon oxides are higher in the deeper samples compared to the near-surface horizons. The highest mercury found in the South Bog soil is 106 ppb.

Weathering of the glacial deposits may be the main source for trace metals detected in soil and water in the North and South Bog. Figure 76 shows that the TREK regional till survey samples have up to 514 ppb mercury at two sample sites south and west of the Nazko Cone compared to up to 3600 ppb in the C soil horizon sampled on the edge of the North Bog. While nickel in the water saturated organic soil reaches 196 ppm the nickel content of the C soil horizon from a bruisolic profile is only 90 ppm, but this compares with up to 110 ppm in the till samples north west of the Nazko Cone (Figure 77). The higher nickel content of the till north west of the bogs suggests that sediment with a greater nickel background has been dispersed by ice-flow from a bedrock source to the south.

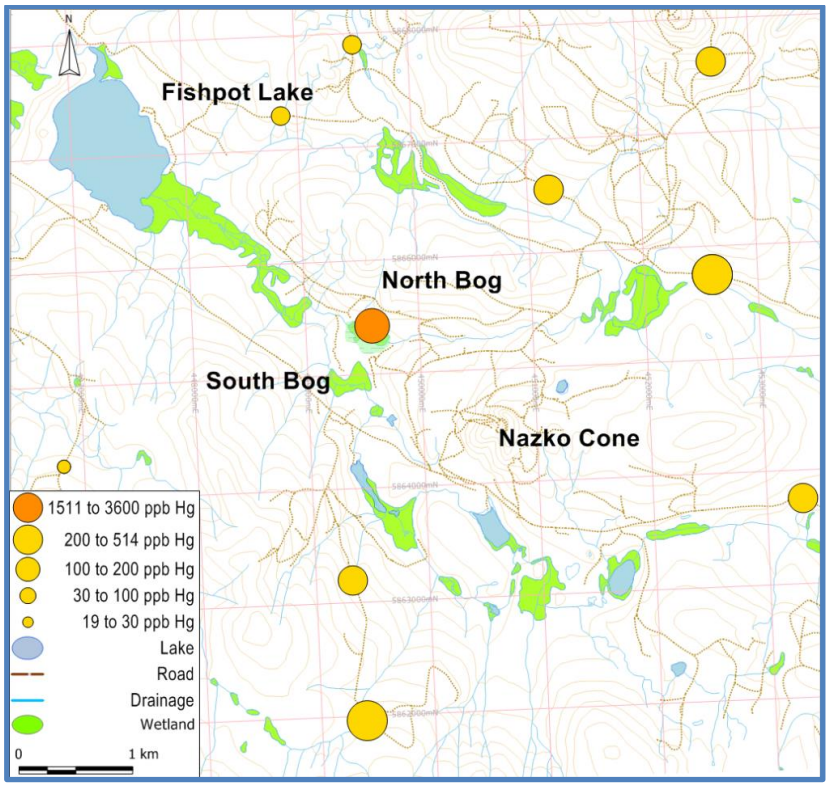

Figure 76 TREK Geothermal project North Bog C horizon and TREK regional till mercury

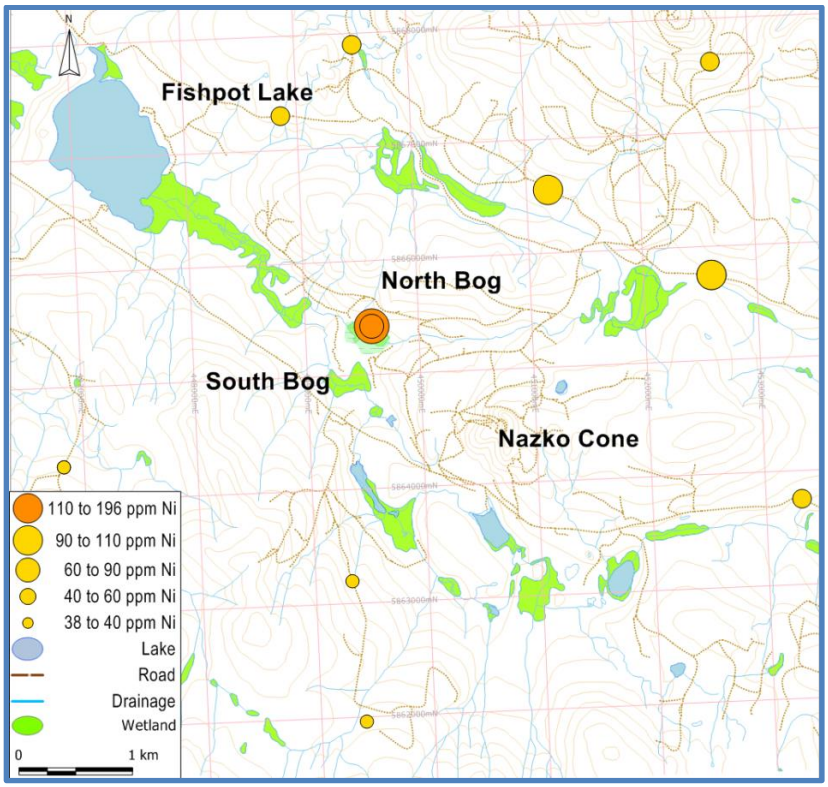

Figure 77 TREK Geothermal project North Bog C horizon and TREK regional till nickel

Rock Geochemistry

Figure 78 shows the location of the rock samples collected in the area surround the bogs and Table 9 gives a description of each sample and sample location coordinates. Trace, minor and major element data for the samples are listed in Tables 10 and 11. While the two bedrock samples, 138003 and 138010, are both identified as basalt they have a different major oxide chemistry. Sample 138010 is from a porphyritic olivine basalt flow mapped by Souther et al. (1987) as bedrock Unit 3b. The major oxide chemistry reported by Souther et al. (1987), for this Unit is similar to those for sample 138010 from a road side outcrop south of the Nazko Cone. However, bedrock sample 138003 from a stream bank outcrop north of the Cone has much less silica and more calcium oxide than the basalt samples reported by Souther et al. 1987 and data for 138010. Compared to basalt sample 138010 this rock also has lower sodium oxide, iron oxide, potassium oxide, magnesium oxide, zirconium and nickel, but higher strontium. The contrasting chemistry of the two basalts might reflect a difference in the volcanic rock and greater weathering of the rock at site 138003 causing a higher calcium coating to the basalt vesicles.

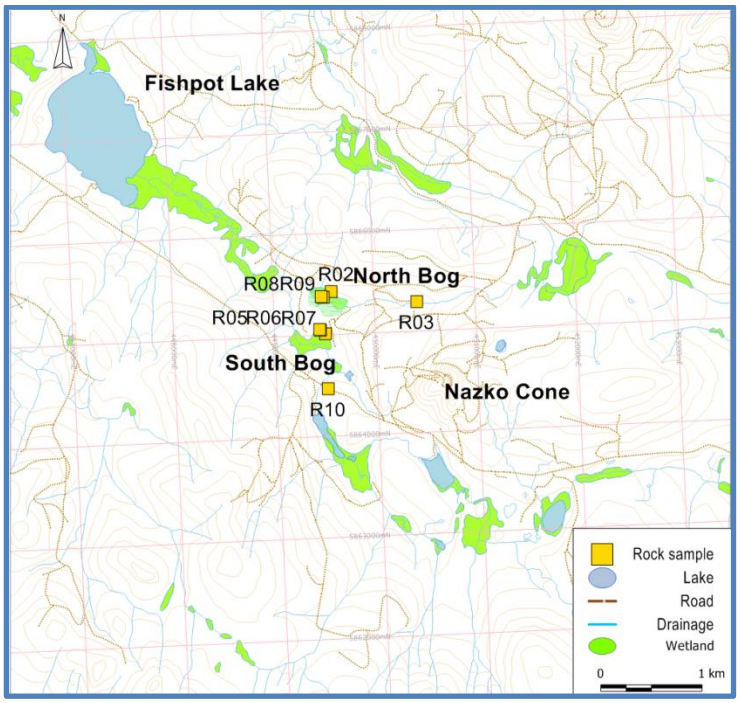

Figure 78 TREK geothermal project rock sample locations. The sample prefix "R" on the map corresponds to "1380" in Tables 9 to 11.

Sample	UTM-East	UTM-North	Description
138002	449579	5865423	Rusty travertine. Forms part of the internal wall of a small cone shaped vent. Active gas bubbling from base of vent.
138003	450422	5865292	Outcrop 2-3 m by 15-20 m of vesicular basalt in creek bank. Vesicles filled with calcite.
138005	449501	5865015	Travertine from slab on surface of south bog.
138006	449454	5865047	Travertine sample from area (1-2 m diameter) in south bog by large area of carbonate mud surface.
138007	449452	5865056	Sample of "white" travertine blocks up to 1 m x 1 m x 25 cm thick from roughly lobate area 100 m x 60 m.
138008	449498	5865373	Rusty travertine from east end on low north-south aligned ridge in northern bog separating carbonate mud from sedge growth bog.
138009	449480	5865377	"White" travertine from west end on low north-south aligned ridge in northern bog about 15 m west from 138008.
138010	449507	5864469	Sample of vesicular basalt from outcrop 3-4 m high 5 m from south side of 4000 road. Calcite coats vesicles.

Table 9. Rock sample descriptions and sample location coordinates.

Analyte	138002	138003	138005	138006	138007	138008	138009	138010
Ag_ppb	4	32	6	6	8	-2	3	22
Al_pct	0.01	3.43	-0.01	-0.01	-0.01	-0.01	-0.01	1.68
As_ppm	13.4	0.8	0.7	0.8	-0.1	0.4	0.2	0.6
B_ppm_Na2O2	6	7	11	9	11	14	13	9
Ba_ppm	324.8	228.9	195.7	263.6	224	364.2	304.7	30.1
Be_ppm	0.3	0.8	-0.1	-0.1	-0.1	-0.1	-0.1	0.7
Ca_pct	31.67	20.48	33.68	32.06	31.37	30.96	32.04	2.26
Cd_ppm	0.55	1.68	0.03	0.02	0.04	-0.01	-0.01	0.1
Ce_ppm	0.4	35.7	-0.1	-0.1	-0.1	-0.1	-0.1	29.7
Co_ppm	10	34.3	2.2	13.3	-0.1	-0.1	-0.1	35.4
Cr_ppm	-0.5	54.4	-0.5	-0.5	-0.5	-0.5	-0.5	53.6
Cs_ppm	-0.02	0.11	0.03	0.05	0.05	0.02	-0.02	0.09
Cu_ppm	1.24	20.94	0.37	0.6	0.39	0.25	0.28	38.69
Fe_%	3.93	4.33	0.04	1.22	0.02	2.45	0.04	4.87
Ga_ppm	-0.1	9.3	-0.1	-0.1	-0.1	-0.1	-0.1	6.5
Hf_ppm	0.02	0.39	-0.02	-0.02	-0.02	-0.02	-0.02	0.22
Hg_ppb	449	56	-5	-5	-5	6	-5	5
In_ppm	-0.02	0.04	-0.02	-0.02	-0.02	-0.02	-0.02	0.03
K_pct	-0.01	0.76	-0.01	-0.01	-0.01	-0.01	-0.01	0.7
La_ppm	-0.5	16.7	-0.5	-0.5	-0.5	-0.5	-0.5	14.5
Li_ppm	2.6	3.5	8.7	8.8	10.6	5.4	5.3	4.6
Mg_pct	0.29	2.39	1.77	2.02	2.57	1.02	0.62	3.74
Mn_ppm	480	1199	490	737	52	371	214	671
Mo_ppm	0.57	1.74	-0.01	0.05	0.02	0.02	-0.01	2.11
Na_pct	0.128	1.386	0.086	0.122	0.099	0.117	0.129	1.231
Nb_ppm	0.05	0.61	-0.02	0.03	0.03	-0.02	-0.02	0.84
Ni_ppm	66	122.3	16.9	13.4	7.1	1.6	1.1	157.2
P_pct	0.03	0.112	0.004	0.008	0.005	0.014	0.009	0.148
Pb_ppm	2.88	9.96	1.97	2.57	1.35	1.5	0.98	7.63
Pd_ppb	-10	-10	-10	-10	-10	-10	-10	20
Rb_ppm	0.2	11.2	-0.1	0.2	-0.1	-0.1	-0.1	8.5
S_pct	0.04	-0.02	0.06	0.04	0.03	0.04	0.05	0.04
Sb_ppm	0.18	-0.02	-0.02	0.03	-0.02	-0.02	-0.02	-0.02
Sc_ppm	6.9	7.1	3.8	5.7	0.1	2.2	0.2	3.3
Sr_ppm_LMBMS	11729	2049	8873	10879	10588	9521	14304	856
Te_ppm	0.54	0.16	0.78	0.63	0.78	0.71	1.41	0.03
Th_ppm	-0.1	1.5	-0.1	-0.1	-0.1	-0.1	-0.1	1.2
Ti_pct	0.001	0.709	-0.001	-0.001	-0.001	-0.001	-0.001	0.442
Tl_ppm	0.21	0.25	0.09	0.08	0.07	-0.02	-0.02	-0.02
U_ppm	0.2	0.9	-0.1	-0.1	0.2	-0.1	-0.1	0.4
V_ppm	9	114	-2	3	-2	-2	-2	115
Y_ppm	3.3	9.34	0.27	1.32	0.06	0.06	0.03	6.86
Zn_ppm	45.5	119.6	3	5.3	2.6	1	1.1	70
Zr_ppm	1.7	31.6	0.6	0.7	1.1	0.5	0.4	15.8

Table 9. Rock samples analysed for trace elements by aqua regia – ICPMS, by lithium metaborate emission spectroscopy for strontium (LMBMS) and by sodium peroxide sinter-mass spectrometry (Na_2O_2) for boron.

Analyte	138002	138003	138005	138006	138007	138008	138009	138010
SiO2_pct	0.48	19.66	0.04	0.18	0.1	0.26	0.03	41.06
Al2O3_pct	0.03	6.07	-0.01	-0.01	-0.01	-0.01	-0.01	12.66
Fe2O3_pct	5.85	6.98	0.06	1.86	0.06	3.78	-0.04	13.37
MgO_pct	0.53	4.28	3.07	3.5	4.49	1.82	1.18	9.19
CaO_pct	47.12	32.64	49.47	47.54	47.88	47.75	50.3	9.58
Na2O_pct	0.14	1.65	0.1	0.14	0.11	0.13	0.15	3.67
K2O_pct	0.02	0.94	-0.01	0.02	0.01	-0.01	-0.01	2.36
TiO2_pct	-0.01	1.74	-0.01	-0.01	-0.01	-0.01	-0.01	3.45
P2O5_pct	0.08	0.35	0.01	0.01	0.02	0.03	0.02	0.72
MnO_pct	0.07	0.17	0.06	0.1	-0.01	0.05	0.03	0.16
Cr2O3_pct	-0.002	0.013	-0.002	-0.002	-0.002	-0.002	-0.002	0.027
Cu_ppm	-5	22	-5	-5	-5	-5	-5	44
Ba_ppm	336	234	194	256	213	349	324	337
Zn_ppm	58	144	-5	7	5	-5	-5	115
Ni_ppm	63	114	-20	-20	-20	-20	-20	168
Co_ppm	-20	43	-20	-20	-20	-20	-20	55
Sr_ppm	11729	2049	8873	10879	10588	9521	14304	856
Zr_ppm	6	130	-5	6	-5	-5	-5	258
Ce_ppm	-30	50	-30	-30	-30	-30	-30	68
Y_ppm	4	12	-3	-3	-3	-3	-3	22
Nb_ppm	6	25	-5	-5	-5	-5	-5	42
Sc_ppm	8	9	5	7	-1	3	-1	18
LOI_pct_IG	44.2	25.1	46.1	45.3	46	45	46.5	3.4
SUM_pct	99.97	99.95	99.99	99.99	99.98	99.98	99.99	99.91
TOT_C_pct	12.39	6.86	12.92	12.81	13.1	12.61	13.28	0.48

Table 10. Rock samples analysed for major oxides and minor element by lithium metaborate emission spectroscopy-ICPES, total carbon analyses by Leco combustion and loss on ignition (LIO) results at 1100°C.

The six travertine samples have an average of 48.34 percent calcium oxide equivalent to more than 88 percent calcite assuming that the travertine mineralogy is mainly formed calcite and aragonite. The remaining 12 percent is most likely magnesium carbonate, iron carbonates, strontianite and trace elements. Most of the minor and trace elements in the travertine samples are present in very low concentrations or not detected by the geochemical analysis. Exceptions are the higher iron, arsenic, mercury and nickel measured in sample 138002 from the travertine cone-carbon dioxide vent.

Discussion of the Results

Several distinctive features of the Nazko wetland geochemistry indicate possible geothermal activity. There is, for example, visible carbon dioxide seepage to the surface through the soil and into the water of many pools in the North and South bogs. A vigorous flow of carbon dioxide from a small travertine cone on the margin of the North Bog suggests an appreciable source for this gas is beneath the bog. Previous studies of carbon isotopes and presence of helium indicate a magmatic source for the gas. Because travertine deposits are commonly associated with natural hot springs and carbon dioxide seeps (Pentecost, 1995) the travertine on the surface of both North and South bogs formed when ground and surface water containing dissolved alkaline earth elements reacted with the carbon dioxide. The thickness and scatter of travertine on the surface of the bogs suggests that it formed periodically over a long period of time and when different carbon dioxide vents became active.

Vigouroux, (pers comm, 2013), reported that the Nazko bog travertine is predominantly composed of aragonite with lesser amounts of calcite and dolomite. From a study of travertine mineralogy and delta ^{13}C values from Mount Etna, Italy, D' Alessandro et al. (2007), concluded that aragonite-rich carbonates enriched in magnesium and strontium were more likely to have been formed by primary deposition from solutions in contact with carbon dioxide degassing from a magmatic source. The higher magnesium and strontium measured in travertine samples from the North and South Bogs is evidence that the carbonate does have appreciable dolomite and strontianite in addition to calcite. One source for the calcium, magnesium and strontium is from weathering and solution of carbonate minerals coating the vesicles in basalt near the Nazko Cone. This basalt (sample 138003) has 23% calcium (LMB-ICPMS) and of this, 87 % of the calcium is aqua regia soluble. The magnesium content of this basalt sample is 2.6 % and strontium content is 0.2%. These elements are carried in solution to the bogs by stream or ground water where they are deposited as primary carbonate minerals by the reaction with carbonate and bicarbonate ions formed when the degassing carbon dioxide dissolves in water. The glacial deposits (till) surrounding the bog might be another source for the calcium, magnesium and strontium, but the C horizon soils has less than 1.5 % calcium and 400 ppm strontium. Also, only 24% of the calcium is aqua regia soluble.

Modeling the solubility of carbonate minerals from the ground and surface water analyses using the chemical equilibrium software PHREEQC (Parkhurst and Appelo, 1999) allows an independent prediction of the travertine mineral composition. Based on the chemistry of the water from inside the travertine cone-carbon dioxide vent on the edge of the North Bog, a PHREEQC simulation predicts that aragonite, calcite, dolomite, chalcedony, iron oxides including goethite and manganese oxides could precipitate. A similar mineral assemblage, but

with the addition of talc, could also precipitate from the alkaline stream water flowing into the North Bog.

Anomalous lithium, boron, arsenic and mercury are known geochemical pathfinders for geothermal activity. Ground water in the Nazko bogs has up to 637 ppb boron and the surface water a maximum of 547 ppb lithium. These concentrations are much lower than those reported from other geothermal fields such as at Waihi, New Zealand and in Eastern Turkey by Pasvanoglu, (2013) where thermal well water contained up to 2.7 ppm lithium, 37 ppm boron, 2000 ppm strontium, 5000 ppb arsenic and 0.3 ppb mercury. Nazko ground and surface water has less than 10 ppm strontium, 3 ppb arsenic and no detectable mercury. Silicon concentrations can also exceed 1000 ppm in hot spring water (Pasvanoglu, 2013) whereas the highest silicon level measured in the Nazko bog water is less than 20 ppm.

One explanation for the 2.4 ppb arsenic and the 44 ppb nickel detected in the water at the bottom of the travertine cone – carbon dioxide vent is that these elements are carried to the surface by artesian ground water from a deeper, bedrock aquifer. However, there is no visible upwelling of water into the bog from the vent and a more probable source for the arsenic and nickel is ground water seeping from the surrounding upland. Since the soil and till covering bedrock northwest of the bogs has an elevated nickel content, the weathering of this sediment and, possibly, volcanic ash erupted from the Nazko cone could explain higher nickel in ground water. Sharply elevated nickel, silver, copper and molybdenum in the water-saturated organic soil along the bog margin reflect the concentration of these metals by soil organic matter from the weakly mineralized ground water. They may also be immobilized and accumulate as hydroxides in response the increasing bog soil pH and, possibly, as sulphides because of the reducing conditions typical of the organic soil.

The calcium oxide-rich, silica poor, alkaline (median pH 8.17) bog soil reflects an accumulation of organic material, sedimentation and the precipitation of carbonate minerals in the wetland basin. From the evidence of plant microfossils identified in a bog profile, Souther et al. (1987) predicted that the original Nazko bog environment in the early Holocene (~ 9000 years BP) was a shallow pond or marsh. A six centimetre thick tephra layer at three metres depth beneath the bog surface dated by Souther et al. (1987) to be between 7100 and 7230 years was interpreted as the last eruption from the Nazko cone generating an extensive, but local ash deposit. Since then, the degassing of carbon dioxide has been a visible evidence for magmatic activity.

Alkaline, anoxic organic bog soil and organic-rich lake sediment control the mobility and distribution of trace metals such as copper, silver, nickel, selenium, molybdenum and rhenium. Copper, silver, nickel cations are most mobile in acid ground water whereas selenium, molybdenum and rhenium (ReO_4^-, MoO_4^{2-}, SeO_4^{2-}) ions are more stable at a higher pH. Hence,

metal cations will concentrate along the bog margin where the groundwater pH increases and organo-metal complex form. More alkaline conditions favour anion mobility and, therefore, selenium, molybdenum and rhenium migrate towards the middle of the North Bog where they may be stabilized as organo-metal complexes and as sulphides. An indication of this mechanism is the association between molybdenum and rhenium in the North Bog soil and in lake sediment.

Silicon oxide is often found as sinter with travertine near hot springs, but the highest silica content of the Nazko bogs travertine is 0.5 percent, the median silica content of the bruisolic C soil horizon is 32 percent whereas modern hot spring deposits have up to 76 percent silica (Caneta et al, 2005). Although lithium and boron in the brunisolic is higher than the organic soil, there is no systematic pattern that would indicate a source for these elements beneath the bogs and they do not appear to suggest a thermal source.

No mercury was detected in surface waters although only a small number of the water samples were analysed for this element. However, there is 3600 ppb mercury in organic soil close to the travertine cone – carbon dioxide vent and over 400 ppb mercury in the travertine sampled from the inner wall of the cone. Mercury levels up to 411 ppb in soil are confined to a few sites around the cone and there is less than 348 ppb mercury in the bog soil. It would be tempting to attribute the high soil mercury to vapour leakage from a geothermal source. However, several of the TREK survey regional till samples around the Nazko bogs have over 500 ppb mercury and also have a varying number of cinnabar (mercury sulphide) grains in till sample heavy mineral concentrates. Figure 79 shows the relationship between the Nazko soil mercury, the TREK regional till mercury and the number of cinnabar grains. The high mercury in the North Bog soil might reflect:

1. Dispersal of cinnabar in the till from bedrock sources that might be epithermal mercury-arsenic-gold mineralization or cinnabar concentrated along geological structures.
2. Remobilization of mercury form cinnabar to vapour by carbon dioxide and then concentration in the soil. Berkovic et al. (2010), demonstrated experimentally that the carbon dioxide radical could reduce to Hg^{2+} ion to elemental mercury**.** Figure 80 summarizes the processes.

One obvious indication of geothermal activity would be the existence of warm ground and surface water. The highest water temperature of 23°C measured in Fishpot lake likely reflects solar heating. Bog surface water typically have a summer temperature below 15°C and there are reports of the bogs being ice and snow free in winter. The low temperature (< 6°C) of the water in the travertine cone – carbon dioxide vent is unusual given the warmer surface water. However, the net heat of reaction between carbon dioxide and water to form carbonic acid,

the predominant ion species in the 6 to 7 pH range, is 1.76 calculated from standard enthalpy values (Fauer, 1995). Since the net standard enthalpy is positive the reaction is endothermic and would absorb heat, thus lowering the water temperature.

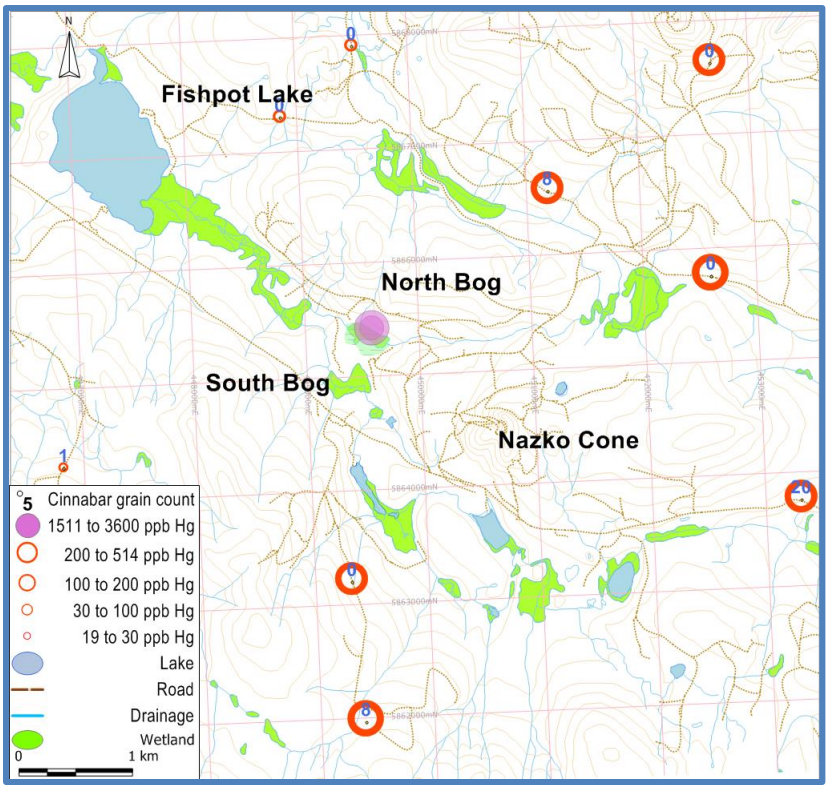

Figure 79 TREK Geothermal project and TREK regional till survey mercury in soil and till and the number of cinnabar grains in till mineral concentrates.

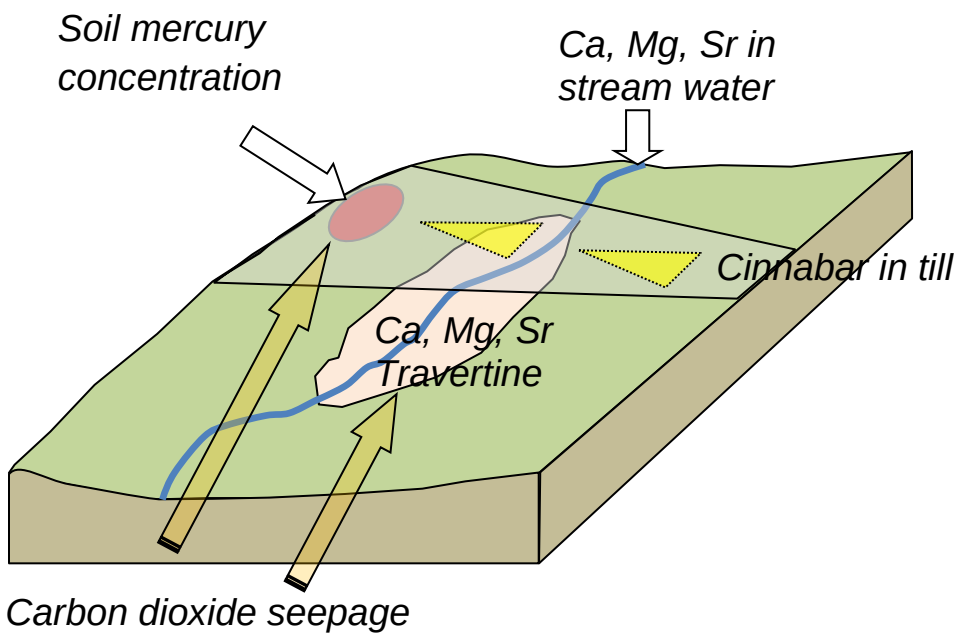

Figure 80 Processes responsible for soil mercury concentration and bog travertine.

Conclusions

Mapping surface features combined with the geochemical analysis of ground water, surface water, soil and rock samples from the Nazko bogs and surrounding area reveals that:

- There is no evidence of a thermal anomaly beneath the bogs and surrounding area. Although the bogs are near the Nazko volcanic cone, the surface travertine deposits that consist of calcium, magnesium and strontium carbonates and the numerous carbon dioxide seepages can be found where there is no geothermal system. A probable source for the calcium, magnesium and strontium in the water are carbonate minerals coating vesicles in the basalt surround the volcanic cone. Travertine forms initially by chemical weathering of the carbonate coating, transport of the dissolved calcium, magnesium and strontium in ground and surface water and finally precipitation as carbonates when the dissolved ions react with carbon dioxide.
- While ground and surface water sampled from the bogs do have elevated geothermal pathfinder elements such as boron and lithium, their concentration is lower than reported in known thermal waters. Other potential geothermal pathfinders such as arsenic and mercury are low or are undetectable in water possibly because of partitioning from a fluid to a vapour phase. The highest arsenic and nickel detected in the water in contact with a vigorous carbon dioxide seep in the Northern Bog are more likely derived from the weathering of minerals in the surrounding soil and till rather than ground water from a deeper aquifer.

- Metals such as copper, nickel and silver are clearly concentrated in organic-carbonate-rich soil close to bog margins where ground water seeps into the wetland basin. Metals that are more stable as anion complexes such as selenium are more mobile in the zone and are more dispersed in the bog soil.
- Very high soil mercury is near an active carbon dioxide seep, but it is likely that the source for the mercury is weathering of cinnabar grains in the till around and beneath the bogs rather than directly from geothermal activity. However, carbon dioxide may improve the mobility of mercury vapour and increase soil concentrations. Although there is no clear evidence for geothermal activity, such as the presence of thermal springs, because of masking by the wetland geochemistry and sediments and possibly owing to the amount of recharge/groundwater flow in the area, it is also possible that any thermal anomaly, i.e., hot water, is lost to deeper aquifers. This condition would explain the sole presence of cold, non-condensable gases at the surface.
- While there is anecdotal evidence of a thermal anomaly beneath the Nazko bogs and surrounding area (e.g., snow-free wetland areas) the ground water over an active carbon dioxide seep has an unusually low temperature. Thermodynamics of reaction between upwelling carbon dioxide and water can predict this low temperature.

Further studies

Additional studies to identify the presence of buried geothermal activity as a source for the geochemical patterns detected in and around the Nazko bogs could include:

- Determining the size of the elevated geothermal indicator element (e.g., B, Rb, Hg, As, Li) patterns in the bog and mineral soil water and vegetation.
- Detecting additional carbon dioxide seepages in the bog and surrounding area and measuring the gas flux to the surface.
- Detecting the presence of mercury vapour at the surface near the travertine cone-carbon dioxide vent and estimating the flux of the mercury to the surface.
- Estimating the geochemical partitioning of mercury in the soil and till into different forms.
- Measuring the seasonal variation of geothermal indicator elements in the surface and ground water.
- Detecting other travertine deposits in the Nazko area and determining geothermal indicators in the travertine and associated water.
- Detecting other gases in the bog seepage carbon dioxide e.g. helium and measuring stable isotope ratios (e.g. ^{3}He:^{4}He, $^{16}O/^{18}O$, $^{13}C/^{12}C$) in the the seepage gas and seep water.

- Measuring stable isotope (e.g., $^{13}C/^{12}C$) ratios and the carbonate mineralogy (e.g. calcite: aragonite) of travertine deposits.

Acknowledgments

In the field, assistance from Jamie Constable, Hazel Paul, Trevor Clement and Dave Sacco with sample collection, sample analysis and data collection was very much appreciated. Nathalie Vigouroux, Glyn Williams-Jones and Brent Ward, (Simon Fraser University), and Catherine Hickson, (Alterra Power Corp.), generously provided information about the Nazko wetlands and loaned sampling equipment. Alexei Rukhlov, (BC Ministry of Energy and Mines), is thanked for allowing use of water testing equipment from the Geological Survey laboratory. Critical reviews of this paper by Travis Ferbey, (BC Geological Survey) and by Nathalie Vigouroux and Glyn Williams-Jones, (Simon Fraser University), are very much appreciated. The project was funding by Geoscience BC as part of the 2013 TREK Project.

References

Bellomo, S and Parello, F. (2007): Geochemistry and mineralogy of travertine deposits of the SW flank of Mt. Etna (Italy): Relationship with past volcanoes and degassing activity; *Journal of Volcanology and Geothermal Research*. Volume 165, pages 64-70.

Berkovic, A. M., Gonzalez, M. C., Russo, N., Michelini, M.C., Diez, R.P., and Mártire, D.O., (2010): Reduction of Mercury(II) by the Carbon Dioxide Radical Anion: A Theoretical and Experimental Investigation; *Journal of Physical Chemistry,* A. 2010, December 16; 114(49), pages 12845-50.

Caneta, C., Prol-Ledesmaa, R.M., Torres-Alvaradob, I., Gilgc, H.A., Villanuevaa, R.E., Cruzd, R.L., (2005): Silica-carbonate stromatolites related to coastal hydrothermal venting in Bahı´a Concepcio´n, Baja California Sur, Mexico, *Sedimentary geology*, 194, pages 97-113.

Ford, T.D. and Pedley, H.M. (1996): A review of tufa and travertine deposits the word*, Earth Science Reviews*, v 41, pages 117-175.

Fouke, B.W. Farmer, J.D. Des Marais, D.J. Pratt, L. Sturchio, N.C. Burns, P.C. and Discipulo, M. (2000): Depositional facies and aqueous-solid geochemistry of the travertine-depositing hot springs (Angel) Terrace , Mammoth hot springs, Yellowstone national Park, U.S.A., *Journal of Sedimentary Research,* Volume 70, pages 565-585.

Jackaman, W. (2014): Regional Geochemical and Mineralogical Data, TREK Project, Interior Plateau, British Columbia, Geoscience BC Report, 2014-10.

Faure, G. (1998): Principles and applications of geochemistry, Prentice Hall, 600 pages.

BC Geological Survey (2013): MINFILE BC mineral deposits database; BC Ministry of Energy and Mines <http://minfile.ca/> [November 2013].

Pasvanoglu, S. (2013): Hydrogeochemistry of thermal an mineralized water in the Diyadin (Agri) area, Eastern Turkey, *Applied Geochemistry*, 38, 70-81.

Parkhurst, D.L. and Appelo, C.A.J. (1999): Users guide PHREEQC (VERSION 2)—a computer program for speciation, batch-reaction, one dimensional transport and inverse calculations, U.S. Geological Survey, water-Resources Investigations Report 99-4259A. 312 pages.

Petecost, A. (1995): Geochemistry of carbon dioxide in six travertine-depositing springs of Italy, Journal of Hydrology, v 167, pages 263-278.

Riddell, J. (2011): Lithostratigraphic and tectonic framework of Jurassic and cretaceous intermountain sedimentary basins of south-central British Columbia; Canadian Journal of Earth Sciences, v. 48, p. 870-896.

Souther, J. G. Clague, J.J. and Mathews. R.W. (1987): Nazko cone: a Quaternary volcano in eastern Anahim Belt; Canadian Journal of Earth Sciences, v. 24, p. 2477-2485.